



PHD

## Hydrodynamics of Migrating Zooplankton in a small lake

Simoncelli, Stefano

*Award date:*  
2018

*Awarding institution:*  
University of Bath

[Link to publication](#)

### Alternative formats

If you require this document in an alternative format, please contact:  
[openaccess@bath.ac.uk](mailto:openaccess@bath.ac.uk)

#### General rights

Copyright and moral rights for the publications made accessible in the public portal are retained by the authors and/or other copyright owners and it is a condition of accessing publications that users recognise and abide by the legal requirements associated with these rights.

- Users may download and print one copy of any publication from the public portal for the purpose of private study or research.
- You may not further distribute the material or use it for any profit-making activity or commercial gain
- You may freely distribute the URL identifying the publication in the public portal ?

#### Take down policy

If you believe that this document breaches copyright please contact us providing details, and we will remove access to the work immediately and investigate your claim.

# Hydrodynamics of migrating zooplankton in a small lake

submitted by

**Stefano Simoncelli**

for the degree of Doctor of Philosophy

**University of Bath**

Department of Architecture and Civil Engineering

February 2018

## **COPYRIGHT**

Attention is drawn to the fact that copyright of this thesis rests with its author. This copy of the thesis has been supplied on the condition that anyone who consults it is understood to recognise that its copyright rests with its author and that no quotation from the thesis and no information derived from it may be published without the prior written consent of the author.

This thesis may be made available for consultation within the University Library and may be photocopied or lent to other libraries for the purposes of consultation.

Signature of Author .....

Stefano Simoncelli



# Abstract

Zooplankton diel vertical migration (DVM) plays a pivotal role in controlling trophic interactions and nutrient transport in lakes and oceans. Understanding behaviours and responses of diel migrators is therefore essential to knowledge of physical processes and ecosystem functioning. This thesis investigated zooplankton hydrodynamics during the DVM in freshwater bodies through two different research topics. The first research explored the potential of swimming zooplankton hydrodynamics in affecting lake turbulent and biological processes. Past research suggests that zooplankton may be able to inject turbulent kinetic energy (TKE) in the water column when organisms swim. This process, referred to as biomixing, may increase vertical mixing in lakes. Since no field studies exist about biomixing by small zooplankton, turbulence and mixing were sampled in a lake during the dusk DVM of *Daphnia*. Results indicate that swimming *Daphnia* did not intensify dissipation rates of TKE and vertical fluxes. This suggests that small zooplankton cannot affect lake mixing even when organisms collectively swim. The second research examined how changes in ecosystem conditions affect zooplankton displacement velocity (DV) during the DVM of *Daphnia*. Currently, it is not known which environmental factors are key in driving this velocity. DV was measured in the field during the sunset migration (upwards DV) and sunrise migration (downwards DV) along with temperature, relative change in light intensity, chlorophyll-*a* and zooplankton concentration, as pos-

---

sible velocity drivers. Results show that upwards velocities were strongly correlated with the water temperature in the migrating layer, suggesting that temperature can control swimming activity, metabolic rates and escape reactions from predators. Downwards velocities were instead constant. Modelling this velocity as a sinking rate indicates that buoyancy and gravity are the governing parameters. The model also suggests that zooplankton favour passive sinking over active swimming to preserve energy and generate hydrodynamic disturbances not detectable by predators.



# Extended abstract

Zooplankton diel vertical migration (DVM) plays a pivotal role in controlling ecologically important processes, trophic interactions and nutrient transport in lakes and oceans. Therefore, understanding behaviour and responses of diel migrators is essential to knowledge of physical processes and ecosystem functioning. The work presented in this thesis investigated zooplankton hydrodynamics during the diel vertical migration (DVM) in freshwater bodies. The aims were to (1) explore the effect of swimming zooplankton hydrodynamics on the lake turbulent environment and biological processes; and (2) understand how changes in ecosystem conditions affect zooplankton hydrodynamics and their swimming behaviour.

The first research topic was addressed by investigating the role of migrating zooplankton in generating turbulence and mixing in lakes. Theoretically, a single swimming organism is not able to enhance vertical mixing because generated hydrodynamics instabilities are too small and smeared out instantaneously by water viscosity. However, several studies in the literature suggest that a high concentration of moving organisms may be able to inject turbulent kinetic energy (TKE) through the turbulent wake created by synchronised motions of their moving appendages. Part of the created TKE may be converted into potential energy to induce vertical mixing. Per this mechanism, vertically-migrating zoo-

---

plankton may be able to transport nutrient-rich water to replenish regions with lower concentrations. This process is referred as biomixing. While past research about biomixing has been conducted in the ocean and laboratory only, for freshwater zooplankton, no *in situ* studies exist that assess the real role of biomixing under real environmental conditions. To tackle this, turbulence and mixing were measured in a small British lake during the dusk vertical migration of *Daphnia* spp. Different datasets of acoustic measurements, dissipation rates of TKE and mixing were collected during the lake stratified season. Results indicate that swimming *Daphnia* did not biologically enhance the dissipation rates of TKE compared to the background level. Observed concentration of migrating zooplankton, as high as 60 org. L<sup>-1</sup>, did not create larger hydrodynamics disturbances via collective motions. Since no turbulent energy was added into the water column by the swimming zooplankton, mixing and vertical fluxes of dissolved substances were not intensified. This suggests that small zooplankton cannot affect lake mixing at the organism concentrations observed in the study site

The second research topic was addressed by examining how changes in lake environmental conditions, such as temperature and food levels, may alter the zooplankton displacement velocity (DV) during the DVM. Currently, it is not known which environmental factors are key in driving the rate of zooplankton migration in the field because available measurements of the zooplankton DV were carried out in laboratory only. For this purpose, the zooplankton DV was continuously measured during the DVM in a small British lake in two different years using the backscatter strength (VBS) from an Acoustic Current Doppler



---

Profiler (ADCP). Two types of velocities were measured: the upwards velocity during the sunset migration and the downwards velocity during the reverse migration at sunrise. Velocity measurements were compared with time series of temperature, relative change in light intensity, chlorophyll-*a* concentration and zooplankton concentration, as possible velocity drivers. Data showed that the upwards velocities increased during the summer and were not enhanced by food, light intensity or by VBS, which is a proxy for zooplankton concentration and size. The upward velocities were strongly correlated with the water temperature in the migrating layer, suggesting that temperature could be a key factor controlling zooplankton swimming activity. Temperature can increase metabolic rates and zooplankton require less effort to propel themselves in a less viscous fluid. Changes in water temperature can also affect, by extension, escape reactions from predators. Since zooplankton are a food resource for planktivorous fish, temperature changes may indirectly alter patterns of predation, and thus trophic interactions and energy flows in lake food webs via this mechanism. Downwards velocities were constant and independent of the DVM drivers. The lack of variation was likely because zooplankton passively sank instead of swimming during the reverse migration. An analytical equation for the downwards velocity was derived by modelling *Daphnia* sinking rate as a function of body size, organism density and water temperature. The good agreement of the sinking model with the field data indicates that the buoyancy and gravity are the governing parameters of the reverse migration and that the sinking rate is temperature-independent. The developed model differs from past model because it also accounts for additional drag from antennas which is fundamental when modelling *Daphnia* sinking rate. The results show that zooplankton

---

favour passive sinking over active swimming to preserve energy and generate hydrodynamic disturbances not detectable by predators.



# Acknowledgements

First and foremost, I would like to express my gratitude to my supervisors Dr. Danielle Wain and Dr. Stephen Thackeray for their unending support during my Ph.D, their enthusiasm, advice and immense knowledge. I could not have imagined better and friendlier mentors during this phase of my professional life. I would like to specifically express my gratitude to Danielle for being always supportive and patient in these three years. I am indebted to her for all the support she gave me, from advising me about my field work to learning new MATLAB tricks and to improving my English skills. My sincere thanks also goes to my other supervisors, Dr. Lee Bryant and Dr. Thomas Kjeldsen. Besides my supervisors, I would like to thank my fellow WEIR(d) students (and friends) for all the support and fun we had in the last three years. I list their names alphabetically to avoid any favouritism: Emily Slavin, Kevin Martins, Ioanna Stamataki, Mahan Amani, Olivia Cooke, Rebecca Ellis and Russell Arnott. I have been lucky to have such friendly and cheerful office mates. I am also very thankful to Sarah Howell, Tobias Woodman, Jake Opher, Zach Wynne and Scott Easter for their assistance in my field campaign also late at night in the cold and damp English weather. I also express my gratitude to Tim Clements for allowing me access to Vobster Quay also past the lake closing time. I am also grateful for the URSA studentship provided by the University of Bath and the Faculty of Engineering and the financial support by the Royal Society and the EU. At last but not the least, I thank my family for their support and patience, in particular my twin brother who endured me during my stressful moments.

# Contents

<b>Abstract</b> . . . . .	<b>1</b>
<b>Extended abstract</b> . . . . .	<b>3</b>
<b>Acknowledgments</b> . . . . .	<b>7</b>
<b>List of Figures</b> . . . . .	<b>12</b>
<b>List of Tables</b> . . . . .	<b>19</b>
<b>1 Introduction</b> . . . . .	<b>21</b>
1.1 Effect of swimming zooplankton on the environment . . . . .	23
1.1.1 Background . . . . .	23
1.1.2 Objectives . . . . .	28
1.2 Effect of the environment on the zooplankton swimming velocity . . . . .	29
1.2.1 Background . . . . .	29
1.2.2 Objectives . . . . .	30
1.3 Dissertation Organisation . . . . .	30
<b>2 Can small zooplankton mix lakes?</b> . . . . .	<b>32</b>
2.1 Introduction . . . . .	34
2.2 Measuring biomixing . . . . .	37
2.3 Biomixing in lakes . . . . .	42

---

2.4	The need for field studies . . . . .	45
2.5	Challenges for future field investigations . . . . .	49
2.6	Conclusions . . . . .	52
<b>3</b>	<b>On biogenic turbulence production and mixing from vertically migrating zooplankton in lakes . . . . .</b>	<b>53</b>
3.1	Introduction . . . . .	58
3.2	Materials and Methods . . . . .	62
3.2.1	Study site . . . . .	62
3.2.2	Zooplankton abundance . . . . .	64
3.2.3	Acoustic measurements . . . . .	65
3.2.4	Microstructure measurements . . . . .	66
3.2.5	Mixing and length scales . . . . .	67
3.2.6	Other measurements . . . . .	68
3.3	Results and discussion . . . . .	68
3.3.1	Zooplankton distribution . . . . .	68
3.3.2	ADCP calibration . . . . .	69
3.3.3	DVM pattern . . . . .	75
3.3.4	Dissipation rates . . . . .	76
3.3.5	Mixing . . . . .	82
3.4	Conclusions . . . . .	85
3.5	Acknowledgements . . . . .	86
3.6	Appendix . . . . .	87
3.6.1	Supplementary material 1 . . . . .	87
3.6.2	Supplementary material 2 . . . . .	88
<b>4</b>	<b>Effect of temperature on zooplankton vertical migration . . . . .</b>	<b>89</b>
4.1	Introduction . . . . .	92
4.2	Materials and Methods . . . . .	95
4.2.1	Study site . . . . .	95
4.2.2	Acoustic measurements . . . . .	96
4.2.3	Bulk velocity estimation . . . . .	97

---

4.2.4	Temperature measurements . . . . .	101
4.2.5	Turbulence estimation . . . . .	102
4.2.6	Chlorophyll- <i>a</i> concentration . . . . .	102
4.2.7	Underwater light conditions . . . . .	103
4.2.8	Zooplankton concentration . . . . .	104
4.3	Results . . . . .	104
4.3.1	Bulk velocity . . . . .	104
4.3.2	Temperature measurements . . . . .	106
4.3.3	Dissipation rates of TKE . . . . .	108
4.3.4	Chlorophyll- <i>a</i> concentration . . . . .	109
4.3.5	Underwater light conditions . . . . .	112
4.3.6	Zooplankton concentration . . . . .	116
4.3.7	Zooplankton position . . . . .	118
4.4	Discussion . . . . .	122
4.4.1	Upwards bulk velocity . . . . .	123
4.4.2	Ecological implications . . . . .	125
4.5	Conclusions . . . . .	126
4.6	Acknowledgements . . . . .	127
4.7	Appendix . . . . .	128
4.7.1	SCAMP fluorometer calibration curve . . . . .	128
<b>5</b>	<b>Modelling sinking rate of <i>Daphnia</i> during the downward vertical migration . . . . .</b>	<b>130</b>
5.1	Introduction . . . . .	133
5.2	Materials and Methods . . . . .	137
5.2.1	Velocity measurements . . . . .	137
5.2.2	Laboratory experiments . . . . .	137
5.3	Results . . . . .	139
5.3.1	Bulk velocity . . . . .	139
5.3.2	Laboratory experiments . . . . .	141
5.3.3	Modelling of $v_{down}$ . . . . .	143
5.4	Discussion . . . . .	147

---

5.5	Conclusions . . . . .	148
<b>6</b>	<b>Conclusions . . . . .</b>	<b>150</b>
6.1	Introduction . . . . .	150
6.2	Effect of swimming zooplankton on the environment . . . . .	151
6.3	Effect of the environment on zooplankton . . . . .	154
6.4	Links between zooplankton hydrodynamics and environment . . . . .	156
<b>7</b>	<b>Prospects for future work . . . . .</b>	<b>159</b>
7.1	Further development of this thesis . . . . .	159
7.2	Future Directions in Zooplankton Hydrodynamics . . . . .	161
	<b>Bibliography . . . . .</b>	<b>165</b>



# List of Figures

1.1	Temperature profile collected on 6 <sup>th</sup> August 2015 in Vobster Quay (black line). The coloured blocks show the partitioning of the water column in three different layers according to the temperature profile. . . . .	24
1.2	The map shows the UK in the background and the location of Radstock (black ellipse), where the sampling site is situated. The inset in the top-left corner shows a magnification of the area with the location of Vobster Quay (red ellipse) with respect to Radstock village (UK grid reference ST 70446 49730) . . . . .	25
1.3	Turbulence level in a medium-sized lake, expressed as dissipation of turbulent kinetic energy, as a function of depth (circles) and as a function of height above bottom (squares). From an energetic point of view the lake has three distinctive layers. The layer of interest in this thesis is the interior. From Wüest and Lorke (2003)	26

---

2.1	Sketch illustrating main mixing processes operating in three different lake regions. In the surface layer, energy from wind (A) leads to mixing by breaking surface waves (B) or via seiching motions (C) or convective mixing can act at night when the surface is cooling (D). Boundaries are subjected to mixing events (E) for example via interactions of internal waves. The lake interior is the calmest region with local and intermittent mixing events (F). Vertical migrators (G) may provide energy for enhancing the mixing in this layer. Eddies indicate layers with mixing, while straight lines in the interior indicate that energy production is extremely weak and sporadic. . . . .	35
2.2	Schematic of the partition of turbulent kinetic energy imparted by a swimmer ( <i>Daphnia</i> spp.). The continuous line depicts the wake left by the swimmer, while the eddies are the turbulent instabilities created within the wake that can be a source of TKE. The source energy is converted into potential energy ( $b$ ), increasing the mixing, and into heat as energy is dissipated ( $\varepsilon$ ) due to water molecular viscosity. . . . .	38
2.3	Eddy diffusivity $K_V$ as a function of zooplankton concentration $C$ from numerical simulations and laboratory experiments. Each study is represented with a different symbol and colour. . . . .	46
3.1	Panel a shows a schematic of swimming <i>Daphnia</i> and their interacting turbulent wakes (continuous lines). The eddies show the turbulent instabilities created within the wake that can be a source of TKE. Panel b shows the experimental setup. The dashed lines shows the acoustic cone of the ADCP, while the gray trapezoids indicate the segments sizes for acoustic and microstructure measurements. . . . .	62

---

3.2	Geometry and bathymetry of Vobster Quay. "S" denotes the sampling station where microstructure and zooplankton measurements were taken. The locations of the thermistor chain (T chain) and ADCP are also shown. . . . .	63
3.3	Conditions before the DVM for the three different sampling dates: (a) average temperature profile from SCAMP data, and (b) buoyancy frequency. The red band shows the average depth range inhabited by zooplankton during the day, just below the depth of maximum buoyancy. . . . .	64
3.4	Profiles of zooplankton concentration for <i>Daphnia</i> spp., copepods, small Cladocera and copepods nauplii collected before the DVM and SCAMP measurements. . . . .	69
3.5	Comparison between the observed <i>Daphnia</i> concentration and that estimated from Eq. 3.5 using the measured VBS. Black dots show the datasets collected on 21 July, 28 July and 18 August used to estimate $k_0$ and $k_1$ in Eq. 3.5. Empty dots show data from the validation dataset collected on 30 June 16. The dashed line is the 1:1 relationship. . . . .	73
3.6	Time series of <i>Daphnia</i> concentration (greyscale colour-bar) for the three different days. Blue line highlights the sunset time when the migration begins. . . . .	74
3.7	Data collected on 21 July 2016. Coloured blocks show the time series of dissipation rate of temperature variance $\chi_T$ (upper panel), dissipation rate of TKE $\varepsilon$ (mid panel), and eddy diffusivity $K_T$ (lower panel). The greyscale background shows the estimated <i>Daphnia</i> concentration. Blue lines highlight the sunset time when the migration begins. Spaces with no colour highlight the parts of the water column with non-stationary turbulence segments and invalid fits of the Batchelor spectrum. . . . .	78
3.8	Data collected on 28 July 2016. Panel descriptions same as in Fig. 3.7 . . . . .	79

---

3.9	Data collected on 18 August 2016. Panel descriptions same as in Fig. 3.7 . . . . .	80
3.10	<i>Daphnia</i> concentration as a function of $\varepsilon$ (black dots) and $\chi_T$ (green triangles) in the turbulent patches during the DVM for the three different datasets. The gray and green area show the mean background dissipation level for $\varepsilon$ and $\chi_T$ respectively . . . . .	82
3.11	Ozmidov scale $L_{OZ}$ as a function of the Thorpe length scale $L_T$ in the turbulent patches inside the migrating layer (filled dots) and outside (empty dots) after sunset. The dashed line is the 1:1 relationship. . . . .	83
3.12	Eddy diffusivity coefficient $K_V$ as a function of <i>Daphnia</i> spp. concentration from different studies in the literature. The green dot represents data from this study. The error bar shows the observed minimum and maximum concentration and the dot its mean. . . . .	84
3.13	Volume backscatter strength from the ADCP vertical beam in grey. Higher values indicate a higher zooplankton abundance, while the minimum is the background echo intensity. Red arrows indicate the time of the zooplankton tows, black arrows the start time of SCAMP casts and the red dashed line sunset when the zooplankton begin migrating. . . . .	87
3.14	Profiles of linear VBS (red line) and <i>Daphnia</i> concentration (black line) collected on the 30 June 2016. . . . .	88
4.1	Bathymetry of Vobster Quay. "S" denotes the sampling station where measurements were taken. "T" and "A" indicate the locations of the thermistor chain and ADCP respectively. . . . .	96

---

4.2	Schematic of how the algorithm computes the bulk velocity. The four panels show the DVM captured by the ADCP on 02/07/16. The grey-scale shading is the VBS and shows the position of the zooplankton in the water column as a function of the time. Panel a shows the green box delimited by $Z_{WINDOW}$ and $T_{WINDOW}$ and used by the model to detect the migrating layer. Red dots in panel b show the zooplankton layer where $81 \text{ dB} \leq VBS \leq 85 \text{ dB}$ . Blue shapes delimit isolated zooplankton patches removed from the algorithm. The red patch in panel c highlights the layer identified by the algorithm. $Z_{s, lower}$ , $Z_{s, upper}$ , $Z_{e, lower}$ and $Z_{e, upper}$ provide the upper and lower position of the layer when the DVM begins and ends. Panel d shows the resulting slope of the layer and the bulk velocity $v_{up,81}$ for $V_{min} = 81 \text{ dB}$ . . . . .	98
4.3	Algorithm results with two other values of $V_{min}$ . Panel a shows the case with a low value, where almost all the points in the target area are selected. When $V_{min}$ is too high as in panel b, the resulting slope is off. In both cases the slope is marked as invalid. Panel c depicts the final result of $v_{up}$ via bootstrapping. . . . .	100
4.4	Time series of bulk velocity $v_{up}$ at sunset in 2015 and 2016. Error bars show the 95% confidence interval from the bootstrap method. The black dashed lines show the trend lines fitted to the points. . . . .	105
4.5	Contour plot of temperature in 2015 (panel above) and 2016 (panel below) from the thermistor chain. . . . .	106
4.6	Mean temperature in the migrating layer (thick line) and its 95% confidence interval (shaded area). . . . .	107
4.7	Mean profiles of TKE dissipation rates $\varepsilon$ (dots) on a logarithmic scale. . . . .	108
4.8	Time series of time and depth-average TKE dissipation rates $\varepsilon$ (dots) on a logarithmic scale. The green areas show the time period when the acoustic measurements are available. . . . .	109

---

4.9	Contour plot of chlorophyll- <i>a</i> concentration profiles collected in the lake in 2015 and 2016. The colour-bar on the right shows the measured concentration while the black triangles indicate the time when vertical profiles were collected with the SCAMP fluorometer. The green lines show the periods when the acoustic measurements were taken. . . . .	110
4.10	Time series of water-column-averaged concentration of chlorophyll- <i>a</i> in 2015 and 2016. Black dots indicate the day when the chlorophyll- <i>a</i> profiles were averaged. The red line represents the time series employed in the correlation. The green areas show the time period when the acoustic measurements are available. . . . .	111
4.11	Photosynthetically active radiation (PAR) profiles in 2015 and 2016 on a logarithmic scale. . . . .	112
4.12	Time series of Secchi disk depth $z_{SD}$ in 2015 and 2016. The dashed horizontal line represents the mean depth from the data. . . . .	113
4.13	Time series of light extinction coefficients from PAR profiles (black circles) and Secchi depths (empty triangles). The green areas show the time period when the acoustic measurements are available. . . . .	114
4.14	Time series of mean relative change in light intensity $S$ during the migration. . . . .	115
4.15	Stacked plots of mean concentration in the water column (panel a and b) and maximum concentration (panel c and d) of <i>Daphnia</i> spp., adult and copepodite-stage copepods, small Cladocera and copepod nauplii. The green areas show the time period when the acoustic measurements are available. . . . .	116
4.16	Mean volume backscatter strength of the migrating layer during the DVM in 2015 and 2016. . . . .	118
4.17	Mean zooplankton position before the DVM (full dots) and after DVM (empty dots) when they reach the surface in 2015 (panel a) and 2016 (panel b). . . . .	120

---

4.18	Panel a shows the correlation between $T$ and the observed upwards velocity. The grey line represents the fitted model to the regression dataset whose equation is reported in the bottom right corner. The upper left corner displays the coefficient of determination $R^2$ and the $p$ value of the regression. Panel b shows the relation between the observed $v_{up}$ from the validation dataset and the prediction from the regression model (dots). The dashed line is the 1:1 relationship. . . . .	122
4.19	In situ calibration curve used to convert the SCAMP voltage profiles to chlorophyll- $a$ concentration. Stars indicate data from the Blagdon lake, while the circles refer to Llandegfedd Reservoir. The conversion equation is reported in the right-bottom corner of the figure along with the coefficient of determination $R^2$ . . . . .	129
5.1	Measured lengths of <i>Daphnia</i> . $l$ is the body length, $w$ its width. The second antennae length is $b_c$ while its width $a_c$ . . . . .	139
5.2	Time series of bulk velocity $v_{down}$ at sunrise (grey triangles) in 2015 and 2016. Error bars show the 95% confidence interval from the bootstrap method. The black dashed lines show the trend lines fitted to the points. . . . .	140
5.3	Frequency distribution of the density of individual <i>Daphnia</i> specimens ( $n=20$ ). The red line is the sample mean and the horizontal error bar its 95% confidence interval. . . . .	141
5.4	<i>Daphnia</i> is modelled using an ellipsoid for the body and two cylinders for the antennae (panel a). The new model (panel b) balances the buoyancy $B$ with the additional drag ( $F_{d,c}$ and $F_{d,e}$ ) accounting for the body lengths $a_e$ , $b_e$ , $a_c$ and $b_c$ . . . . .	144

5.5	Average sinking rates of <i>Daphnia</i> as a function of the temperature $T$ . Orange line shows the organism modelled as a spherical body (with $R = b_E = 0.433$ mm), the green line as an ellipses (with $a_e = 0.189$ mm and $b_e = 0.443$ ) and the blue line with the new model (with $a_c = 0.425$ mm and $b_c = 0.039$ mm). Each thick line shows the mean velocity and the shaded areas the 95% confidence intervals. Dots report the measured values of $v_{down}$ with the corresponding temperature $T$ observed in the migrating layer. Grey box shows instead the observed range of $v_{down}$ and $T$ . . . . .	146
6.1	Conceptual diagram showing interactions between zooplankton hydrodynamics and their environment during the DVM. Block (a) and (b) show the two explored research topics, while numbers 1 to 5 indicate the connections between different elements. . . . .	151
7.1	Vertical velocities (upper panel) and turbulence dissipation rates (lower panel) measured from an Aquadopp and 1000-kHz ADCP in Lake Stechlin, Germany. Black lines highlight the time when night convection approximately begins. . . . .	162
7.2	Sketch of interaction between convective cells and plumes during penetrative convection at nighttime. . . . .	163

## List of Tables

2.2	Main biomixing studies in the literature classified by type of study. For the different kind of analysed organisms and swimming behaviours, we reported the main results for generated turbulence and mixing. Grey-shaded rows show the few biomixing observations for freshwater zooplankton. . . . .	41
-----	--	----



---

3.1	Regression coefficient $k_g$ and $p$ values from multiple regression analysis between the zooplankton groups and the linear VBS using the data from the three sampling days . . . . .	71
3.2	Mean and maximum <i>Daphnia</i> concentration ( $C_{Daphnia}$ ) in the migrating layer estimated from the simplified regression model. . .	76
4.1	Correlation matrix of the regression coefficient for the volume backscatter strength ( $VBS$ ), temperature ( $T$ ), chlorophyll concentration ( $Chl$ ) and relative change in light intensity ( $S$ ) . . . . .	121
4.2	Variance inflation factor (VIF) for the predictors . . . . .	121
5.2	Sinking rates of <i>Daphnia</i> from the literature . . . . .	136
5.3	Body sizes (see Fig. 5.1) measured for <i>Daphnia</i> . The last two rows report the mean and the 95% confidence interval $CI_{95}$ via bootstrapping. . . . .	142

## Introduction

Zooplankton diel vertical migration (DVM) plays a pivotal role in controlling ecologically important processes, trophic interactions and nutrient transport in lakes and oceans. Understanding hydrodynamics, behaviour and responses of zooplankton during the DVM is therefore essential to knowledge of physical processes and ecosystem functioning.

Several studies in the literature have investigated the role of zooplankton in affecting the environment where they reside and how their hydrodynamics may influence water quality in lakes and oceans. When these organisms ingest food resources, the organic matter not directly assimilated, can be respired as CO<sub>2</sub> or released as dissolved compounds for phytoplankton and bacteria (Castellani and Edwards, 2017). Egestions can create fluxes of dissolved organic carbon which are again made available to bacteria for decomposition (Castellani and Edwards, 2017; Hessen and Kaartvedt, 2014). During the vertical migration, zooplankton may also be responsible for transporting nutrients by ingestion in the hypolimnion and later release in the surface lake layer (Haupt et al., 2010). Recent studies also suggested that zooplankton in lakes and oceans may be able to generate turbulence and enhance mixing while swimming, affecting vertical fluxes of dissolved substances during the stratification period (Huntley and Zhou, 2004; Katija, 2012; Wang and Ardekani, 2015; Wilhelmus and Dabiri,

2014). Finally, zooplankton are also regarded as an important food resource for fish and other invertebrate predators and are the main grazers of phytoplankton, bacteria and protozoa (Stoecker and Capuzzo, 1990; Work and Havens, 2003).

While zooplankton can influence directly and indirectly a variety of ecological and physical process in lakes, another branch of the literature approached the opposite research question: how are zooplankton hydrodynamics and their biological demands affected by the environment where they reside? During the stratified period, organisms experience varying conditions of temperature, food availability, light and other environmental factors. Changes in these parameters can alter zooplankton swimming response and their interactions with the fluid (Larsen et al., 2008; Ringelberg and Flik, 1994; Van Gool and Ringelberg, 2003; Wickramarathna, 2016) and influence their habitat back again. For example, when zooplankton assimilate organic matter, the availability of food resources in the environment is reduced. However, since their metabolism is temperature-regulated, the process decelerates when zooplankton is exposed to colder waters and may also be inhibited when conditions are too adverse. This may further complicate the study of these phenomena because processes are strongly interconnected with each other.

The aims of the work presented in thesis are twofold: (1) explore the effect of swimming zooplankton hydrodynamics on the lake turbulent environment and biological processes and (2) understand how changes in ecosystem condition affect zooplankton hydrodynamics and their swimming behaviour. The first research topic is described in Section 1.1, while the second point is addressed in Section 1.2.

## 1.1 Effect of swimming zooplankton on the environment

### 1.1.1 Background

Understanding how physical processes generate turbulence and mixing in fresh water bodies is a problem of fundamental importance because mixing events can impact ecosystem processes and water quality (Imboden and Wuest, 1995; Wüest and Lorke, 2003). In the temperate zone, freshwater lakes are frequently typified by annual cycles of mixing and stratification. Figure 1.1 shows an example of a temperature profile collected in July 2016 in Vobster Quay Reservoir, an oligotrophic basin in Radstock, England (see Fig. 1.2, UK grid reference ST 70446 49730). The summer density stratification, which can persist all year long in deep lakes, partitions the water column into three distinctive layers: the surface mixed layer (epilimnion), the metalimnion, with a sharp density gradient, and the mixed bottom (hypolimnion). The presence of the stratification has an impact on several environmental parameters, as the basin does not reach uniform and well-mixed conditions. As a consequence, for example, low oxygen concentrations in the stratified part of the water column can have adverse effects on organisms, impairing their reproductive cycle or leading to the disappearance of local species and the appearance of new invasive ones (Wu et al., 2003). Anoxic conditions can result in the release of nutrients, such as phosphorus or nitrogen, from the lake sediment, leading to a further deterioration of the water quality (Beutel et al., 2007; Boehrer and Schultze, 2008; Rao et al., 2008).

In lakes, the main source of mixing is the wind which adds kinetic energy and generates internal waves and seiches. However during the stratification period, the wind mostly enhances mixing only in the surface layer (see Fig. 1.3). In this layer, the dissipation of turbulent kinetic energy (TKE), a quantity often used as a

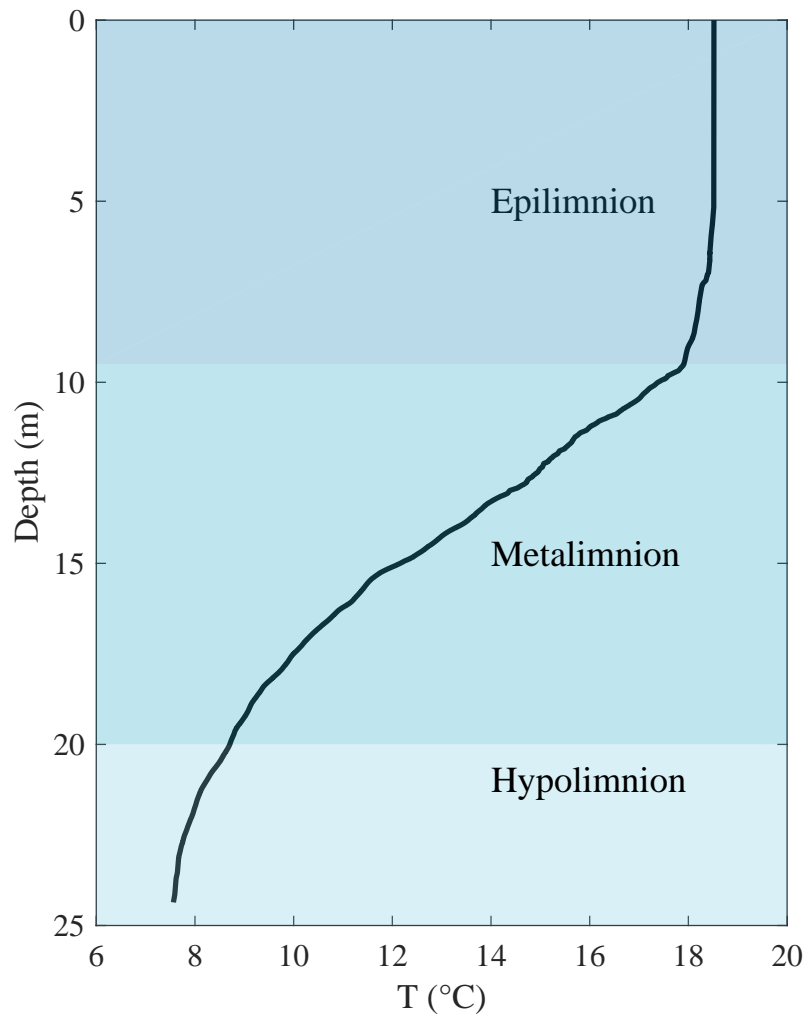


Figure 1.1: Temperature profile collected on 6<sup>th</sup> August 2015 in Vobster Quay (black line). The coloured blocks show the partitioning of the water column in three different layers according to the temperature profile.

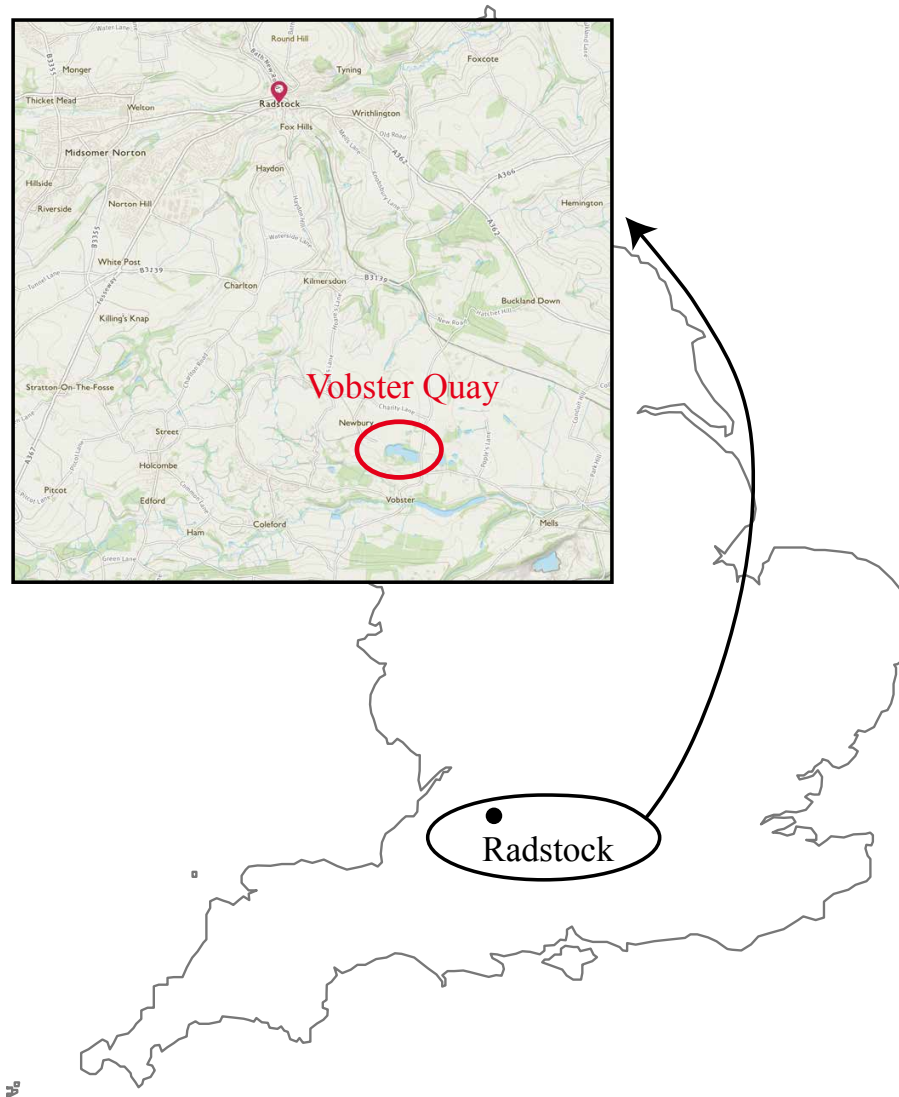


Figure 1.2: The map shows the UK in the background and the location of Radstock (black ellipse), where the sampling site is situated. The inset in the top-left corner shows a magnification of the area with the location of Vobster Quay (red ellipse) with respect to Radstock village (UK grid reference ST 70446 49730)

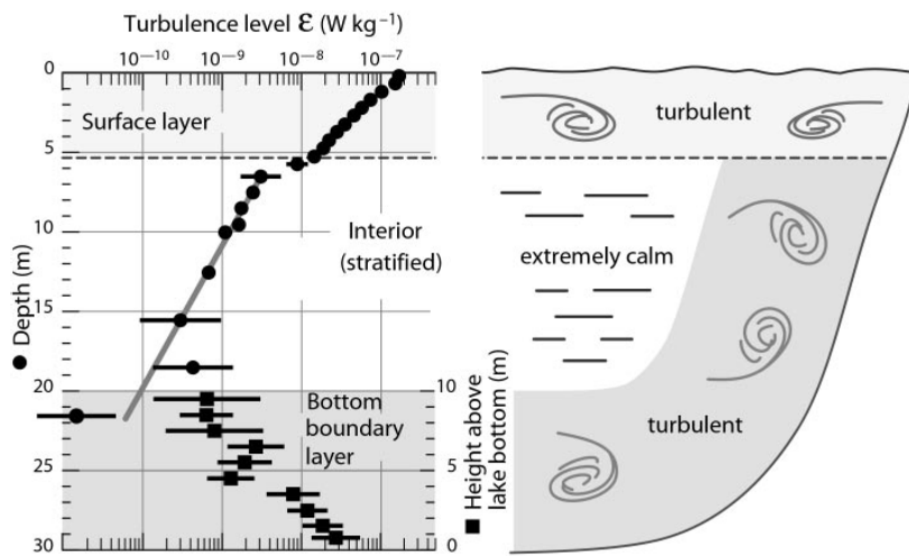


Figure 1.3: Turbulence level in a medium-sized lake, expressed as dissipation of turbulent kinetic energy, as a function of depth (circles) and as a function of height above bottom (squares). From an energetic point of view the lake has three distinctive layers. The layer of interest in this thesis is the interior. From Wüest and Lorke (2003)

proxy to infer the available energy in the water for mixing, can be as high as  $10^{-7}$   $\text{W Kg}^{-1}$  (circles between 0 and 5 m in the figure). These values are an indication that the turbulent level is high and mixing is very likely. In the interior, the part of the lake away from the physical boundaries (see Fig. 1.3), mixing is instead highly patchy and unsteady. This is suggested by the black circles in Fig. 1.3, between 5 and 20 m, where the level of turbulent dissipations reaches values as low as  $10^{-10}$   $\text{W Kg}^{-1}$ . The interior is the calmest part of the lake where instabilities generating mixing are sporadic and local processes only.

In recent years, several studies have suggested that swimming organisms, when migrating vertically, may create turbulence and mixing in the ocean interior, as effectively as winds and tides do in the ocean surface layer (Huntley and Zhou, 2004; Katija, 2012). This mixing-generation mechanism is referred to in the literature as biomixing. The impact of swimming animals on the interior of lakes, which share some similarities with oceans, has not been investigated yet from an experimental point of view. The only *in situ* study of biologically-generated mixing in lakes was conducted by Lorke and Probst (2010) for perch (*Perca fluviatilis*) and other investigations about mixing by small zooplankton have been performed in the laboratory only (Noss and Lorke, 2012; 2014; Wickramarathna et al., 2014). Theoretically, a single swimming organism is not able to enhance lake mixing because of their small size. The generated hydrodynamic instabilities would be too small and smeared out instantaneously by the water viscosity. Very recently, some laboratory and modelling studies have suggested that a high concentration of moving organisms may be able to inject turbulent kinetic energy (TKE) through the turbulent wake created by collective motions of their moving appendages. Part of the created TKE may be converted into potential energy, resulting in vertical mixing. Since no field studies are available on biomixing from small zooplankton, this precludes definitive conclusions regarding the potential importance of this mixing-generation mechanism. By studying the process in the field, when zooplankton may create synchronised motions, we can overcome limitations arising from laboratory studies and understand the



real contribution of zooplankton towards mixing water.

### 1.1.2 Objectives

In order to build upon, and advance, knowledge of zooplankton biomixing in freshwaters, the following objectives have been tackled:

1. Measure the turbulence generated by swimming zooplankton during the diel vertical migration in a lake environment by using a microstructure profiler.
2. Estimate the mixing and Thorpe overturning scales due to zooplankton migration.
3. Compare the results and the importance of this mechanism with existing investigations and models.

The objectives were addressed by collecting field data in Vobster Quay, a small made-man lake in Radstock (UK). The lake was chosen because of its simple bathymetry which makes this site ideal for the isolation of biomixing processes. As part of the investigation other lake data were also collected: bathymetry, currents, temperature profiles, chlorophyll-a profiles, acoustic backscatter strength and zooplankton abundance and composition.

## 1.2 Effect of the environment on the zooplankton swimming velocity

### 1.2.1 Background

Several studies in the literature have shown that zooplankton motility and swimming behaviour can be affected by the environment in which they swim. During the lake stratification period, zooplankton are exposed to varying environmental conditions which can influence the velocity at which the organisms swim. Zooplankton swimming speed has two components. The swimming velocity (SV) is the organism's instantaneous velocity during a reactive phase (Ringelberg, 2010); and the displacement velocity (DV) is instead the vertical displacement of the organism divided by the time taken to perform the movement (Gool and Ringelberg, 1995). The DV is smaller than SV because it includes various animal reactions including latent periods when the organism pauses or sinks. Experimental studies demonstrated that SV and DV can be affected by changes in environmental turbulence (Alcaraz et al., 1994; Seuront et al., 2004; Wickramarathna, 2016), temperature variations (Beveridge et al., 2010; Larsen et al., 2008; Moison et al., 2012), predation (Van Gool and Ringelberg, 1998a; Van Gool and Ringelberg, 1998b; 2003), food concentration (Rinke and Petzoldt, 2008; Van Gool and Ringelberg, 2003) and light intensity (Ringelberg and Flik, 1994; Ringelberg et al., 1991; Van Gool and Ringelberg, 1998a). However, as most of the past research on zooplankton swimming velocity was carried out in laboratory only, there is little knowledge about which parameter really drives the zooplankton velocity in the field and how it may vary during the stratified period. Moreover, laboratory studies addressed the effect of one parameter on the zooplankton swimming speed without assessing the net effects of multiple, interacting environmental factors.

### 1.2.2 Objectives

In order to address the current knowledge gap regarding correlates of zooplankton swimming velocity in the field, the DV was measured in the field during the diel vertical migration (DVM) of zooplankton. The DV was assessed at sunset, when organisms actively swim upwards, and at sunrise, when they passively sink towards the lake bottom. The objectives of this work were to:

1. Measure the zooplankton displacement velocity during the DVM at sunset and sunrise with a new technique based upon acoustic measurements and image analysis.
2. Correlate the time series of the measured velocity at sunset with time series of possible DVM drivers in the field, such as chlorophyll-*a* concentration, underwater light conditions, water temperature, and zooplankton concentration and size.
3. Explain and model the zooplankton sinking velocity at sunrise.

The mean DV was estimated using a 2-year dataset from an Acoustic Current Doppler Profiler deployed in Vobster Quay. The lake was also sampled for temperature, chlorophyll-*a* concentration, underwater light intensity and zooplankton during the stratification period. Additional laboratory analyses were also performed on zooplankton specimens to model their sinking rate.

## 1.3 Dissertation Organisation

The thesis is divided into seven chapters. Chapter 1 is this introductory chapter. Chapter 2 is an original contribution published in *Limnology and Oceanography*

*Letters.* It is a review of the existing literature about biomixing, with particular emphasis on small zooplankton in lakes. The chapter addresses the importance of biomixing in lakes and the need for field studies to properly understand the potential of biomixing. Chapter 3 presents measurements of turbulence and mixing during the DVM of zooplankton in a small man-made lake. Chapter 4 presents measurements of zooplankton displacement velocity (DV) during the upwards DVM. The DV is correlated with potential DVM drivers affecting this velocity. Chapter 5 deals with the zooplankton sinking rate measured in the field during the reverse DVM. The sinking velocity is modelled via the formulation of a physical-based model and laboratory measurements performed on specimens collected in the lake. Chapter 6 synthesises the results and draws the conclusions of this thesis. Chapter 7 delineates potential future works related to a better understanding of zooplankton hydrodynamics.

# Can small zooplankton mix lakes?

S. Simoncelli<sup>1</sup>, S. J. Thackeray<sup>2</sup> and D. J. Wain<sup>1</sup>


<sup>1</sup> Department of Architecture and Civil Engineering, University of Bath

<sup>2</sup> Centre for Ecology & Hydrology, Lancaster Environment Centre

## Abstract

**T**HE idea that living organisms may contribute to turbulence and mixing in lakes and oceans (biomixing) dates to the 1960s, but has attracted increasing attention in recent years. Recent modelling and experimental studies suggest that marine organisms can enhance turbulence as much as winds and tides in oceans, with an impact on mixing. However, other studies show opposite and contradictory results, precluding definitive conclusions regarding the potential importance of biomixing. For lakes, only models and lab studies are available. These generally indicate that small zooplankton or passive bodies generate turbulence but different levels of mixing depending on their abundance. Nevertheless, biogenic mixing is a complex problem, which needs to be explored in the field, to overcome limitations arising from numerical models and lab studies, and without altering the behaviour of the animals under study.

## Statement of Authorship

<b>This declaration concerns the article entitled</b>				
Can small zooplankton mix lakes?				
<b>Authors</b>				
Simoncelli, S. (SS), Thackeray, S. J. (SJT) and Wain, D. J. (DJW)				
<b>Publication status (tick one)</b>				
Draft manuscript	Submitted	In review	Accepted	✓ <u>Published</u>
<b>Publication details (reference)</b>				
Simoncelli, S., Thackeray, S. J., & Wain, D. J. (2017). Can small zooplankton mix lakes? <i>Limnology and Oceanography Letters</i> . <a href="https://doi.org/10.1002/lol2.10047">https://doi.org/10.1002/lol2.10047</a>				
<b>Candidate's contribution to the paper (detailed, and also given as a percentage)</b>				
DJW developed the research question and designed the research in conjunction with SJT. SS synthesised the literature on the topic and wrote the paper (100%) with inputs from all the co-authors.				
<b>Statement from Candidate</b>				
This paper reports on original research I conducted during the period of my Higher Degree by Research candidature.				
<b>Signed</b>			<b>Date</b>	13/02/2018

## 2.1 Introduction

Mixing is defined as the combined action of dispersion of dissolved or suspended substances (chemicals or sediment) and enhancement of diffusion of fluid properties, such as heat or salinity (Thorpe, 2007). Mixing in lakes plays an important role because it can affect biological and chemical processes (Fischer et al., 1979). External forces acting on lakes can deliver energy into the water column and can drive different local mixing mechanisms depending on the part of the lake under investigation (*see* Fig. 2.1). The surface layer is the most dynamic and energetic environment; here wind events (A in Fig. 2.1) usually provide most of the kinetic energy, creating shear, and inducing mixing. During storms, intense mixing can also be generated close to the surface via formation and breaking of surface waves (B) or seiche activity (C). Other processes, such as nocturnal convection (D), when the lake surface cools at night, may alter the potential energy of the water column and affect the lake stratification (Jonas et al., 2003). In the littoral zone, mixing can be enhanced when physical processes (E), such as seiches or wind-generated internal waves, interact with lake physical boundaries and generate boundary mixing with a possible impact on nutrient fluxes (MacIntyre et al., 1999).

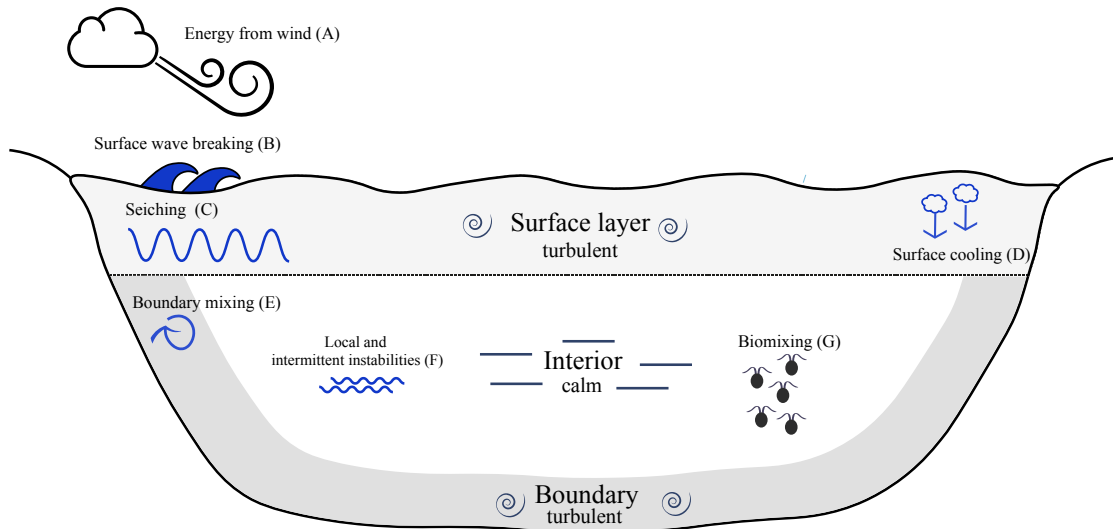


Figure 2.1: Sketch illustrating main mixing processes operating in three different lake regions. In the surface layer, energy from wind (A) leads to mixing by breaking surface waves (B) or via seiching motions (C) or convective mixing can act at night when the surface is cooling (D). Boundaries are subjected to mixing events (E) for example via interactions of internal waves. The lake interior is the calmest region with local and intermittent mixing events (F). Vertical migrators (G) may provide energy for enhancing the mixing in this layer. Eddies indicate layers with mixing, while straight lines in the interior indicate that energy production is extremely weak and sporadic.

The lake interior, below the surface and away from the bottom and shores, responds differently to external forces because of the vertical temperature stratification. The lake interior is the most quiescent part of a lake where mixing events (F in Fig. 2.1) are intermittent and localised processes (Bouffard and Boegman, 2012; Wüest and Lorke, 2003). For this reason, understanding which mechanisms drive interior mixing is of crucial importance for lake ecosystem functioning. Recent research suggests that swimming organisms may operate as a previously neglected mixing mechanism in the interior (Fig. 2.1, G): by creating hydrodynamic disturbances, such as jets or turbulent eddies, organisms may deliver potential energy to the water column, with a significant contribution toward interior mixing. Recent investigations show that the contribution



of horizontal migrators, such as fish, is usually negligible (Gregg and Horne, 2009; Pujiana et al., 2015) and attention should instead be focused on vertically migrating zooplankton.

There is currently insufficient understanding of the role of vertically migrating zooplankton as agents of biomixing: these organisms can swim against the stable density stratification, with potential effects on water column mixing and ecological processes. For example, biomixing from vertical migrators may be able to replenish nutrients in surface-depleted waters and stimulate primary production by phytoplankton. If nutrients are brought to the surface, they can also be redistributed via other surface mixing events (such as wind-driven transport or river inflows) to other regions. Oxygen distribution may be altered as well: biomixing enhancement of oxygen fluxes between the surface and metalimnion could reduce deep-water oxygen depletion, with impacts on habitat quality and biogeochemical cycling. Vertical migrators, once they reach the epilimnion, may still enhance turbulence and mixing in unstratified surface waters. Zooplankton-generated turbulent motions can alter ecological interactions by advecting passive bodies such as algae, and increasing encounter rates between zooplankton grazers and their phytoplankton resources (Harris et al., 2000). Given these under-studied possibilities, it is important to study the ecological significance of biomixing in lakes.

Quantifying biomixing is a complex problem because results depend on several factors such as the organisms under investigation, their swimming mode, their concentration and their interactions with the environment. Direct comparisons between current models in the literature and field measurements is not always possible, because probes are not able to sample what happens near the organism's body while swimming.

In the following, we provide a theoretical framework to understand the fundamental physics of biomixing along with some results from *in situ* ocean observations. We then discuss current studies in lakes and suggest that there is

insufficient evidence about the role of biomixing in freshwater bodies. Field observations are needed to overcome some limitations of current studies, and to verify the potential role of biomixing in lakes.

## 2.2 Measuring biomixing

Mixing in lakes can be generally described through a turbulent kinetic energy (TKE) balance, which in the simplest case reads (Ivey and Imberger, 1991; Osborn, 1980):

$$m = b + \varepsilon \quad (2.1)$$

where  $m$  is the production of TKE,  $b$  is the buoyancy flux accounting for the vertical mixing and  $\varepsilon$  the TKE dissipation rate. External forces, such as wind at the lake surface or eddies generated by swimming organisms in the interior, can provide TKE and contribute to the production term ( $m$ ) in Eq. 2.1. Part of the source energy is inevitably dissipated as heat ( $\varepsilon$ ) by viscous processes acting at the molecular level. However, some energy may be converted into potential energy ( $b$ ) and affect the position of fluid particles. Changes in the potential energy of the water column can partially destroy the stable vertical stratification and lead to mixing (Fig. 2.2). Dissipation rates  $\varepsilon$  can be measured *in situ* through specific devices, such as shear probes or temperature micro-structure profilers, but  $\varepsilon$  does not provide direct information about mixing. When an increase of  $\varepsilon$  is observed, it means that energy ( $m$ ) is transferred in the fluid but mixing may not occur, if no input energy is transferred into the component  $b$ .

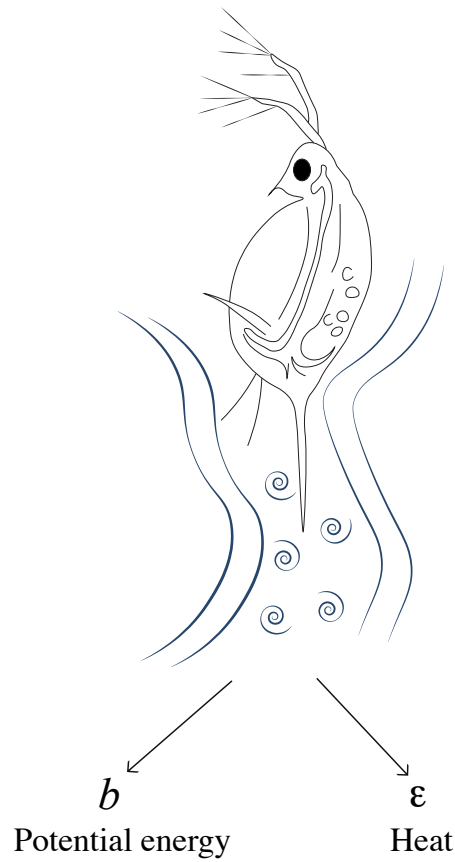


Figure 2.2: Schematic of the partition of turbulent kinetic energy imparted by a swimmer (*Daphnia* spp.). The continuous line depicts the wake left by the swimmer, while the eddies are the turbulent instabilities created within the wake that can be a source of TKE. The source energy is converted into potential energy ( $b$ ), increasing the mixing, and into heat as energy is dissipated ( $\varepsilon$ ) due to water molecular viscosity.

Energy dissipation rates ( $\varepsilon$ ) can however be linked to vertical mixing ( $b$ ) via the vertical eddy diffusion coefficient  $K_V$  (Osborn, 1980):

$$K_V = b/N^2 = \Gamma \cdot \varepsilon/N^2 \quad (2.2)$$

where  $N = [-(g/\rho)\partial\rho/\partial z]^{1/2}$  is the buoyancy frequency describing the vertical

stratification which depends on the gravitational acceleration  $g$ , the water depth  $z$ , the density  $\rho$  and its gradient  $\partial\rho/\partial z$ . The estimation of the eddy diffusion coefficient  $K_V$  is relevant for the quantification of mass vertical fluxes and mixing: when the coefficient is enhanced with respect to background conditions, oxygen or other nutrients can spread in the water column and to different lake layers. The flux  $F_S$  of a substance with concentration  $C_S$  in the lake can be described using Fick's law, once  $K_V$  is known:

$$F_S = K_V \frac{dC_S}{dz} \quad (2.3)$$

For waters stratified by temperature, mixing can be enhanced if  $K_V > D_T$ , where  $D_T = 10^{-7} \text{ m}^2 \text{ s}^{-1}$  is the molecular temperature diffusivity. However, when  $K_V \approx D_T$  dissolved substances will spread very slowly at the molecular level only.

In Eq. 2.2,  $\Gamma$  is a parameter representing the efficiency of the mixing and provides an estimate of how much energy is converted to mixing ( $b$ ) with respect to the dissipated energy  $\varepsilon$ . Laboratory and experimental observations suggest  $\Gamma < 0.2$  (Bouffard and Boegman, 2013; Ivey et al., 2008) for wind-generated turbulence. However, for biogenic mixing the value for is still not known. Several conditions and parameters affect the biomixing process, and thus  $\Gamma$ , such as the species of organisms concerned, their size, concentration, swimming behaviour, and the environmental conditions such as the stratification strength and the background turbulence dissipation level. If swimming organisms do not efficiently mix the water column, creating small water disturbances,  $\Gamma$  would be too small and  $K_V$  does not increase.

Kunze et al. (2006) measured for the first time  $\varepsilon$  generated by the vertical migration of a population of krill (organism's length  $l_{OR} = 1 - 2 \text{ cm}$ ) in Saanich Inlet (Canada). Observed dissipation rates of TKE from biogenic inputs peaked between  $10^{-4}$  and  $10^{-5} \text{ W Kg}^{-1}$ , compared to typical background level of  $10^{-9} \text{ W Kg}^{-1}$ . Dissipation spanned five orders of magnitude, suggesting an impor-

tant krill biomixing contribution as much as mixing from wind and tides. High concentration, and associated multi-body hydrodynamic interactions, probably played an important role, despite weak wind forcing and the strong stratification gradient. The estimated eddy diffusivity from Eq. 2.2, assuming  $\Gamma=0.2$ , ranged between  $2 \cdot 10^{-1}$  and  $2 \cdot 10^{-2} \text{ m}^2 \text{ s}^{-1}$ , an increase of five orders of magnitude when compared to the daily-averaged level. However, elevated TKE rates were observed by Kunze only for a few minutes during the migration, indicating that the source of turbulence is not constant in time, as was later observed by Rousseau et al. (2010). Rippeth et al. (2007) drew the same conclusions and did not observe such important increases in turbulence from their measurements of TKE dissipation rates in stratified coastal waters of the UK.

Other ocean studies estimated dissipation rates  $\varepsilon$  and eddy diffusivity  $K_V$  through laboratory experiments and models. A summary is presented in Table 2.2. These studies show that mixing by krill is not feasible (Rousseau et al., 2010) and only possible with high concentrations (Dean et al., 2016; Kunze et al., 2006) but other vertical migrators, such as copepods or other small zooplankton, may still be able to enhance ocean mixing (Huntley and Zhou, 2004; Katija, 2012). Direct comparisons of dissipation  $\varepsilon$ , between current models in the literature and field measurements, is not always possible because micro-structure profilers, such as the one used by Kunze et al. (2006), are not able to sample turbulence near the organism's body, providing smaller turbulence dissipations than those estimated from models. Finally, the quantification of biomixing, as done by Kunze et al. (2006), must not rely only on the estimation of dissipation rates ( $\varepsilon$ ) and on the assumption that  $\Gamma = 0.2$  (Subramanian, 2010; Visser, 2007a; Visser, 2007b) but must also be based on direct assessment of  $\Gamma$  and  $K_V$  in Eq. 2.2.

Reference	Type of study	Organism (size)	Swimming behaviour	Average $\varepsilon$ (W Kg <sup>-1</sup> )	Mixing
Huntley and Zhou (2004)	Model	Euphausiids-Whales	Aggregated	$10^{-5}$	-
Kunze et al. (2006)	Field (ocean)	Krill (1-2 cm)	Aggregated	$10^{-5} - 10^{-4}$	$K_V = 2 \cdot 10^{-1} - 2 \cdot 10^{-2}$ $\text{m}^2 \text{s}^{-1}$ (with $\Gamma = 0.2$ )
Rippeth et al. (2007)	Field (ocean)	Krill	Aggregated	No enhancement	-
Gregg and Horne (2009)	Field (ocean)	Nekton	School	$10^{-6} - 10^{-5}$	No enhancement
Rousseau et al. (2010)	Field (ocean)	Euphausiids	Aggregated	$< 10^{-8}$	$K_V \sim 10^{-5} \text{ m}^2 \text{ s}^{-1}$ (with $\Gamma = 0.2$ )
Thiffeault and Childress (2010)	Model	Krill	Aggregated	$\sim 10^{-6}$	-
Lorke and Probst (2010)	Field (lake)	Perch	Aggregated	$3 \cdot 10^{-9} - 10^{-8}$	-
Leshansky and Pismen (2010)	Model	Small zooplankton	Aggregated	$2 \cdot 10^{-7}$	-
Kunze (2011)	Model	Small zooplankton	Aggregated	$10^{-9}$ (assumption)	$K_V = 2 \cdot 10^{-7} \text{ m}^2 \text{ s}^{-1}$
Noss and Lorke (2012)	Laboratory	<i>Daphnia magna</i> (4 mm)	Tethered on a filament	$8 \cdot 10^{-7}$ (max: $2 \cdot 10^{-5}$ )	-
			Freely swimming	$2 \cdot 10^{-6}$ (max: $3 \cdot 10^{-4}$ )	$K_V \sim 10^{-5} \text{ m}^2 \text{ s}^{-1}$
Noss and Lorke (2014)	Laboratory	<i>Daphnia magna</i> (3 mm)	Aggregated	-	$K_V \sim 10^{-9} \text{ m}^2 \text{ s}^{-1}$
Wagner et al. (2014)	Model	Small zooplankton	Single organism	-	$\Gamma \sim 0.03$
Dean et al. (2016)	Model	Krill	Aggregated	$10^{-6} - 10^{-7}$ (highest concentration)	$\Gamma \sim 0.03$
Wang and Ardekani (2015)	Model	Small zooplankton	Aggregated	-	$K_V \sim 10^{-6} \text{ m}^2 \text{ s}^{-1}$
Tanaka et al. (2017)	Laboratory	Sardine	Aggregated	$2.3 \cdot 10^{-4}$	$K_V \sim 10^{-2} - 10^{-1} \text{ m}^2 \text{ s}^{-1}$ $\Gamma = 0.02 - 0.08$

Table 2.2: Main biomixing studies in the literature classified by type of study. For the different kind of analysed organisms and swimming behaviours, we reported the main results for generated turbulence and mixing. Grey-shaded rows show the few biomixing observations for freshwater zooplankton.

## 2.3 Biomixing in lakes

Biomixing observations in lakes are very limited. So far, the only experimental biomixing study in a lake was conducted by Lorke and Probst (2010) for perch (*Perca fluviatilis*), while the first investigations of zooplankton-generated mixing were carried out under controlled laboratory conditions for *Daphnia* only. *Daphnia* is a very common zooplanktonic genus in lakes, with body lengths approximately between 1 mm and 3 mm. Organisms within this genus often undertake diel vertical migration (DVM), ascending at dusk toward the food-rich surface layer to forage on phytoplankton, and sinking back at dawn into deeper, aphotic waters (Ringelberg, 1999). DVM is mainly adopted as a predator-avoidance mechanism but other migratory drivers, such as UV exposure or temperature, may play a role (Williamson et al., 2011). Migrations can last anywhere from minutes to a few hours, and their magnitude differs among lakes and between seasons (Ringelberg, 2010).

Noss and Lorke, 2012 conducted the first laboratory study of dissipation rates ( $\varepsilon$ ) of TKE produced by *Daphnia*. By using a particle image velocimetry (PIV) technique combined with laser-induced fluorescence, they could estimate some energetic parameters of the planktonic organism swimming in different configurations with a density gradient typical of the thermocline ( $N = 0.07 \text{ s}^{-1}$ ). TKE dissipation rates ( $\varepsilon$ ) and diffusion coefficients ( $K_V$ ) were estimated considering the water volume influenced by the organism while swimming, which is usually larger than the organism size. Estimated average dissipation was  $2 \cdot 10^{-6} \text{ W kg}^{-1}$  with a maximum of  $3 \cdot 10^{-4} \text{ W kg}^{-1}$  in accordance with results from Huntley and Zhou (2004)'s model. Eddy diffusivity was enhanced in the organism vicinity ( $K_V \sim 10^{-5} \text{ m}^2 \text{ s}^{-1}$ ) and was two orders of magnitude bigger than the molecular heat diffusivity ( $D_T \sim 10^{-7} \text{ m}^2 \text{ s}^{-1}$ ), indicating the potential for an impact on temperature gradients in lakes. However, during the experiment,  $K_V$  was not measured in the whole tank, therefore it is not certain whether the zooplankton could have affected mixing on scales larger than the organism size. Moreover,

the impact of the restratification was not evaluated and no conclusion can be drawn about the mixing efficiency  $\Gamma$ .

Later Noss and Lorke (2014) studied the same organism in different swimming configurations and quantified mixing via the diffusion of a fluorescent dye (Rhodamine 6G) injected into a stratified water tank ( $N = 0.08 \text{ s}^{-1}$ ). *Daphnia* (max. concentration  $\sim 4 \text{ org. L}^{-1}$ ) were forced to vertically migrate generating a global diffusivity in the tank as low as  $10^{-9} \text{ m}^2 \text{ s}^{-1}$ . Even when swimming in aggregations, *Daphnia* had a small impact on dissolved substances or gases, whose molecular diffusivity  $D_G$  is  $10^{-10} \text{ m}^2 \text{ s}^{-1}$ . This result differs however from the previous study, because it provides the diffusion coefficient affected at larger scales, while Noss and Lorke (2012) measured the diffusivity in the near vicinity of a single organism only. For *Daphnia*, at organism-scale dissipation  $\varepsilon$  and mixing can be enhanced, but when  $K_V$  is assessed over the effective and larger volume influenced by *Daphnia* migration, the impact on mixing is negligible if compared to wind-induced mixing. To affect temperature stratification in lakes, *Daphnia* aggregation must be able to increase  $K_V$  above  $D_T = 10^{-7} \text{ m}^2 \text{ s}^{-1}$ .

Wilhelmus and Dabiri (2014) later performed another laboratory experiment in an unstratified tank to analyse the fluid instabilities and mixing induced by *Artemia salina*, a small zooplanktonic species ( $l_{OR} = 5 \text{ mm}$ ) that lives in saline lakes. During the vertical migration, induced artificially with a laser, collective swimming dynamics from different organisms created a large downward jet. The length of the generated eddies near its boundary was considerably larger ( $l \sim 1 \text{ cm}$ ) than a single organism. Their measurements clearly show that swimmers, when present at high concentration, can deliver kinetic energy at scales bigger than the single organism's length with a possible impact on mixing. However, the lack of a stable stratification did not allow the estimation of the real migration effect on mixing after buoyancy restores the initial density gradient: displaced water parcels and properties can return to their initial position with no effect on mixing if swimmers are not sufficiently efficient.



Physics-based models can also be used to evaluate biogenic mixing for lakes. Kunze (2011) estimated the eddy diffusivity coefficient from simple physical considerations and by assuming that each organism can transport a water volume comparable to its size as it swims in a dense aggregation. Kunze (2011) found that the apparent diffusivity depends on the organism concentration  $C$  and for *Daphnia* with  $C = 100 \text{ org. L}^{-1}$ , the resulting diffusivity is  $K_V = 1.7 \cdot 10^{-7} \text{ m}^2 \text{ s}^{-1}$ , suggesting a negligible enhancement in mixing. More importantly, the model does not consider any restratification effect and is not suitable for small zooplankton, such as for *Daphnia*, because it assumes that the organism Reynolds number  $Re = U \cdot l_{OR}/\nu < 1$ , where  $U$  is the organism's speed and  $\nu$  the kinematic water viscosity.

Laboratory experiments show that  $Re \sim 30 - 80$  for *Daphnia* (Noss and Lorke, 2014; Wickramarathna et al., 2014). Furthermore, inertial forces neglected by the model, can further enhance mixing (Noss and Lorke, 2014). Another simple and similar approach was previously proposed by Leshansky and Pismen (2010). In their model, swimmers can disperse the turbulent local flow as a function of the school concentration  $C$ , the turbulent dissipation  $\varepsilon$ , the size  $l$  of the produced hydrodynamic instabilities, and speed  $U$ . By assuming that for a *Daphnia* swarm,  $C = 100 \text{ org. L}^{-1}$ ,  $\varepsilon = 10^{-9} \text{ W kg}^{-1}$ ,  $U = 30 \text{ mm s}^{-1}$  and  $l = l_{OR} = 1 \text{ mm}$  (Gries et al., 1999; Wickramarathna et al., 2014), the diffusion coefficient is  $4 \cdot 10^{-7} \text{ m}^2 \text{ s}^{-1}$ . Diffusivity increases to  $K_V = 10^{-5} \text{ m}^2 \text{ s}^{-1}$  when  $C = 10,000 \text{ org. L}^{-1}$ . Estimated coefficients from these models provide a lower bound of mixing and generally suggest that zooplankton may not be able to alter vertical temperature stratification, since  $K_V \approx D_T$ .

Wagner et al. (2014) provided instead an estimation of mixing in terms of its efficiency  $\Gamma$  (Eq. 2.2). In their model, each organism is considered very small and swimming in a stable stratified fluid. For a single vertically migrating zooplankton  $\Gamma \sim 0.03$ , but it may achieve unity depending on the organism's length, swimming mode, and stratification. The model suggests that biomixing seems a feasible mechanism but does not provide any information about the eddy diffu-

sion coefficient  $K_V$ . Moreover, the model is more suitable for micro-organisms and does not consider any influence of the zooplankton packaging density  $C$ , which may be the main boosting factor for the mixing.

Finally, Wang and Ardekani (2015) numerically resolved the flow field influenced by an aggregation of interacting swimmers in a stratified medium in the intermediate Reynolds number regime. The model is particularly suitable to model small zooplankton and provide a complete description of biomixing. Simulations were performed with a small number of swimmers and aggregations corresponding to very high densities of  $C = 10,000 \text{ org. L}^{-1}$  to provide an upper-bound for mixing. In particular, organism swimming behaviour was modelled as a "squirmers" (Blake, 1971; Lighthill, 1952) and controlled by a parameter  $\beta$  which scales with the organism's size  $l_{OR}$ , velocity  $U$  and fluid generated vorticity; for *Daphnia*  $\beta = 1$  (Wickramarathna, 2016; Wickramarathna et al., 2014). From this model, the estimated mixing efficiency  $\Gamma$  for *Daphnia* was 0.01, and eddy diffusivity  $K_V$  is as low as  $2 \cdot 10^{-7} \text{ m}^2 \text{ s}^{-1}$  but for a very strong density stratification with  $N = 1.9 \text{ s}^{-1}$ . However, for a weaker but more realistic stratification, the numerical model by Wang and Ardekani (2015) showed that swimmers were less efficient ( $\Gamma = 3 \cdot 10^{-4}$ ) but generate a higher diffusivity, with  $K_V = 10^{-6} \text{ m}^2 \text{ s}^{-1}$ . Change of swimming trajectories, vertical orientation as well as organism buoyancy can further enhance these values (Wang and Ardekani, 2015).

## 2.4 The need for field studies

Biomixing studies for oceans cannot be used to draw conclusions for lakes because oceans are physico-chemically different to freshwater bodies, and because marine planktonic organisms are more diverse and potentially larger than their freshwater counterparts (Hessen and Kaartvedt, 2014), and biomixing is an organism-dependent mechanism. The few studies in the literature for freshwater

zooplankton collectively yield differing conclusions about the role of biomixing (Fig. 2.3). Numerical simulations by Wang and Ardekani (2015) show that biomixing by *Daphnia* is a feasible process when the zooplankton concentration is as high as  $C = 10,000 \text{ org. L}^{-1}$ . On the other hand, the experimental study by Noss and Lorke (2014) suggests that mixing is negligible with a smaller concentration of organisms from the same genus ( $4 \text{ org. L}^{-1}$ ). In the two studies  $K_V$  varies by three orders of magnitude, while the concentration  $C$  covers four orders of magnitude. Zooplankton abundance depends on both biotic and abiotic environmental conditions; their density in lakes can vary greatly and can be substantially higher than that used in the experiment by Noss and Lorke (2014), especially during the DVM (George and Hewitt, 1999; Hembre and Megard, 2003; Straile and Adrian, 2000; Talling, 2003).

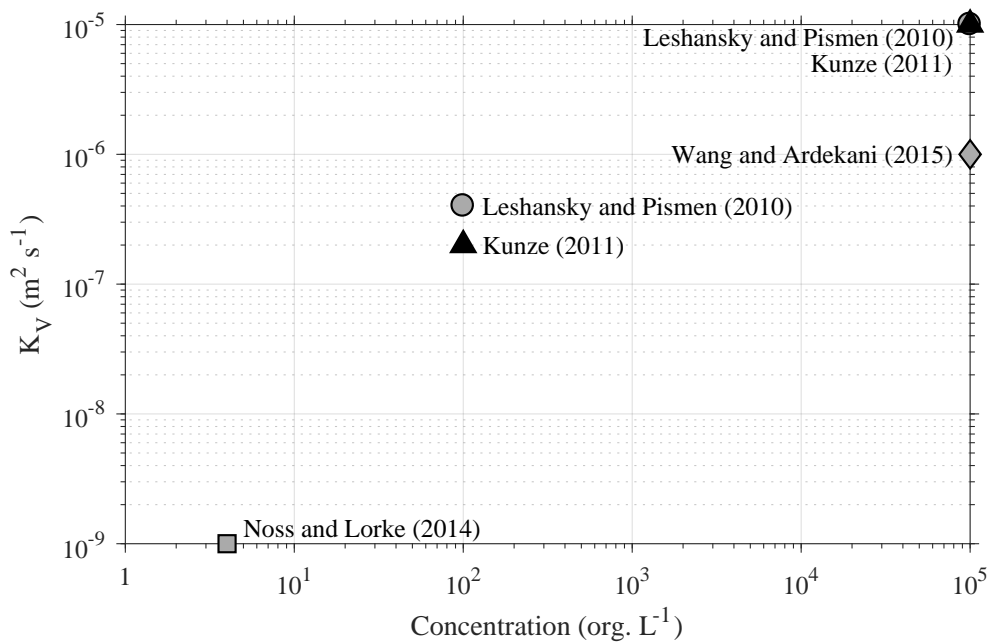


Figure 2.3: Eddy diffusivity  $K_V$  as a function of zooplankton concentration  $C$  from numerical simulations and laboratory experiments. Each study is represented with a different symbol and colour.

Zooplankton aggregation density is important and may have emergent effects on biomixing: higher concentrations can enable interactions of wakes originating from single organisms and enhance shear and mixing in the same fashion as observed by Wilhelmus and Dabiri (2014). The form of the relationship between zooplankton density and biomixing is currently not known e.g., there may be a concentration threshold over which biomixing is enhanced. In addition, numerical simulations currently simplify taxonomic variability in biomixing potential e.g., Kunze (2011) and Wang and Ardekani (2015) describe all the zooplanktonic species with general models, while in reality zooplankton species swim in different ways, and species-specific models may be more suitable to model *Daphnia* and to describe their particular swimming behaviour (Jiang and Kiørboe, 2011). These interactions, taking place in a real environment, between individuals from multiple species may be stochastic and challenging to describe mathematically. However, community-level effects may be observable in the field.

Field observations are needed to understand the feasibility of biomixing by freshwater zooplankton communities generally, and *Daphnia* specifically, for several reasons. With field studies, it is possible to overcome limitations arising from laboratory experiments under controlled conditions. In the laboratory, diel vertical migration cycles are artificially simulated by alternating light and dark periods with LED panels or using laser beams with a constant intensity. These methods trigger the zooplankton primary phototaxis, which is the movement toward or away from a light beam. *Daphnia* DVM in the field is instead triggered by the secondary phototactic behaviour, which is the reaction due to the rate of change in light intensity, usually peaking at dusk and sunrise only (Ringelberg, 1999; 2010). These two different behavioural responses also explain why the DVM does not occur during the day or at night and therefore zooplankton responses in lab tanks may be very different from those in the field. Without field observation, it is not known whether the difference in the DVM trigger can affect *Daphnia* swimming responses and, thus, biomixing. Moreover, it is not

certain how laser beams, used to fluoresce the fluid in the tank, impact upon zooplankton migration behaviour. The use of artificial light, generated by LEDs in Noss and Lorke (2014) to trigger the migration, may explain why only 16% of the organisms into the tank moved and why some of them remained at the tank top or bottom. Field sampling allows the study of organisms in their natural environment without altering the behaviour, potentially increasing the realism of biomixing estimates. Field studies also allow understanding the zooplankton concentration during the DVM, compared to the daily zooplankton densities in the lake. Finally, lakes are populated by variable abundances of zooplanktonic species (species of *Daphnia*, *Bosmina*, *Cyclops*, etc.) and other migrators that can interact with *Daphnia*. Other species can affect *Daphnia* density and force them to frequently change their swimming direction in the migrating layer, which could affect the vertical mixing. Such species interactions cannot be easily reproduced in lab experiments, and they may be difficult to address numerically with models. However, field studies would allow us to construct empirical relationships between abundance and biomixing for communities of different compositions, against which to test developing theoretical expectations.

Migration frequently acts as an avoidance mechanism from visual predators such as larval or juvenile fish (De Robertis, 2002; Ringelberg, 1999; Waya, 2004). The presence of chemical substances released by predators, such as kairomones, and sensed by zooplankton, affect DVM leading to increased migration amplitude or faster swimming reactions (Dodson et al., 1997a; Loose and Dawidowicz, 1994; Ringelberg, 1999; 2010). These behavioural responses can increase the size of the generated instabilities and may increase the vertical diffusion  $K_V$ . Moreover, food in lab experiments is usually absent and its availability in real lakes, such as a surface or deep chlorophyll maxima, may be another key factor affecting migration amplitude (Dodson et al., 1997a; Ringelberg, 1999; Rinke et al., 2007). Tank size, light distribution, temperature, and other features of the environment can also change the swimming behaviour and limit the swimming reaction (Buchanan et al., 1982; Dodson et al., 1997a). Field studies are needed

to confirm whether results from experiments under simplified conditions and numerical models are applicable to biomixing mechanisms in complex natural environments. Only field measurements can tell us which lakes are, and are not, prone to such effects so that we can make generalisations about the importance of biomixing.

## 2.5 Challenges for future field investigations

Field investigation should be performed on vertical migrators during the DVM of zooplankton. *Daphnia* are a good candidate to develop our understanding of freshwater biomixing because (1) they are a very common and abundant migrating species in lakes. (2) Despite their smaller size, dissipation rates of kinetic energy are higher for *Daphnia* compared to theoretical estimates for other zooplanktonic species due to their unique swimming mode (Wickramarathna et al., 2014). (3) Finally, they have been studied in the lab, therefore field studies can be used to validate numerical models and compare experimental results under very controlled conditions.

In particular, the DVM can be directly studied both through zooplankton collection and analysis and indirectly via acoustic devices such as ADCPs or echo sounders, allowing a higher spatial and temporal resolution (Huber et al., 2011; Lorke et al., 2004; Rinke et al., 2007). These instruments are usually employed to measure current velocities in three dimensions and to infer turbulence levels as well. The backscatter strength (BS) or amplitude of the scattered wave provided by ADCPs can be used as a proxy for the zooplanktonic concentration and to estimate zooplankton velocities. Higher values of BS indicate higher zooplankton abundance while lower values usually indicate a lack of scatterers in the water. Recent studies by Huber et al. (2011) and Lorke et al. (2004) suggest that ADCPs can be calibrated against the zooplankton concentrations estimated by more traditional means, allowing continuous estimation of their abundance in

the water column. However, these devices do not directly provide any information about the zooplankton abundance, size or taxonomy, but they can be used to track their displacement, to understand the timing of the migration and the part of the water column they inhabit during the day.

A first step in assessing biomixing in the field is to measure TKE dissipation rates  $\varepsilon$ . Generated turbulence during the DVM in lakes can be measured with microstructure profilers which are nowadays normally employed in sampling TKE dissipation rates. In particular, turbulence should be sampled before and after the DVM, to characterise the background turbulence condition without migrators, and during the zooplankton ascent. The duration of observations depends on the time scale of biomixing and measurements should continue for the whole migration duration to understand whether turbulence is patchy and short-lived or energy production by zooplankton is a regular process. Vertical migrators usually swim unsteadily (Noss and Lorke, 2012) but asynchronous motions of organisms in the migrating layer may lead to quasi-stationary conditions of turbulence production. If turbulence is enhanced during the migration, this is an indication that energy is generated by zooplankton but, alone, this is not a sufficient proof of biologically-generated mixing. Available energy ( $m$  in Eq. 2.1) can be dissipated as heat with no changes in the potential energy  $b$ . However, if no turbulence is observed, zooplankton DVM is not a feasible mechanism for mixing water. Eddy diffusivity  $K_V$  can also be inferred from turbulence measurements by using parametrisation of Eq. 2.2, but attention must be paid to the models used because the underlying hypotheses of the mixing parametrisations may not be applicable to biomixing.

If turbulence is generated during the DVM, the next natural step would be to directly measure mixing efficiency  $\Gamma$  or eddy diffusivity  $K_V$  via tracer injections (Goudsmit et al., 1997; Wain et al., 2013; Wüest et al., 1996) to measure the effect of the DVM on the eddy diffusivity  $K_V$ . This assessment should rely on measurements and comparison of diffusion before and during the DVM. The duration of tracer sampling should continue until after the migration is com-

pleted, and longer than the dissipation measurements. This allows understanding of how tracer diffusion is affected over longer time scales, when stratification restores the initial water column density structure affected by the zooplankton migration.

Attempts to study biomixing in the field can however pose important challenges. For example, zooplankton may avoid plankton nets (Brinton, 1967; Harris et al., 2000) but disturbance can be limited by using nets with mouth-reducing cones or by reducing the towing speed (Unesco, 1968). The same avoidance mechanisms might be adopted toward free-falling probes (Benoit-Bird et al., 2010; Ross, 2014) however, probes are usually designed to avoid any forward disturbances while sampling turbulence. Moreover, turbulence probes may not be able to resolve turbulence produced by a single organism: generated fluid structures from a single individual are generally smaller than the instrument spatial resolution or the turbulence signal may be contaminated by noise.

Zooplankton spatial heterogeneity is another important issue relevant to the role of biomixing in the field. If biologically generated mixing is sampled in the field, results of the measurements may depend on the chosen location within the lake interior because of horizontal zooplankton patchiness (Blukacz et al., 2009; Thackeray et al., 2004). Turbulence profile collection should therefore be coupled with ADCP measurements to continuously measure zooplankton concentration. ADCPs with multiple beams, bottom-mounted in different lake locations, or surveys with a boat-mounted ADCP, allow understanding of vertical and horizontal variations in abundance in the migrating layer and during the DVM. Vertical distribution before DVM and also horizontal patchiness and temporal variation in zooplankton concentration in the migrating layer are relevant to the spatio-temporal dynamics of biomixing. These dynamics can only be observed in the natural environment.



## 2.6 Conclusions

In this paper, we presented an overview of existing studies of turbulence and mixing generated by small zooplankton in lakes. Lake research currently yields mixed conclusions about the feasibility of biomixing, generally showing that small zooplankton can generate turbulence but different levels of mixing depending on the type of study and on the zooplankton abundance. Field studies are needed to overcome limitations arising from lab studies and to confirm the importance of biomixing in complex natural environments such as lakes, and without altering the behaviour of the animals generating the biomixing under study.

Chapter **3**

# **On biogenic turbulence production and mixing from vertically migrating zooplankton in lakes**

S. Simoncelli<sup>1</sup>, S. J. Thackeray<sup>2</sup> and D. J. Wain<sup>1</sup>

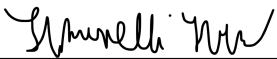
<sup>1</sup> Department of Architecture and Civil Engineering, University of Bath

<sup>2</sup> Centre for Ecology & Hydrology, Lancaster Environment Centre

## Abstract

**V**ERTICAL mixing in lakes is a key driver of transport of ecologically important dissolved constituents, such as oxygen and nutrients. In this study we focus our attention on biomixing, which refers to the contribution of living organisms towards the turbulence and mixing of oceans and lakes. While several studies of biomixing in the ocean have been conducted, for freshwater zooplankton, no *in situ* studies exist that assess the turbulence induced by zooplanktonic organisms under real environmental conditions. Here, turbulence is sampled during three different sampling days during the sunset diel vertical migration (DVM) of *Daphnia* spp. in a small man-made lake. This common genus may create hydrodynamic disturbances in the lake interior where thermal stratification usually suppresses vertical diffusion. Concurrent biological sampling assessed the zooplankton vertical concentration profile. An acoustic-Doppler current profiler was also used to track zooplankton concentration and migration via the backscatter strength. Our datasets do not show biologically-enhanced dissipation rates of temperature variance and turbulent kinetic energy in the lake interior, despite *Daphnia* concentrations as high as 60 org. L<sup>-1</sup>. No large and significant turbulent patches were created within the migrating layer to generate irreversible mixing. This suggests that *Daphnia* do not affect the mixing in the lake at the organism concentrations observed here.

## Statement of Authorship

<b>This declaration concerns the article entitled</b>				
On biogenic turbulence production and mixing from vertically migrating zooplankton in lakes				
<b>Authors</b>				
Simoncelli, S. (SS), Thackeray, S. J. (SJT) and Wain, D. J. (DJW)				
<b>Publication status (tick one)</b>				
Draft manuscript	Submitted	<input checked="" type="checkbox"/> <u>In review</u>	Accepted	Published
<b>Publication details (reference)</b>				
Aquatic Sciences				
<b>Candidate's contribution to the paper (detailed, and also given as a percentage)</b>				
Designed the experiments: DJW, SJT, SS (75%).				
Performed the experiments: DJW, SS (90%).				
Analysed the data: SS (100%).				
Wrote the paper: SS.				
Editorial support in writing the manuscript: DJW, SJT				
Interpretation of the results: DJW, SJT, SS (80%).				
<b>Statement from Candidate</b>				
This paper reports on original research I conducted during the period of my Higher Degree by Research candidature.				
<b>Signed</b>			<b>Date</b>	13/02/2018

## List of symbols

- $a$  Particle or zooplankton radius in acoustic measurements (m)
- $b$  Buoyancy flux of turbulent kinetic energy, ( $\text{W kg}^{-1}$ )
- $C_g$  Concentration of zooplankton group  $g$ , ( $\text{org. L}^{-1}$ )
- $C_{Daphnia}$  Concentration of *Daphnia* group, ( $\text{org. L}^{-1}$ )
- $\chi_T$  Dissipation rate of temperature variance, ( $\text{K}^2 \text{s}^{-1}$ )
- $d$  Diameter of zooplankton net mouth, (m)
- $D_G$  Gas molecular diffusivity, ( $\text{m}^2 \text{s}^{-1}$ )
- $D_T$  Molecular diffusivity of heat, ( $\text{m}^2 \text{s}^{-1}$ )
- $\varepsilon$  Dissipation rate of turbulent kinetic energy, ( $\text{W kg}^{-1}$ )
- $g$  Gravitational acceleration, ( $\text{m s}^{-2}$ )
- $\Gamma$  Coefficient of mixing efficiency, (-)
- $h$  Thickness of sampling layer in zooplankton collection, (m)
- $k_0$  Regression intercept of ADCP calibration, (-)
- $k_1$  Regression slope of ADCP calibration for *Daphnia* group, ( $\text{L org.}^{-1}$ )
- $k_g$  Regression slope of ADCP calibration for zooplankton group  $g$ , ( $\text{L org.}^{-1}$ )
- $K_V$  Vertical eddy diffusivity, ( $\text{m}^2 \text{s}^{-1}$ )
- $\lambda$  Acoustic wavelength (m)
- $l$  Length scale of fluid instability, (m)
- $l_O$  Organism's length, (m)
- $L_P$  Segment length in patch analysis (m)
- $L_T$  Thorpe scale (m)
- $L_{Tmax}$  Maximum Thorpe scale (m)

$m$  Production of turbulent kinetic energy, ( $W\text{ kg}^{-1}$ )

$N$  Buoyancy frequency, ( $s^{-1}$ )

$p$   $p$  value in regression analysis, (-)

$R^2$  Coefficient of determination in regression analysis, (-)

$R_f$  Flux Richardson number, (-)

$\rho$  Water density, ( $kg\text{ m}^{-3}$ )

$V$  Filtered volume from zooplankton net, ( $m^3$ )

$VBS$  Volume backscatter strength from ADCP, (dB)

$VBS_{linear}$  Linear volume backscatter strength, (-)

### 3.1 Introduction

The role of swimming organisms in enhancing turbulence and mixing in stratified water bodies is still uncertain. Experiments, observational studies, and numerical simulations have tried to determine whether biogenic turbulence may be an underrepresented source of energy in oceans and lakes, in particular when compared to other mechanisms, such as winds and tides (Dewar et al., 2006; Gregg and Horne, 2009; Katija, 2012; Kunze et al., 2006). Of particular relevance to lakes is the question of whether migrations of small zooplankton can elevate turbulence relative to the generally quiescent levels typically observed in the lake interior. While migrations of smaller zooplankton in ocean environments have shown negligible increases compared to the higher background turbulence levels in the ocean (Dean et al., 2016; Rousseau et al., 2010), recent lab (Wilhelmus and Dabiri, 2014) and numerical (Wang and Ardekani, 2015) studies indicate that aggregations of small zooplankton at sufficient concentrations can elevate turbulence and mixing through interactions between the swimmers.

Biologically-generated turbulence and mixing can be qualitatively described considering the turbulent kinetic energy (TKE) budget, which for steady state and spatially homogenous conditions, reads (Ivey and Imberger, 1991):

$$m = b + \varepsilon \quad (3.1)$$

where  $m$  is the production term of TKE,  $b$  the buoyancy flux which accounts for changes in the potential energy field, and  $\varepsilon$  is the rate at which energy is lost from the fluid due to water viscosity. Swimming organisms, by moving their appendages, can create hydrodynamic instabilities and energetic eddies (see Fig. 3.1a), usually comparable with the organism's size, and supply TKE ( $m$ ) to the fluid (Huntley and Zhou, 2004). This additional energy  $m$  can either be converted into potential energy ( $b$ ) to achieve mixing or be dissipated and

lost as heat via  $\varepsilon$ . This energy-conversion process from  $m$  to  $b$  is efficient and can lead to substantial mixing, as long as the size of the biologically-generated instabilities are sufficiently large and energy is constantly added to the fluid.

Eq. 3.1 can also be re-arranged to explain mixing in terms of eddy diffusivity  $K_V$ . Using the generalised flux Richardson number  $R_f = b/m$  and a flux-gradient relationship yields (Ivey and Imberger, 1991):

$$K_V = \frac{R_f}{1 - R_f} \frac{\varepsilon}{N^2} = \Gamma \frac{\varepsilon}{N^2} \quad (3.2)$$

where  $N = -[(g/\rho)\partial\rho/\partial z]^{1/2}$  is the buoyancy frequency depending on the gravitational acceleration  $g$  and the density  $\rho$ . In Eq. 3.2,  $\Gamma$  describes how efficient the energy-conversion process is. Osborn (1980) suggested that  $\Gamma$  reaches the maximum of 0.2 for shear-generated turbulence, however, the value for bioturbulence is currently unknown. Visser (2007b) argued that  $\Gamma$  scales as  $(l/L_{OZ})^{4/3}$  within the biosphere, where  $l$  is the scale of the biologically-generated overturn and  $L_{OZ} = (\varepsilon/N^3)^{1/2}$  the Ozmidov length scale. For example, for krill, no important mixing can occur because  $\Gamma \approx 10^{-4} - 10^{-2}$  (Kunze, 2011; Rousseau et al., 2010; Visser, 2007b). On the other hand, for a small freshwater zooplanktonic organism ( $l \approx 1$  mm),  $\Gamma$  can range between  $10^{-3}$  and  $10^{-1}$  depending on the stratification and turbulence conditions (Visser, 2007b). Moreover, zooplankton aggregations can create larger hydrodynamic disturbances via collective or synchronised motions which may increase the effective value of  $l$  by a few orders of magnitude (Noss and Lorke, 2014). For waters stratified by temperature, the vertical eddy diffusivity  $K_V$  can typically range between  $10^{-7}$  and  $10^{-3}$  m<sup>2</sup> s<sup>-1</sup>. When  $K_V > D_T$ , where  $D_T \approx 10^{-7}$  m<sup>2</sup> s<sup>-1</sup> is the molecular temperature diffusivity, turbulence can efficiently mix the water column. However, when  $K_V = D_T$ , heat will spread slowly at the molecular level only.

The first observations of biogenic turbulence from migrators were made by Kunze et al. (2006), who measured enhanced turbulent dissipation rates ( $\varepsilon$ ) be-



tween  $10^{-5}$  and  $10^{-4}$   $\text{W Kg}^{-1}$  during krill vertical migration in a Canadian inlet. Maximum diffusivities  $K_V$  reached  $10^{-2}$   $\text{m}^2 \text{s}^{-1}$ , as large as those from winds and tides, but assuming  $\Gamma = 0.2$ . Dissipation rates agreed with those found in the model by Huntley and Zhou (2004) that suggests that biosphere can deliver a significant amount of mechanical energy regardless of the species. Later measurements by Rippeth et al. (2007), however, did not show such dramatic dissipation rates in a different coastal environment, suggesting that measurements may be limited to that particular coastal system. Numerical simulations by Dean et al. (2016) suggest that TKE enhancements observed by Kunze et al. (2006) are only possible with very high krill density above  $10 \text{ org. L}^{-1}$ . Later measurements by Rousseau et al. (2010) concluded and supported the hypothesis that biologically-generated turbulence from krill vertical migration is an intermittent mechanism and no mixing can occur.

Other studies focused on small but more abundant zooplankton. Noss and Lorke (2014) performed a laboratory experiment in a stratified tank on the mixing induced by the vertical motion of *Daphnia magna*. For this species, they found that vertical mixing is not enhanced; the observed vertical eddy diffusivity was as low as  $10^{-9}$   $\text{m}^2 \text{s}^{-1}$ , an order of magnitude smaller than the diffusivity of the stratifying agent. Despite *Daphnia* being able to generate turbulence as high as  $10^{-5}$   $\text{W Kg}^{-1}$  in their turbulent wake (Noss and Lorke, 2012; Wickramarathna et al., 2014), no mixing occurred because  $\Gamma$  was too small (Eq. 3.2). However, the result may depend on the organisms' concentration and how the migration was triggered in artificial laboratory conditions (Simoncelli et al., 2017). Experimental measurements in an unstratified tank by Wilhelmus and Dabiri (2014) indicate instead that collective motions, arising from small zooplankton swimming at high concentration, can trigger fluid instabilities bigger than the size of the individual organism and may enhance mixing. Nevertheless density stratification was not included in the experiment and so no final conclusions can be drawn about the efficiency of the mixing. Very recent numerical simulations by Wang and Ardekani (2015), in the intermediate Reynolds number regime, show that

millimetre-sized organisms swimming with collective motions, can enhance  $K_V$  up to  $10^{-6} \text{ m}^2 \text{ s}^{-1}$  but at a high concentration of zooplankton. Heat and gas fluxes can still be affected by biomixing, as the molecular diffusivity of heat  $D_T \approx 10^{-7} \text{ m}^2 \text{ s}^{-1}$  and gases  $D_G \approx 10^{-9} \text{ m}^2 \text{ s}^{-1}$  are smaller than the enhanced  $K_V$ . A simple model by Leshansky and Pismen (2010) reported instead a smaller diffusivity of  $10^{-7} \text{ m}^2 \text{ s}^{-1}$ , with no enhancement of heat diffusion.

Other studies in the ocean and lakes suggest instead that mixing by bacteria or micro-zooplankton is feasible under certain conditions. At very high concentrations, small organisms can enhance vertical mixing via creation of convective cells (Kils, 1993; Sommer et al., 2017) rather than via turbulent wake formation from the moving appendages. This mechanism, however, does not seem to govern TKE energy production for high abundances of meso-zooplankton, such as *Daphnia*, where energy can be supplied via Kelvin-Helmholtz instabilities (Wilhelmus and Dabiri, 2014).

A full review of previous studies of small zooplankton can be found in Simoncelli et al. (2017). To date, observational studies on zooplankton biomixing have been limited to oceanic species only and no field studies exist on the turbulence production and mixing due to small zooplankton in freshwaters. We present a field study of turbulence measurements during the vertical migration (DVM) of small zooplankton in the interior of a small lake, where the community is dominated by *Daphnia* spp. This genus frequently engages in a DVM at sunset, with many organisms crossing the thermocline, despite the density stratification. During the ascent phase, they may create interacting wake or jet structures (see Fig. 3.1a) and large scale motions, and add mechanical energy in the quiescent part of the lake, away from the boundaries, where the thermal stratification usually suppresses turbulence and vertical diffusion (Wüest and Lorke, 2003). Temperature instabilities and turbulence were sampled before and during the DVM under calm conditions to isolate the biologically-generated temperature perturbations from those originating from other processes such as the wind. Measurements can be used to infer the zooplankton contribution towards

interior mixing and the likely ecological importance in lake ecosystems.

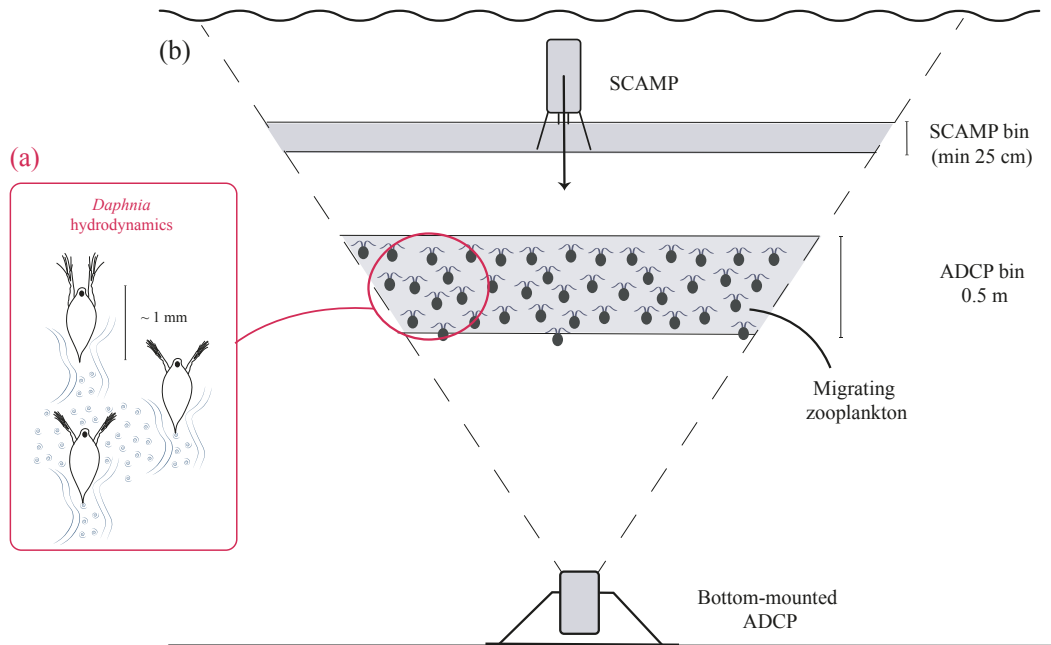


Figure 3.1: Panel a shows a schematic of swimming *Daphnia* and their interacting turbulent wakes (continuous lines). The eddies show the turbulent instabilities created within the wake that can be a source of TKE. Panel b shows the experimental setup. The dashed lines show the acoustic cone of the ADCP, while the gray trapezoids indicate the segments sizes for acoustic and microstructure measurements.

## 3.2 Materials and Methods

### 3.2.1 Study site

Measurements were carried out on three different days during the summer stratification period (21 July, 28 July and 18 August 2016) in Vobster Quay, a shallow man-made lake situated in Radstock, UK (Fig. 3.2). The lake, with an average

depth of 15 m and maximum depth of 40 m, is wind-sheltered with a fetch of approximately 500 m. It was originally created by filling a decommissioned quarry, so has very steep sloping boundaries and a flat bottom, providing a very simple bathymetry ideal for this study. It is fed by rainfall and infiltration of cold groundwater on the northwest side during heavy rainfall events. The lake stratifies from early May until late August with a maximum surface temperature of 22 °C and a bottom temperature between 9 °C and 12°C. Fig. 3.3 shows the temperature profiles for the three sampling dates as well as the buoyancy frequency. The metalimnion usually extends from 5 m to 17 m. The water had an average Secchi depth of 10 m over the summer. The lake was chosen because of its simple shape, small wind fetch, and the lack of topographic features or boundary effects which might affect mixing during the measurement campaign.

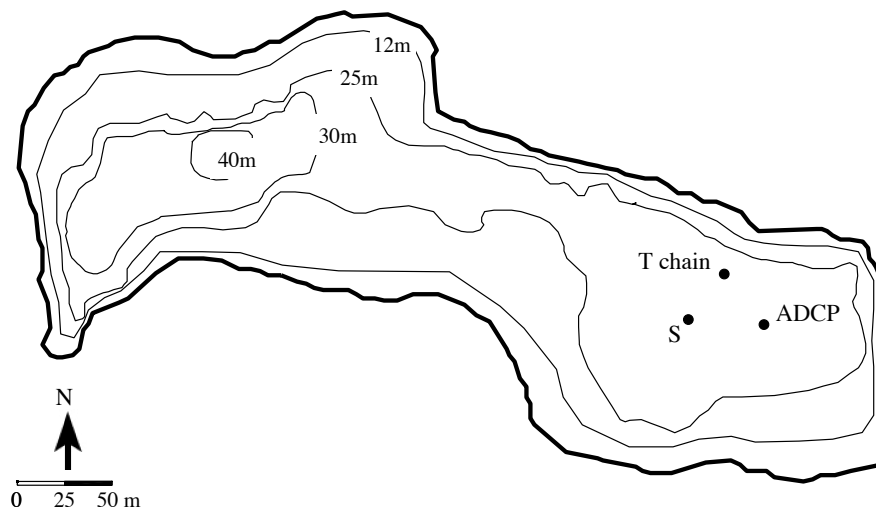


Figure 3.2: Geometry and bathymetry of Vobster Quay. "S" denotes the sampling station where microstructure and zooplankton measurements were taken. The locations of the thermistor chain (T chain) and ADCP are also shown.

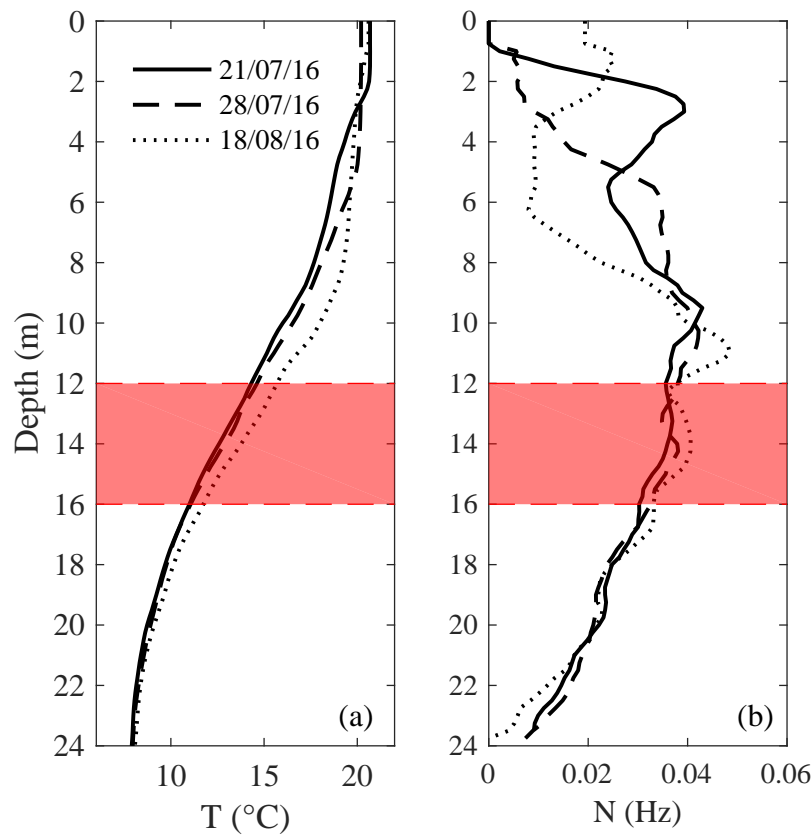


Figure 3.3: Conditions before the DVM for the three different sampling dates: (a) average temperature profile from SCAMP data, and (b) buoyancy frequency. The red band shows the average depth range inhabited by zooplankton during the day, just below the depth of maximum buoyancy.

### 3.2.2 Zooplankton abundance

In order to gather data on crustacean zooplankton population density and vertical distribution, zooplankton samples were collected using a conical net (HydroBios) mounted on a stainless-steel hoop with a cowl cone (mesh=100  $\mu\text{m}$ , diameter  $d=100$  mm, length approximately 50 cm). Samples were collected within con-

secutive strata of thickness  $h=3$  m, from the surface up to 24 m, in daytime. Three samples ( $n = 3$ ) were collected and pooled for each stratum. Samples were collected before the DVM at location S (Fig. 3.2) and were stored in a 70% ethanol solution to fix and preserve the organisms (Black and Dodson, 2003). Sample collection from the entire water column took about 80 minutes. Zooplankton were enumerated by counting the organisms under a dissecting microscope and distinguishing four taxonomic groups: *Daphnia* spp., small Cladocera, copepod adults and copepodites and copepod nauplii. Due to the high numbers of organisms present in each sample, enumeration of zooplankton was conducted on three replicate sub-samples of each sample. The concentration  $C_g$  of a group  $g$  was then estimated by dividing the abundance by the filtered water volume  $V = \pi/4 \cdot d^2 \cdot h/n$ .

### 3.2.3 Acoustic measurements

A bottom-mounted 500-kHz acoustic-Doppler current profiler (ADCP, Nortek Signature 500) was also deployed at a depth of 25 m (Fig. 3.1b) to record the acoustic backscatter strength (BS) and velocities during the summer stratification (ADCP, Fig. 3.2). The device has four acoustic transducers slanted at  $25^\circ$  to the vertical and one additional beam pointing vertically. The ADCP was set up to measure with a ping frequency of 0.5 Hz for the vertical beam and 1 Hz for the others, with a vertical resolution of 0.5 m. Data approximately 1 m below the surface were removed due to surface reflection of the pings, while data 1 m above the sediment are not available due to the deployment configuration and the ADCP blanking distance. Velocity data are not reported here because the observed velocity range was too low to provide reliable information.

The strength of the returned signal or backscatter strength (BS) from the vertical beam can be used as a proxy to track the position of the zooplankton layer and the timing of the migrations potentially relevant for turbulence measure-

ments (Noss and Lorke, 2014; Record and de Young, 2006). The BS however needs to be converted to the relative volume backscatter strength (VBS) to account for any transmission loss of the intensity signal. For this purpose, a simplified version of the sonar equation was applied to the vertical beam only (Huber et al., 2011; Noss and Lorke, 2014):

$$VBS = BS - P_{DBW} - L_{DBM} + 2 \cdot \alpha \cdot R + 20 \log_{10} \cdot R \quad (3.3)$$

where  $P_{DBW}$  is the transmitted power sent in the ensonified water,  $L_{DBM}$  the  $\log_{10}$  of the transmit pulse length  $P$ ,  $R$  the slant acoustic range and  $\alpha$  the acoustic absorption coefficient.  $P_{DBW}$  was set to zero because the transmit power is not a function of the battery for short period measurements, while  $P$  was set to 0.5 m being close to the cell size (Nortek, *pers. comm.*). The sound absorption was estimated from the model by Francois (1982) and using the temperature profiles from the thermistor chain. The result of the conversion process for the three datasets is reported in the Appendix 3.6, "Supplementary Material 1".

### 3.2.4 Microstructure measurements

Profiles of temperature fluctuations were acquired at the same location "S" (Fig. 3.2) before and during the DVM with a Self-Contained Autonomous MicroProfiler (SCAMP, PME), a temperature microstructure profiler using two Thermometrics FP07 thermistors. The SCAMP was deployed in downwards mode to sink at  $10 \text{ cm s}^{-1}$  (Fig. 3.1b). Expecting very small currents in the lake interior, each SCAMP cast was separated by a distance of at least 5 m with a GPS, but always kept near the sampling location, to avoid sampling the wake generated from the device itself when recovered after a previous profile. Fifteen SCAMP profiles were acquired on the 21 July, 19 on 28 July and 19 on the 18 August, approximately every 5 minutes. Turbulence was also sampled before the DVM

to characterise the background condition in absence of vertical migrators.

Each profile was split into segments of variable length, following the segmentation method by Chen et al. (2002). The method employs a wavelet-based test, sensitive to changes in spectral shape and magnitude, to ensure that each segment is statistically stationary. The dissipation of temperature variance  $\chi_T$  was computed for each segment by integrating the observed spectrum assuming isotropy (Thorpe, 2005). Dissipation rates of TKE  $\varepsilon$  were then estimated for each segment by fitting the data to the theoretical spectrum (Batchelor, 1959). Bad fits, with invalid TKE dissipation rates, were rejected and removed using the statistical criteria proposed by Ruddick et al. (2000).

### 3.2.5 Mixing and length scales

The eddy diffusivity coefficient  $K_T$  was estimated for each segment using the model by Osborn and Cox (1972), assuming steady-state and spatial homogeneity in each segment. Each SCAMP segment was also analysed to compute characteristic length scales: the Thorpe scale  $L_T$ , the maximum Thorpe displacement  $L_{Tmax}$  and the Ozmidov scale  $L_{OZ}$ . The scales  $L_T$  and  $L_{Tmax}$  were calculated after denoising the temperature and pressure profiles using the procedure by Piera et al. (2002) based on wavelet analysis. The advantage of the method is that it removes small but spurious patches generated by instrumental noise. The scale  $L_{OZ}$  was instead calculated using the buoyancy frequency  $N$  following the procedure by Wain and Rehmann (2010) and using the dissipation rate  $\varepsilon$  estimated from the spectral analysis. Each segment was then considered as a valid patch if  $L_{Tmax} < L_P$  and  $\int d_T(z) < 0.05 \cdot L_P$ , where  $L_P$  is the segment length (Piera et al., 2002).



### 3.2.6 Other measurements

A Secchi disk was employed to provide an estimation of the water transparency and compare it to the zooplankton daytime depth distribution. A thermistor chain (Fig. 3.2) was also deployed near the location "S" with 10 RBR thermistors (Solo T, RBR Ltd.) and 5 Hobo loggers (TidbiT v2, Onset Computer) sampling every 5 minutes.

## 3.3 Results and discussion

### 3.3.1 Zooplankton distribution

The zooplankton community was mainly composed of *Daphnia* spp. and copepods which accounted for about 70% of the total abundance in spring and summer. The average size ( $l_0$ ) of both *Daphnia* and adult copepods was approximately 1 mm, with some organisms reaching 2 mm. The zooplankton maximum concentration in the lake usually varies with the season with highest values in late May. The profiles of *Daphnia* concentration (Fig. 3.4) show that this taxon exhibited a similar vertical distribution during the three sampling days, with low population densities near the surface and the lake bottom, and peaks in the metalimnion. On 21 July, Daphnids were mostly located in the 12-15m layer at a concentration of 20 org. L<sup>-1</sup> and were also abundant near the lake bottom, at concentrations of less than 15 org. L<sup>-1</sup>. Copepods nauplii were as abundant as *Daphnia* below 12 m, but were unlikely to generate turbulence because of their small body size ( $l_0 \ll 1mm$ ). On 28 July, *Daphnia* were more abundant between 9 m and 12 m with a maximum concentration of 23 org. L<sup>-1</sup>, which is the maximum observed in July from the zooplankton tows. Concentrations below 12 m decreased abruptly to approximately 5 org. L<sup>-1</sup>. The next most abundant group, the adult and copepodite stage of copepods, reached a maximum density of 10

org. L<sup>-1</sup> in the 9-12m layer. On 18 August, the zooplankton concentration were at their lowest, with a maximum of *Daphnia* spp. density of only 10 org. L<sup>-1</sup> between 12 m and 15 m.

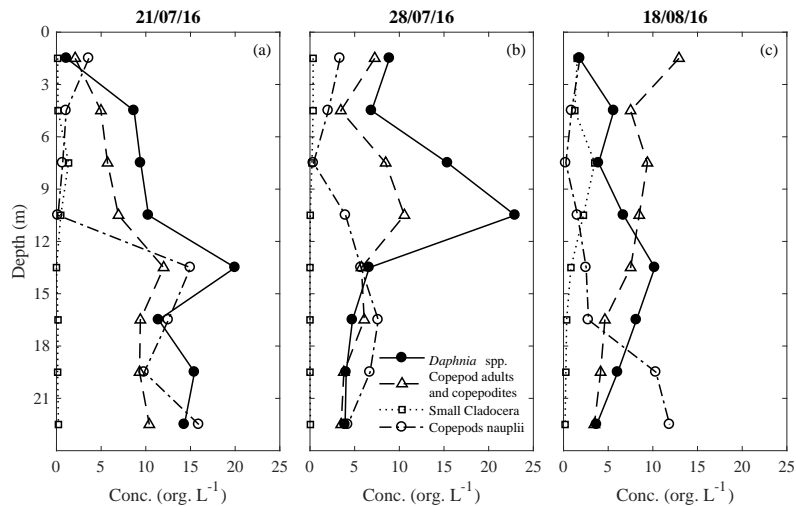


Figure 3.4: Profiles of zooplankton concentration for *Daphnia* spp., copepods, small Cladocera and copepods nauplii collected before the DVM and SCAMP measurements.

### 3.3.2 ADCP calibration

Data from the zooplankton net tows (Fig. 3.4) offer only a snapshot of the situation during daytime, and before the DVM begins. To overcome this limitation, the measured ADCP echo intensity (see "Supplementary material 1" in Appendix 3.6) can be used as a proxy for the zooplankton abundance, where the highest values correspond to the highest abundance, while the lowest value corresponds to those parts of the water column free of zooplankton or with a negligible concentration. Several studies in the ocean and lakes (Fielding et al., 2004; Huber et al., 2011; Lorke et al., 2004; Rahkola-Sorsa et al., 2014; Record and de Young, 2006) show that the concentration of different taxonomic groups can

be related to the linear volume backscatter strength ( $VBS_{linear} = 10^{VBS/10}$ ) via a physical and acoustic-based model. This ADCP calibration allows us to (1) continuously estimate zooplankton concentration without resorting to multiple net tows; (2) use a finer vertical resolution (0.5 m) than zooplankton tows (3 m); (3) provide an estimation of the concentration within the migrating layer during the DVM, as it is not possible to sample the water column with the net during the migration and obtain a concentration profile under reasonably stationary conditions because the concentration changes too quickly during the DVM; (4) understand which taxonomic groups explain and contribute the most to the acoustic signal and to its variation. It is possible to express the concentration  $C_g$  of a taxonomic group  $g$  as a function of  $VBS_{linear}$  through a multiple linear regression as:

$$VBS_{linear} = k_0 + \sum_{g=1}^4 k_g \cdot C_g \quad (3.4)$$

where  $C_g$  is the abundance measured from net hauls and  $k_g$  is its calibration coefficient. In the equation above,  $VBS_{linear}$  can be computed by averaging the backscatter in each of the depth strata sampled for zooplankton at the time of the net tows. Deviations from the model relating  $VBS_{linear}$  and  $C_g$  may be due to omitted loss terms in Eq. 3.3, surface reflection of the acoustic signal or net avoidance reactions by zooplankton (Brinton, 1967; Ianson et al., 2004). Despite the fact the zooplankton may be able to sense pressure variation when the net is approaching, the towing speed was controlled and kept very low to limit this artefact during sample collection. Finally the presence of the mouth-reducing cone helps reduce forward physical disturbances caused by the net itself (Unesco, 1968).

Table 3.1 shows the coefficients  $k_g$  and  $p$  values from the multiple regression analysis to test the statistical significance of each taxonomic group against the VBS. Results show that *Daphnia* spp. make the most significant contribution to

Table 3.1: Regression coefficient  $k_g$  and  $p$  values from multiple regression analysis between the zooplankton groups and the linear VBS using the data from the three sampling days

	<i>Daphnia</i> spp.	Copepods	Small Cladocera	Copepods nauplii
$k_g$ ( $10^6$ L org. $^{-1}$ )	$2148.3 \pm 0.61$	$2273.2 \pm 1.21$	$-5816.3 \pm 0.55$	$-8271.8 \pm 4.02$
$p$ value	0.00248	0.85364	0.16585	0.15552

$k_0 = 1.4846 \pm 0.66 \cdot 10^7$ ,  $R^2 = 0.657$

the VBS signal ( $p = 0.0024$ ). The abundances of the other taxa were poorly correlated with the VBS ( $p > 0.1$ ), indicating that *Daphnia* are the major contributor to the observed acoustic strength. For this reason it is possible to simplify the model by regressing  $VBS_{linear}$  with  $C_{Daphnia}$  only:

$$VBS_{linear} = k_0 + k_1 \cdot C_{Daphnia} \quad (3.5)$$

From the analysis,  $k_0 = 7.144 \pm 4.481 \times 10^6$  and  $k_1 = 2.315 \pm 0.425 \times 10^6$  L org. $^{-1}$ ; the coefficient of determination ( $R^2$ ) only reduces to about 0.6 from 0.7 using the model described by Eq. 3.5, still indicating a good fit. The standard deviation of the regression is  $\pm 5$  ind. L $^{-1}$ . A comparison between the measured  $C_{Daphnia}$  and that estimated from Eq. 3.5 is reported in Fig. 3.5 (black dots). The significant correlation between the VBS and *Daphnia* concentrations is linked to the balloon-like shape of Daphnids that scatter back acoustic waves more effectively than the other species (Huber et al., 2011; Lorke et al., 2004; Rinke et al., 2007). Sound wave reflection does not depend on *Daphnia*'s orientation or on their acoustic cross-section area, as much as for the elongated copepods. The regression coefficients for copepod nauplii and small Cladocera have a negative sign, indicating the lack of statistical dependence with the VBS. Their effect upon VBS is negligible because of their small size. The target strength of scatterers in the water becomes negligible when  $2\pi/\lambda \cdot a = 1$ , where  $\lambda$  is the acoustic wavelength and  $a$  the zooplankton radius. For a 500 kHz ADCP, this occurs when

$a \sim 0.44$  mm. Therefore zooplankton, whose size  $l_O < 2a$  (i.e. copepod nauplii and small Cladocera), do not contribute to the VBS as much as *Daphnia*. This is also suggested by the coefficient of determination  $R^2$  not changing significantly after removing these taxonomic groups.

Eq. 3.5 was also validated by using a validation dataset of  $C_{Daphnia}$  and  $VBS_{linear}$  measured in the lake on 30 June 2016 (see "Supplementary material 2" in Appendix 3.6). The empty dots in Fig. 3.5 show the comparison between the observed *Daphnia* concentrations and those estimated via Eq. 3.5 by using the  $VBS_{linear}$  acquired on that date. The good agreement between the observation and the estimation ( $R^2 = 0.75$ ,  $p = 6 \cdot 10^{-10}$ ) indicates that Eq. 3.5 can be reliably used to estimate  $C_{Daphnia}$ , when  $VBS_{linear}$  is only available, also for higher *Daphnia* concentrations.

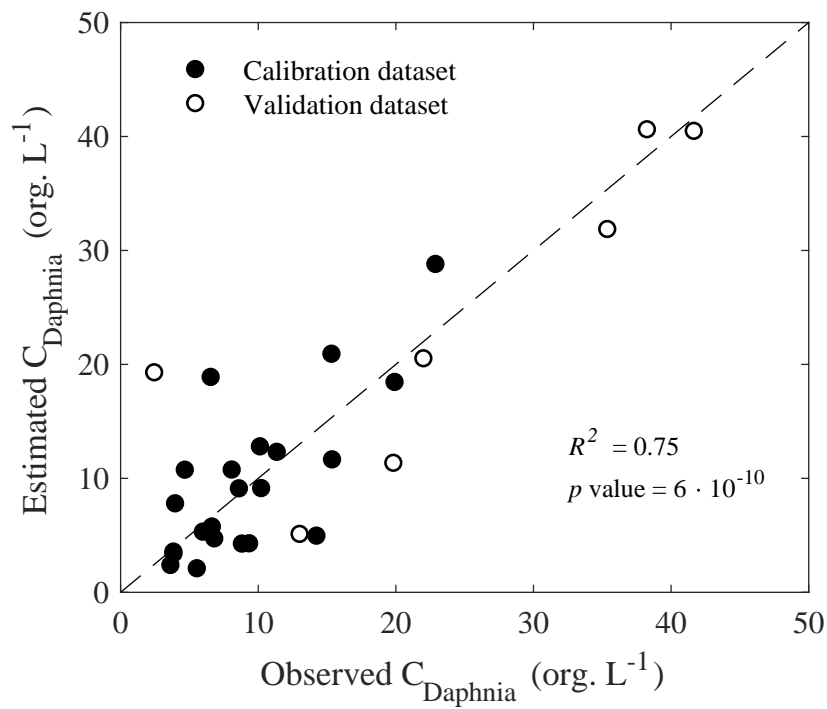


Figure 3.5: Comparison between the observed Daphnia concentration and that estimated from Eq. 3.5 using the measured VBS. Black dots show the datasets collected on 21 July, 28 July and 18 August used to estimate  $k_0$  and  $k_1$  in Eq. 3.5. Empty dots show data from the validation dataset collected on 30 June 16. The dashed line is the 1:1 relationship.

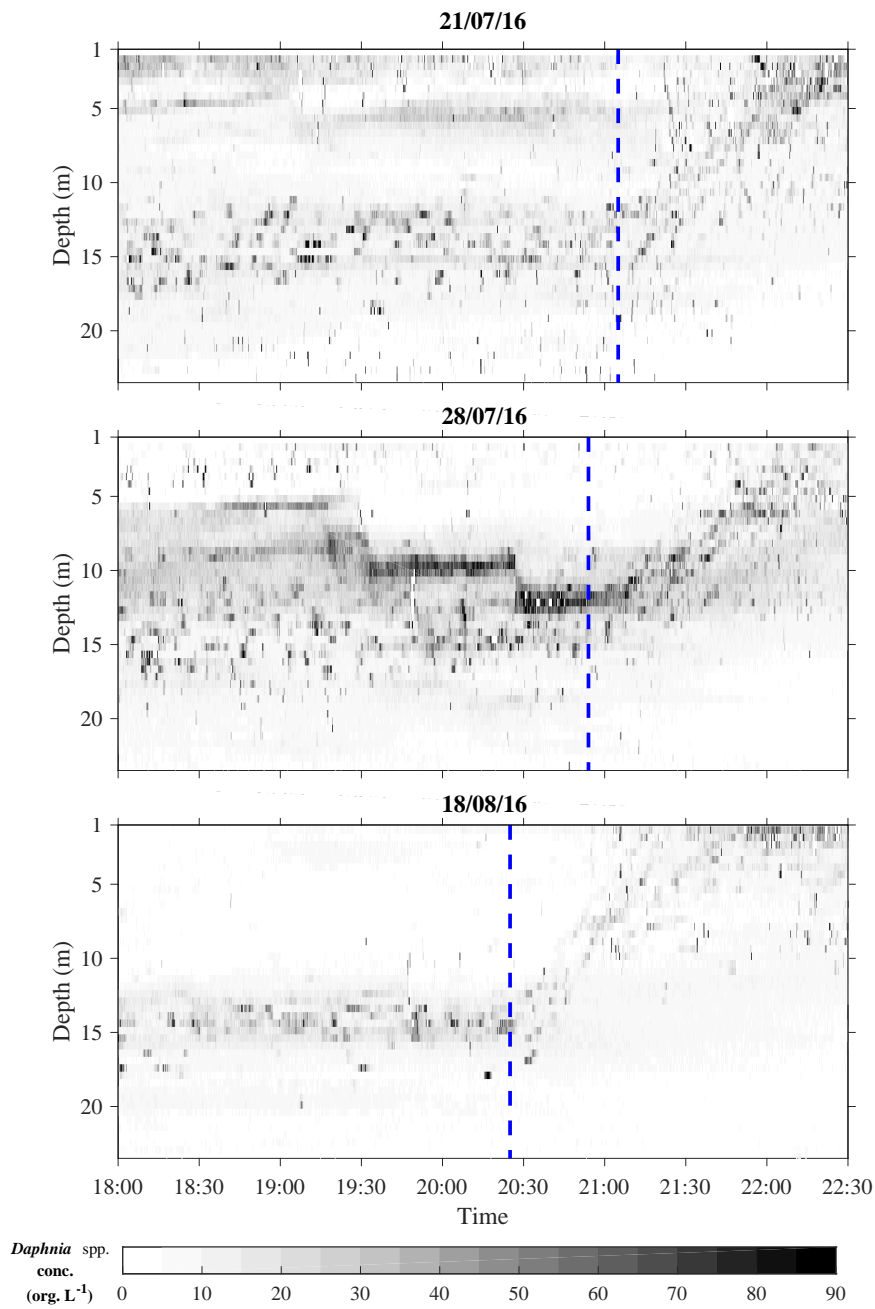


Figure 3.6: Time series of *Daphnia* concentration (greyscale colour-bar) for the three different days. Blue line highlights the sunset time when the migration begins.

### 3.3.3 DVM pattern

By inverting Eq. 3.5, it is possible to plot a time series of *Daphnia* concentration (Fig. 3.6). The figure shows that the *Daphnia* layer occupies the metalimnion during the day and is scattered around a stationary depth but always below the depth of maximum buoyancy frequency (see red bands in Fig. 3.3). Patches of higher concentration can be identified in the time series as well, but they are usually short-lived, suggesting that organisms are swimming either vertically or horizontally outside the acoustic cone of the ADCP. *Daphnia* begin migrating towards the epilimnion at sunset (blue dashed lines in Fig. 3.6), reaching the surface layer in approximately one hour with a bulk velocity of 3.4, 3.0 and 4.3 mm/s on the three dates respectively. Secchi depths were 10 m on 21 July, between 7.5 m and 8 m on 28 July, and 8 m for the last sampling date, indicating that *Daphnia* spp. resided in the low-light region of the lake water column during daylight hours.

Fig. 3.6 also suggests that the DVM pattern adopted by *Daphnia* is light-driven (Iwasa, 1982; Ringelberg, 1999; Rinke and Petzoldt, 2008) and migration took place in response to visual predation. However, *Daphnia* may change position in the water column during daytime as well. This happened on 28 July after 19:30 when the zooplankton layer at 10-m depth migrated downward before the beginning of the DVM at 21:00. The reasons for this unexpected behaviour are currently unknown: local cloud cover or other weather conditions did not change during the measurements, but the presence of chemical substances released by predators, such as kairomones, may have affected the vertical distribution during the day (Cohen and Forward, 2009).

Table 3.2 shows a summary of the estimated mean and maximum concentration of *Daphnia* within the migrating layer during the DVM, based upon ADCP data and extrapolation from the simplified regression model (see Eq. 3.5). Concentrations were lowest on 18 August, with a few zooplankton patches reaching a maximum of 70 org. L<sup>-1</sup>. The maximum observed concentrations in the mi-



Table 3.2: Mean and maximum *Daphnia* concentration ( $C_{Daphnia}$ ) in the migrating layer estimated from the simplified regression model.

	21 July	28 July	18 August
Mean $C_{Daphnia}$ (org. L <sup>-1</sup> )	15	38	12
Max $C_{Daphnia}$ (org. L <sup>-1</sup> )	90	99	70

grating layer were found on 28 July, with some small patches reaching almost 99 org. L<sup>-1</sup>. Moreover, data on the same day show a zooplankton band homogeneously distributed between 5 m and 10 m which is not well captured by the zooplankton profile (Fig. 3.4b) because of the coarse 3-m resolution of the net tows. This layer starts descending at 19:20 (local time) and again at 20:20, finally merging with the main zooplankton layer few minutes after 20:30. After 20:30, *Daphnia*'s abundance declines in the 6-9m strata and increases instead between 12 m and 15 m, where average concentration peaks at  $70 \pm 5$  org. L<sup>-1</sup>. Before 21:00, at sunset, the whole band begins to migrate upwards.

### 3.3.4 Dissipation rates

The upper and mid panels in Fig. 3.7-3.9 show the time series of the dissipation rates of thermal variance  $\chi_T$  and TKE  $\varepsilon$  for the three datasets. Data were overlapped upon the estimated *Daphnia* concentration (greyscale background). The empty blocks in the panels, where data are not present, represents non-stationary turbulent segments for which spectral analysis was not performed. The panels of  $\varepsilon$  show additional empty regions corresponding to rejected fits of the Batchelor spectrum, where the dissipation rates were ignored. Forty-five spectral fits out of 537 were invalid on 21 July, 66 out of 727 on 28 July, and 56 out of 618 on 18 August 2016.

An important condition for turbulence measurements is related to the sta-

tionarity of the flow field generated by *Daphnia*. A single organism swims unsteadily most of the time, creating an unsteady flow field in their wake (Kiorboe et al., 2014). However, a hopping and sinking *Daphnia* generates a quasi-stationary flow (Gries et al., 1999) and stationarity may be satisfied during the DVM when *Daphnia* usually adopts a fast-swimming behaviour (Dodson et al., 1997a).

The measurements showed the highest dissipations in the epilimnion, confined to 3m in depth on 21 July, 6m on 28 July, and 7m on 18 August 2016. Below this depth, turbulence was suppressed by the vertical stratification and dissipation rates rarely exceeded  $\varepsilon = 10^{-8} \text{ W kg}^{-1}$  and  $\chi_T = 10^{-6.5} \text{ K}^2 \text{ s}^{-1}$ . Because turbulent production is a patchy and intermittent process by nature, a turbulence burst of  $\chi_T$  or  $\varepsilon$  above the background level in a few patches within the migrating layer, is not proof of turbulent energy production by zooplankton. If zooplankton-generated turbulence occurred, we would expect to observe persistent turbulence dissipations in the migrating layer only. However, in our measurements, patches of enhanced  $\chi_T$  were present after sunset in all the three datasets and production of thermal anomalies took place outside the *Daphnia* migrating layer as well. Our measurements therefore suggest that the swimming zooplankton are not an efficient energy production mechanism in the lake.

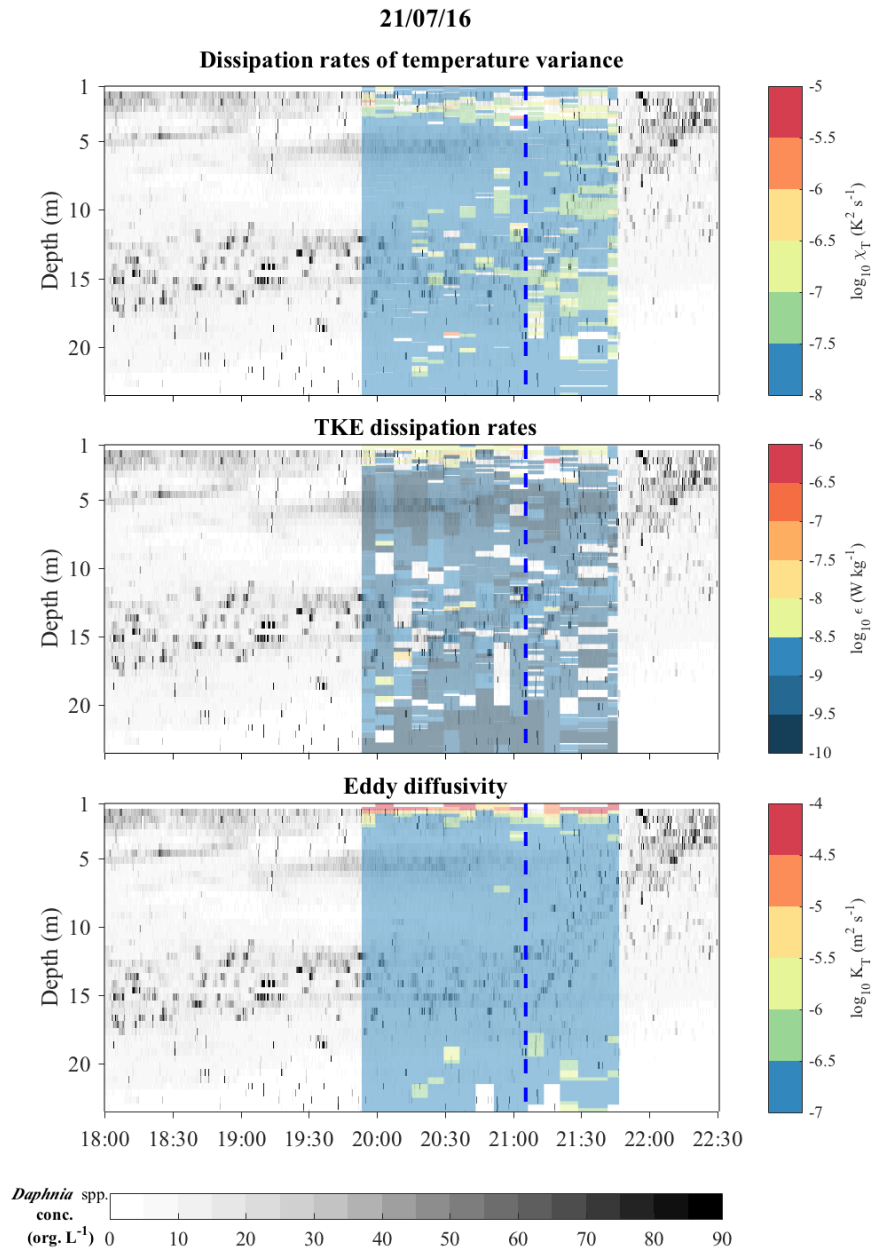


Figure 3.7: Data collected on 21 July 2016. Coloured blocks show the time series of dissipation rate of temperature variance  $\chi_T$  (upper panel), dissipation rate of TKE  $\epsilon$  (mid panel), and eddy diffusivity  $K_T$  (lower panel). The greyscale background shows the estimated *Daphnia* concentration. Blue lines highlight the sunset time when the migration begins. Spaces with no colour highlight the parts of the water column with non-stationary turbulence segments and invalid fits of the Batchelor spectrum.

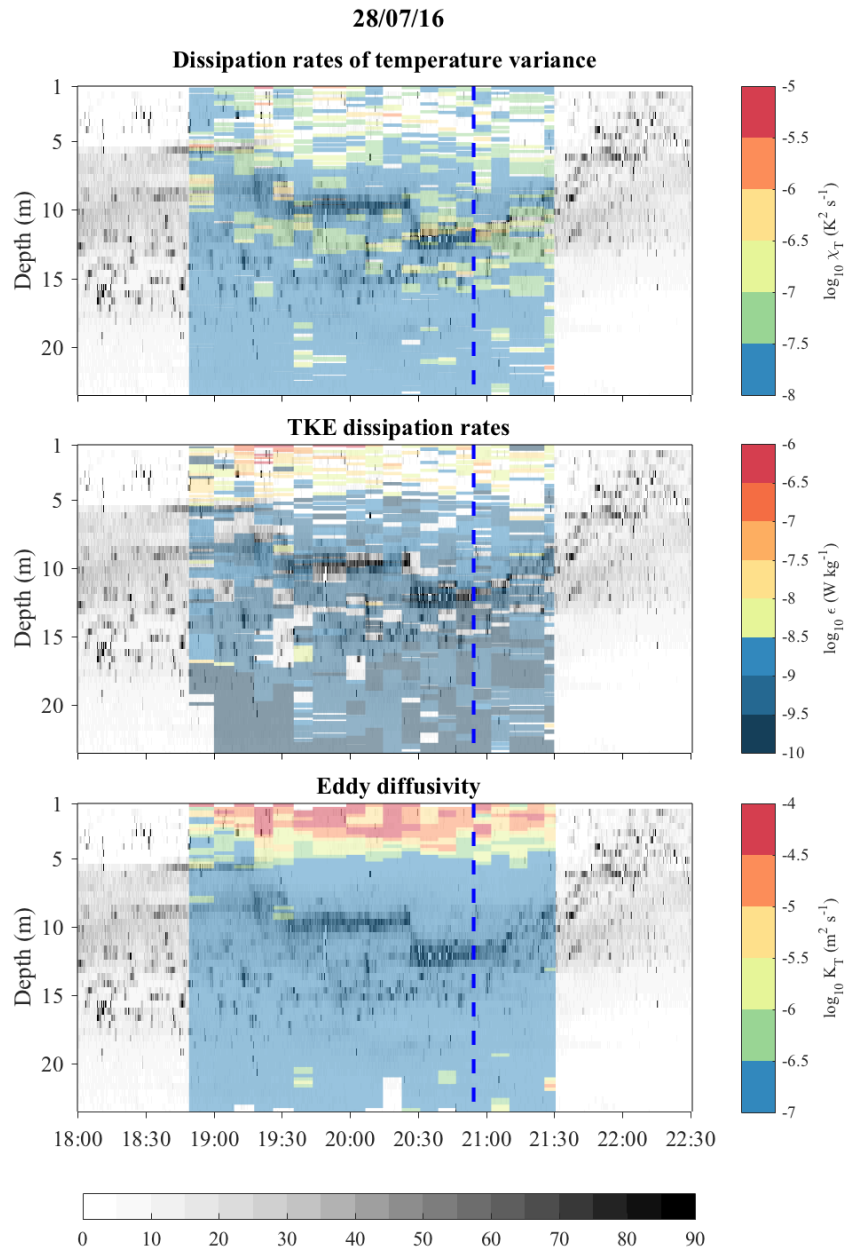


Figure 3.8: Data collected on 28 July 2016. Panel descriptions same as in Fig. 3.7

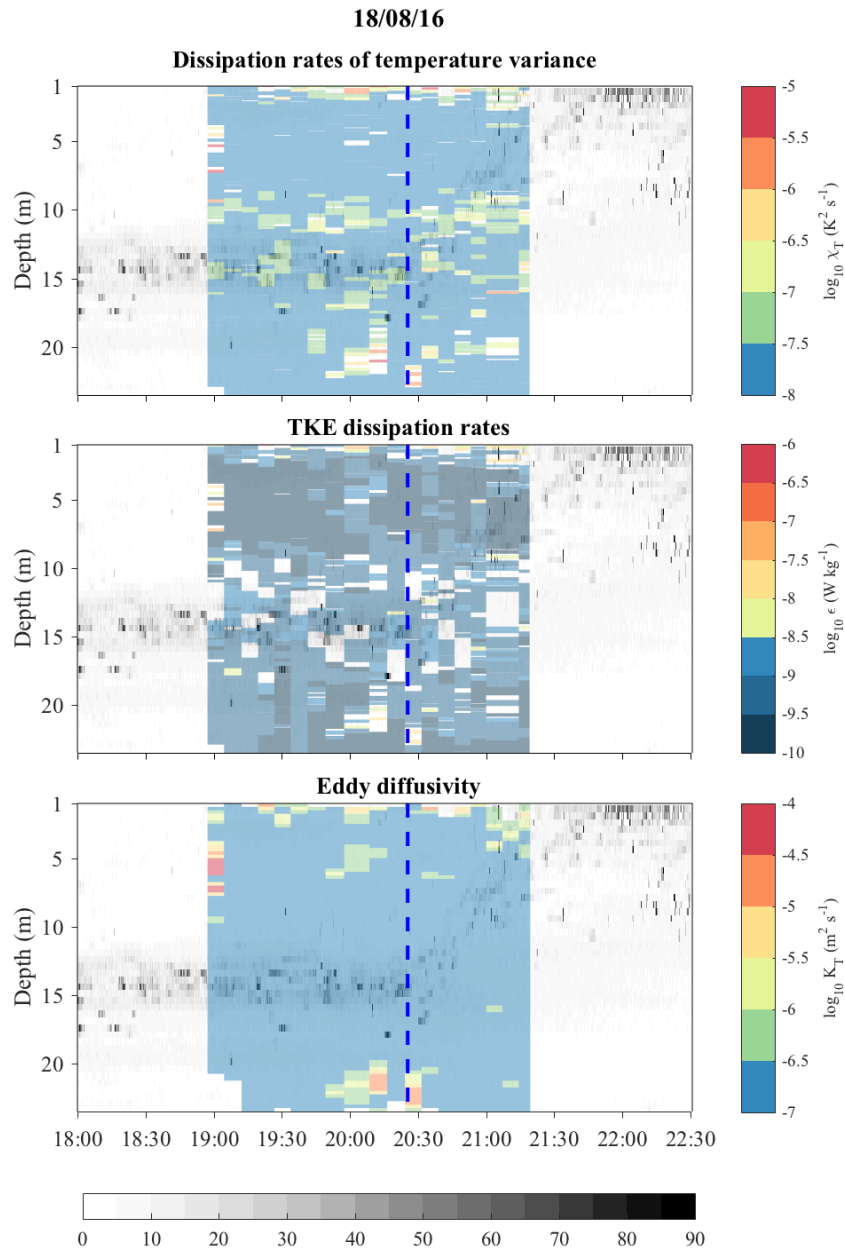


Figure 3.9: Data collected on 18 August 2016. Panel descriptions same as in Fig. 3.7

From the time series in Fig. 3.6-3.9, it is possible to extract and correlate the

dissipation rates against the mean *Daphnia* concentration, measured in each turbulent segment within the migrating layer. The result is reported in Fig. 3.10 for  $\chi_T$  (green triangles) and  $\varepsilon$  (black dots) for all the three datasets. The lack of any correlation clearly demonstrates that turbulence was not intensified during the dusk ascent, even for concentrations as high as 60 org. L<sup>-1</sup>. A few patches showed increased bursts of  $\chi_T$  for concentrations above 40 org. L<sup>-1</sup>, however, data constantly approached the mean background dissipation level of  $\varepsilon \sim 10^{-9}$  W kg<sup>-1</sup> (gray-shaded area) and  $\chi_T \sim 10^{-8}$  K<sup>2</sup> s<sup>-1</sup> (green-shaded area). Noss and Lorke (2012) measured  $\varepsilon \sim 10^{-6}$  W kg<sup>-1</sup> near the body of a single swimming *Daphnia*, but this was not observed in our data in the vicinity of multiple swimming organisms. Dissipation rates of TKE were also below the prediction of Huntley and Zhou (2004)'s model with  $\varepsilon \sim 10^{-5}$  W kg<sup>-1</sup>. Finally, according to acoustic measurements, *Daphnia* concentration peaked at 99 org. L<sup>-1</sup> on 28 July (see Table 3.2). However, denser patches of zooplankton are usually very small and are short-lived in a turbulent patch. After averaging the concentration in each SCAMP segment, the maximum concentration reduced to 60 org. L<sup>-1</sup> (Fig. 3.10). This concentration may have been too low to enhance dissipations as there was likely no superposition of the organisms' volume of influence.

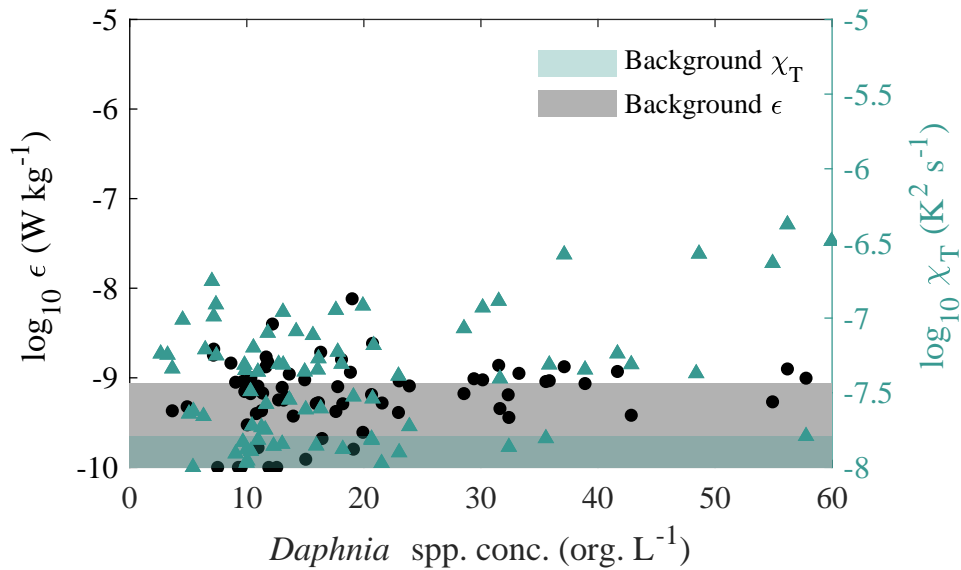


Figure 3.10: *Daphnia* concentration as a function of  $\epsilon$  (black dots) and  $\chi_T$  (green triangles) in the turbulent patches during the DVM for the three different datasets. The gray and green area show the mean background dissipation level for  $\epsilon$  and  $\chi_T$  respectively

### 3.3.5 Mixing

Lower panels in Fig. 3.7-3.9 show the time series of  $K_T$  from the Osborn and Cox model. Below the epilimnion, mixing did not increase, consistently approaching the molecular heat diffusivity ( $D_T = 10^{-7} \text{ m}^2 \text{ s}^{-1}$ ). Limited patches in the metalimnion with higher mixing up to  $K_T = 10^{-6} \text{ m}^2 \text{ s}^{-1}$  were short-lived. The assumption of stationary and homogenous turbulent conditions may not be applicable to the case of biomixing.

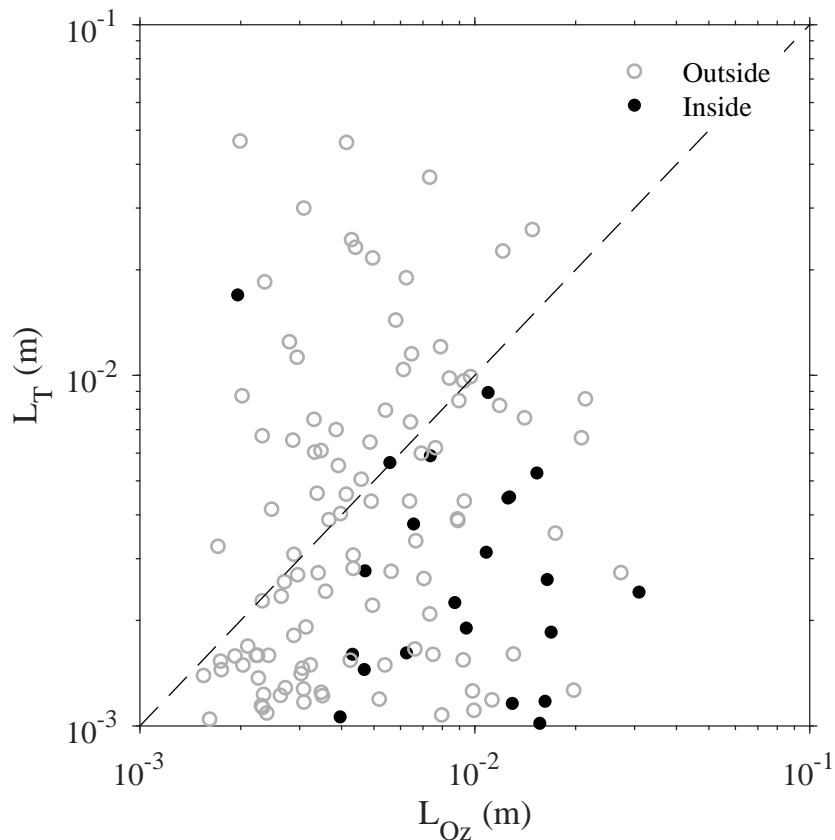


Figure 3.11: Ozmidov scale  $L_{OZ}$  as a function of the Thorpe length scale  $L_T$  in the turbulent patches inside the migrating layer (filled dots) and outside (empty dots) after sunset. The dashed line is the 1:1 relationship.

The analysis of the overturning length scales (see Fig. 3.11) shows that the scales inside the migrating layer (filled dots) were characterised by  $L_T$  constantly below  $L_{OZ}$ . Overturns outside the layer (empty dots) were instead scattered around  $L_T \sim L_{OZ}$ . The same difference was observed by Gregg and Horne (2009), but over a wider range for pelagic nekton. The fluctuations were also above the size of a single *Daphnia* ( $l_O = 1$  mm). However, no significant and persistent differences in the displacements were generally observed between the



situation outside and inside the migrating layer. This further suggests the hypothesis that no important fluctuations were generated by the migrating *Daphnia* and that no potential energy was created.

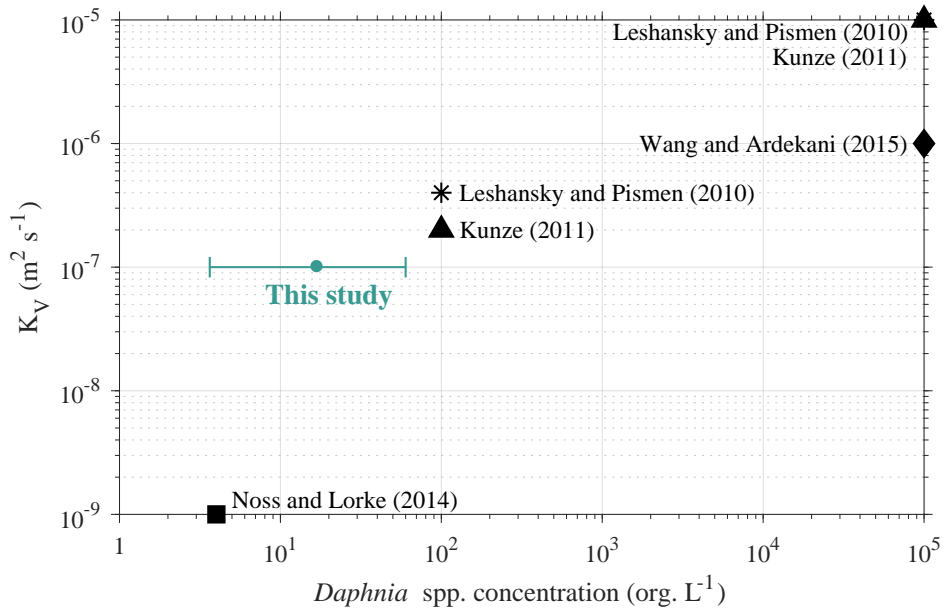


Figure 3.12: Eddy diffusivity coefficient  $K_V$  as a function of *Daphnia* spp. concentration from different studies in the literature. The green dot represents data from this study. The error bar shows the observed minimum and maximum concentration and the dot its mean.

Available estimations of the eddy diffusivity coefficient provide different values of  $K_V$ , depending on the concentration of the swimming *Daphnia* aggregation (see Fig. 3.12). Laboratory experiment by Noss and Lorke (2014) provided  $K_V = 10^{-9} \text{ m}^2 \text{ s}^{-1}$  with 4 org. L<sup>-1</sup>. Numerical simulations by Wang and Ardekani (2015) suggest instead that biomixing by zooplankton is a likely mechanism.  $K_V$  can be enhanced up to  $10^{-5} \text{ m}^2 \text{ s}^{-1}$ , but only using unrealistic concentrations of *Daphnia*. The observed mean concentration within the turbulent patches in our data varied instead between 4 and 60 org. L<sup>-1</sup>. These values were above the con-

centration employed by Noss and Lorke (2014) and three orders of magnitude smaller than those used in numerical estimations. In our study we estimated  $K_V = K_T = 10^{-7} \text{ m}^2 \text{ s}^{-1}$ , therefore vertically-swimming zooplankton did not affect the vertical thermal stratification in the lake.

Other field studies report *Daphnia* daytime concentration similar to those measured in Vobster Quay (Hembre and Megard, 2003; Rinke et al., 2007). However, it is not certain how the concentration, in other lakes and during the DVM, differs from that observed in this study. The concentration may depend on the presence of other migrating species, predators and light conditions (Ringelberg, 2010; Simoncelli et al., 2017). Since zooplankton abundance is a lake and time-dependent factor, this does not rule out the possibility that collective action and synchronised movements of larger zooplankton and/or higher abundances may produce significant instabilities in other lakes. If this is the case, the process would be limited only to those specific basins and would not be a widespread mechanism.

### 3.4 Conclusions

In this study we measured *in-situ* dissipation rates of temperature variance and estimated dissipation rates of TKE and eddy diffusivity in the metalimnion of a small lake during the diurnal vertical migration of a small zooplankton species to verify whether migrating zooplankton can trigger hydrodynamic instabilities and enhance vertical mixing in the lake interior. We did not observe important and persistent turbulent enhancements with respect to the background levels during the DVM of the zooplankton layer. No correlations between concentration and dissipation rates were observed. No biomixing was detected even though the estimated *Daphnia* abundances of almost  $60 \text{ org. L}^{-1}$  were fifteen times larger than those used in the laboratory experiment by Noss and Lorke (2014). This suggests that migrating *Daphnia* do not affect mixing at these con-

centrations. However, there might still be a concentration threshold over which synchronised movements of *Daphnia* may become relevant.

### 3.5 Acknowledgements

Funding for this work was provided by a UK Royal Society Research Grant (Y0106-WAIN) and an EU Marie Curie Career Integration Grant (PCIG14-GA-2013-630917) awarded to D. J. Wain. We would also like to thanks Tim Clements for allowing us access to Vobster Quay and Scott Easter, Zach Wynne and Emily Slavin (from the University of Bath) for the help provided during the field campaign. Data are available in the University of Bath Research Data Archive repository at <http://researchdata.bath.ac.uk/344>

## 3.6 Appendix

### 3.6.1 Supplementary material 1

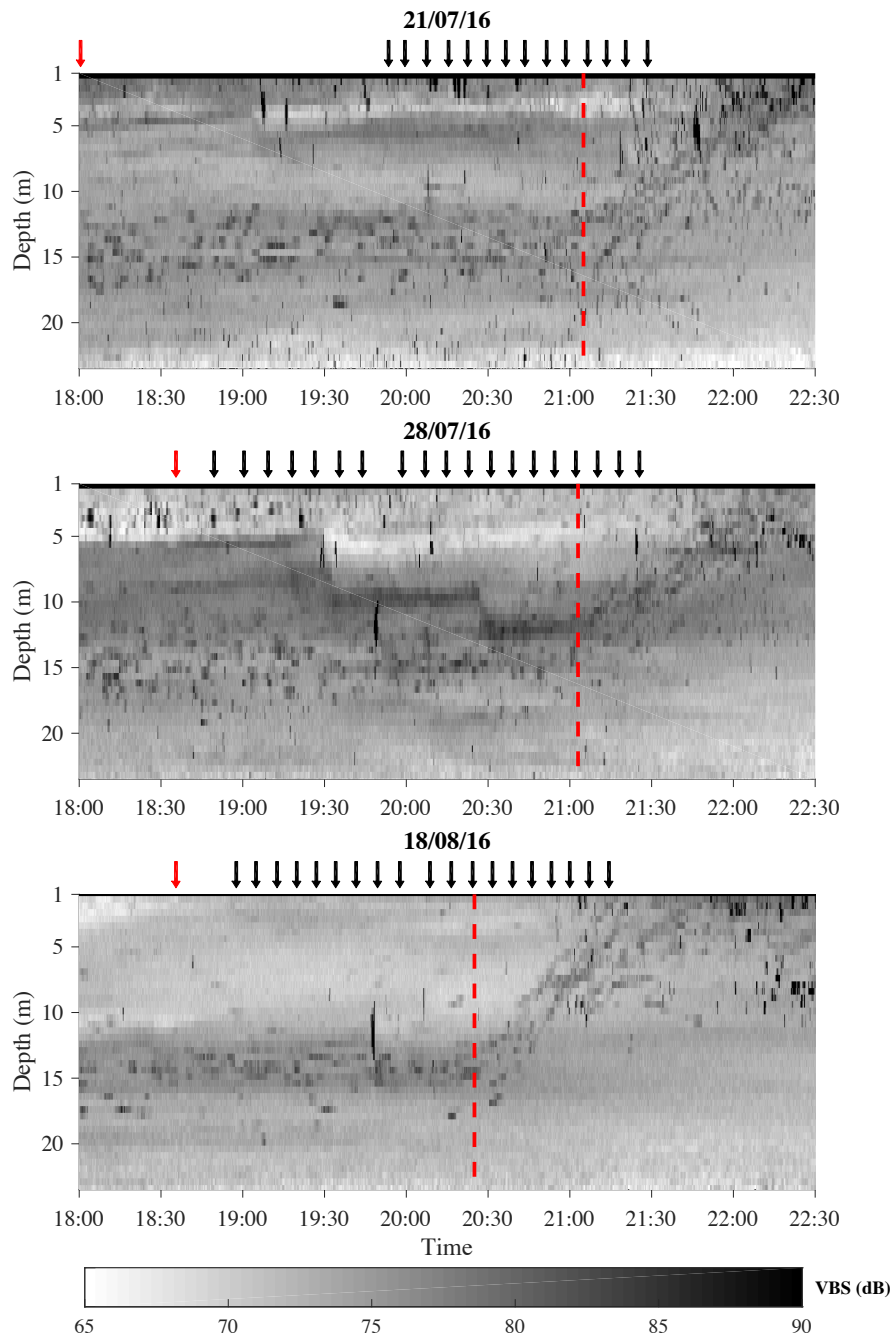


Figure 3.13: Volume backscatter strength from the ADCP vertical beam in grey. Higher values indicate a higher zooplankton abundance, while the minimum is the background echo intensity. Red arrows indicate the time of the zooplankton tows, black arrows the start time of SCAMP casts and the red dashed line sunset when the zooplankton begin migrating.

## 3.6.2 Supplementary material 2

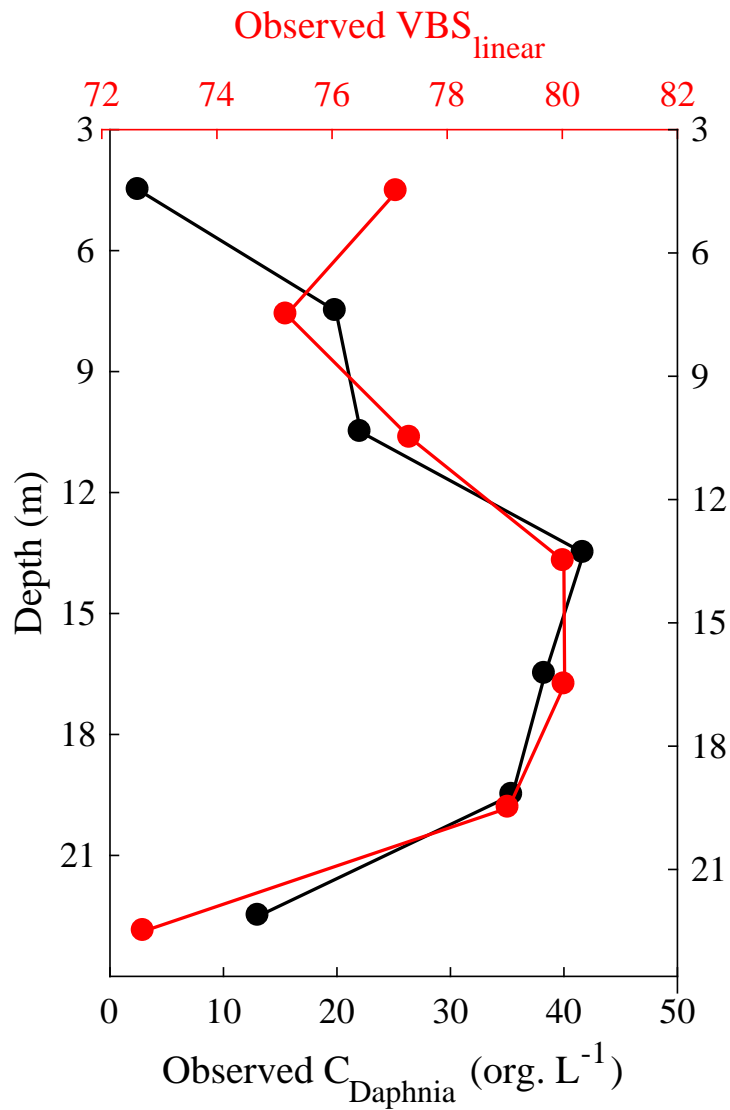


Figure 3.14: Profiles of linear VBS (red line) and *Daphnia* concentration (black line) collected on the 30 June 2016.

# Effect of temperature on zooplankton vertical migration

S. Simoncelli<sup>1</sup>, S. J. Thackeray<sup>2</sup> and D. J. Wain<sup>1</sup>

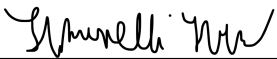
<sup>1</sup> Department of Architecture and Civil Engineering, University of Bath

<sup>2</sup> Centre for Ecology & Hydrology, Lancaster Environment Centre

## Abstract

**Z**OOPLANKTON diel vertical migration (DVM) is an ecologically important process, affecting nutrient transport and trophic interactions. Available measurements of zooplankton displacement velocity during the DVM in the field are rare, therefore it is not known which factors are key in driving this velocity. We measured the velocity of the migrating layer at sunset (upwards bulk velocity), in summer 2015 and 2016 in a lake, using the backscatter strength (VBS) from an acoustic Doppler current profiler. We collected time series of temperature, relative change in light intensity, chlorophyll-a concentration and zooplankton concentration. Our data show that upwards velocities increased during the summer and were not enhanced by food, light intensity or by VBS, which is a proxy for zooplankton concentration and size. Upward velocities were strongly correlated with the water temperature in the migrating layer, suggesting that temperature could be a key factor controlling swimming activity. Zooplankton migrations mediate trophic interactions and web food structure in pelagic ecosystems. An understanding of the potential environmental determinants of this behaviour is therefore essential to our knowledge of ecosystem functioning.

## Statement of Authorship

<b>This declaration concerns the article entitled</b>				
Effect of temperature on zooplankton vertical migration				
<b>Authors</b>				
Simoncelli, S. (SS), Thackeray, S. J. (SJT) and Wain, D. J. (DJW)				
<b>Publication status (tick one)</b>				
Draft manuscript	Submitted	<input checked="" type="checkbox"/> <u>In review</u>	Accepted	Published
<b>Publication details (reference)</b>				
Hydrobiologia <i>(Chapter 4 and 5 have been submitted as one paper)</i>				
<b>Candidate's contribution to the paper (detailed, and also given as a percentage)</b>				
Designed the experiments: DJW, SJT, SS (90%).				
Performed the experiments: DJW, SS (90%).				
Analysed the data: SS (100%).				
Wrote the paper: SS.				
Editorial support in writing the manuscript: DJW, SJT				
Interpretation of the results: DJW, SJT, SS (90%).				
<b>Statement from Candidate</b>				
This paper reports on original research I conducted during the period of my Higher Degree by Research candidature.				
<b>Signed</b>			<b>Date</b>	13/02/2018



## 4.1 Introduction

Population dynamics and physiological responses of zooplankton in stratified lakes are a result of a complex interplay of endogenous and exogenous factors and their seasonal variations throughout the year (Masson et al., 2001; Ringelberg, 2010). One of the most studied behavioural responses of zooplankton is the diel vertical migration (DVM) that is typical of crustacean zooplankton, but has also been observed in other marine and freshwater species (Ringelberg, 1999). In a typical DVM, organisms migrate from deep and cold waters towards the warmer surface at sunset and they descend at sunrise (Ringelberg, 2010; Williamson et al., 2011). Predation, light, food availability and temperature are recognised as the main DVM drivers. However, avoidance of visually-hunting juvenile fish and food requirements are generally considered the most significant factors (Hays, 2003; Ringelberg, 1999; Van Gool and Ringelberg, 2003; Williamson et al., 2011). According to this reasoning, zooplankton hide during the daytime in the deep and dark layers of the lake in response to chemical cues released by fish (kairomones) (Beklioglu et al., 2008; Boeing et al., 2003; Cohen and Forward, 2009; Dodson, 1988; Lass and Spaak, 2003; Loose and Dawidowicz, 1994; Neill, 1990). Zooplankton then graze on phytoplankton in surface waters at night, minimising at the same time their mortality risk. Food availability can modify migration behaviour as well (Van Gool and Ringelberg, 2003); if a deep chlorophyll maximum is present, zooplankton may not migrate (Rinke and Petzoldt, 2008). Finally, DVM can still take place in very transparent and fishless lakes where zooplankton hide to prevent damage from surface UV radiation (Leach et al., 2014; Tiberti and Iacobuzio, 2013; Williamson et al., 2011).

During the lake stratification period, zooplankton are exposed to different DVM drivers. These drivers can influence the speed at which the organisms migrate. This speed has two components. The swimming velocity (SV), which is the organism's instantaneous velocity during a reactive phase (Ringelberg, 2010). And the displacement velocity (DV), which is instead the vertical dis-

placement of the organism divided by the time taken to perform the movement (Gool and Ringelberg, 1995). The DV is smaller than SV because it combines various animal reactions, including latent periods.

Field observations, by Ringelberg et al. (1991) and Ringelberg and Flik (1994), showed that the DV at dusk of *Daphnia galeata x hyalina* was well-correlated with the change of light intensity ( $S$ ) measured in the water column at the time of the migration. The response of the animals was strongly light-driven but not influenced by food concentration or water transparency. Moreover, acceleration and deceleration in  $S$  can also play a role in determining the *Daphnia* swimming response (Van Gool, 1997).

The dependence of the zooplankton SV on the presence of predators in the water column is species-specific. Beck and Turingan (2007) showed that the swimming speed of brine shrimp (*A. franciscana*) and two copepod species (*Nitokra lacustris* and *Acartia tonsa*) increased when zooplankton were exposed to water with larval fish. However, this was not the case for the rotifer *Brachionus rotundiformis*. Dodson et al. (1995) theorised instead that *Daphnia* may adopt a conservative-swimming behaviour, because faster swimming velocity would increase predator-prey encounter rates and therefore predation risk. In their experiment they did not observe increases in SV of *Daphnia pulex* when exposed to *Chaoborus*-enriched water. However, Weber and Van Noordwijk (2002) later showed that the swimming response of *D. galeata* to info-chemicals can be clone-specific and that *Perca* kairomone can positively affect their speed. Finally, Van Gool and Ringelberg (1998a) and Van Gool and Ringelberg (1998b; 2003) observed that the *Daphnia* swimming response to  $S$  can be enhanced by chemical signal from *Perca fluviatilis* and by food concentration as well.

Turbulence in the environment can affect zooplankton motility behaviour. Marine copepods can enhance their metabolism when swimming in high turbulence (Alcaraz et al., 1994) but some species avoid a highly energetic environment if it can prevent them from feeding (Saiz et al., 2013). Swimming ability can also

be negatively affected by turbulence (Prairie et al., 2012; Visser and Stips, 2002), but some copepod species can retain their swimming velocity (Michalec et al., 2015) or enhance their speed (Webster et al., 2015), even in highly turbulent eddies. Other experiments on *Daphnia* showed that *D. pulicaria* and *D. magna* can overcome eddy turbulent velocity (Seuront et al., 2004; Wickramarathna, 2016), but they avoid very high turbulence environments (Wickramarathna, 2016).

Zooplankton swimming velocity may also be size-dependent. Laboratory studies and empirical correlations show that bigger organisms can propel themselves faster in the water (Andersen Borg et al., 2012; Gries et al., 1999; Huntley and Zhou, 2004; Wickramarathna et al., 2014) because of their larger swimming appendages.

Recent research has focused on assessing the impact of other factors on the swimming speed of other zooplanktonic species. Although these studies did not focus specifically on the DVM, results can still be applied to organism behaviour during their vertical movement. Laboratory observations, on live samples of marine copepods *Temora longicornis* by Moison et al. (2012), showed that the organism's swimming speed was greatly enhanced when organisms were exposed to a higher water temperature. Temperature has in fact a twofold effect. It can boost the biological and metabolic activity of zooplankton, increasing the energy available for locomotion and therefore the power available for thrust generation (Beveridge et al., 2010). At the same time, it can reduce the fluid kinematic viscosity ( $\nu$ ) and therefore the drag on the zooplankton beating appendages, so that they can swim faster. Experimental data by Larsen et al. (2008) showed that the swimming velocities of the rotifer *Brachionus plicatilis* and copepod *Acartia tonsa* were mostly determined and correlated with  $\nu$ . This effect is not limited to mesozooplankton only, but it can influence the velocity of fish larvae and micrometer-sized organisms where the propulsion mechanisms are controlled by cilia or flagella (Humphries, 2013; Jung et al., 2014; Larsen and Riisgård, 2009; Macheimer, 1972). Larsen and Riisgård (2009) proposed that  $\nu$ , and not the organism's biological activity, mainly controls the organisms response.

Finally, Van Gool and Ringelberg (2003) observed that *Daphnia* phototactic response varied more with temperature changes than with food availability and kairomone concentration.

Available measurements of zooplankton swimming velocity during the DVM in the field are rare. Ringelberg and Flik (1994) estimated for the first time the zooplankton DV relying on successive net hauls to measure the zooplankton position in the water column. This method only offers a coarse resolution of the organism's position and is time-consuming. More recent studies by Lorke et al. (2004) and Huber et al. (2011) measured instead the DV using velocity data and variations of the backscatter strength signal from an Acoustic Current Doppler Profiler (ADCP). However, their objective was not to analyse variations in time series of the zooplankton DV. In this study, we continuously measured the velocity of the migrating layer (bulk velocity or mean DV) from the backscatter strength of an ADCP in two different years. We quantified  $v_{up}$  as the bulk velocity at dusk, when zooplankton actively swim to reach the surface. We then employed a correlative approach to infer the dependence of  $v_{up}$  upon possible DVM drivers in the field. This allowed the first field exploration of seasonal variability of the DV and of environmental parameters that potentially drive the rate of zooplankton migration in lakes.

## 4.2 Materials and Methods

### 4.2.1 Study site

Measurements were carried out in 2015 and 2016 in Vobster Quay, a shallow man-made lake located in Radstock, UK. The lake has an average depth of 15 m and maximum depth of 40 m (see Fig. 4.1). It has a very simple bathymetry, with very steep shores and a flat bottom. The lake is oligotrophic, with an average

chlorophyll-*a* concentration of about  $1 \mu\text{g L}^{-1}$ . During the summer stratification, the surface temperature reaches a maximum of  $21 \text{ }^\circ\text{C}$  and a bottom temperature of  $9 \text{ }^\circ\text{C}$ . The metalimnion usually extends from 5 m to 17 m. The water transparency is very high, with an average Secchi depth of 10 m over the summer. The lake was stocked in August 2004 with a population of *Perca fluviatilis* and *Rutilus rutilus*.

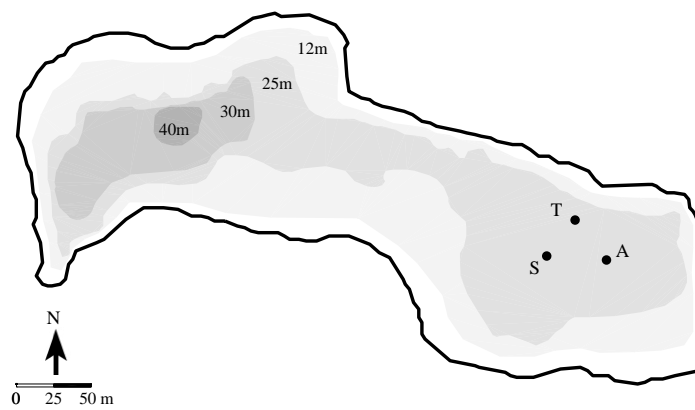


Figure 4.1: *Bathymetry of Vobster Quay*. “S” denotes the sampling station where measurements were taken. “T” and “A” indicate the locations of the thermistor chain and ADCP respectively.

### 4.2.2 Acoustic measurements

Acoustic measurements were employed to track the position of the zooplankton layer during the DVM (e.g. Lorke et al., 2004) and to estimate their DV at sunset and sunrise using the acoustic backscatter strength. An acoustic Doppler current profiler (ADCP Signature 500 by Nortek) was bottom-deployed at location “A” in Fig. 4.1. The device was set-up to record the acoustic backscatter strength

(*BS*) every 30 seconds from the vertical beam. The *BS* 1 m below the surface and above the bottom was removed due to surface reflection and the ADCP blanking distance. Data were available from 7 July to 27 July of 2015, 24 June to 7 July 2016, and from 21 July to 19 August 2016.

The *BS* was then converted to the relative volume backscatter strength (*VBS*) to account for any transmission loss of the intensity signal, using the sonar equation (Deines, 1999):

$$VBS = BS - P_{dbw} - L_{dbm} + 2 \cdot \alpha \cdot R + 20 \log_{10} \cdot R \quad (4.1)$$

where  $P_{dbw}$  is the transmitted power sent in the water,  $L_{dbm}$  the  $\log_{10}$  of the transmit pulse length  $P = 0.5$  m (Nortek, *pers. comm.*) and  $R$  the slant acoustic range.  $\alpha$  is the acoustic absorption coefficient estimated following Francois (1982) and using the temperature profiles from the thermistors chain ("T" in Fig. 4.1).

### 4.2.3 Bulk velocity estimation

The bulk velocity of the migrating layer is defined as the slope of the zooplankton layer during the DVM. Fig. 4.2d shows an example of the migration on 2 July 2016, where the VBS in black depicts the zooplankton in the water column. When the zooplankton start swimming upwards after sunset (21:45 local time), a line can be fit to the migrating layer, whose slope is constant throughout the ascending phase (red line in Fig. 4.2d). This slope is the upward bulk velocity ( $v_{up}$ ) and provides the mean DV of the organisms.

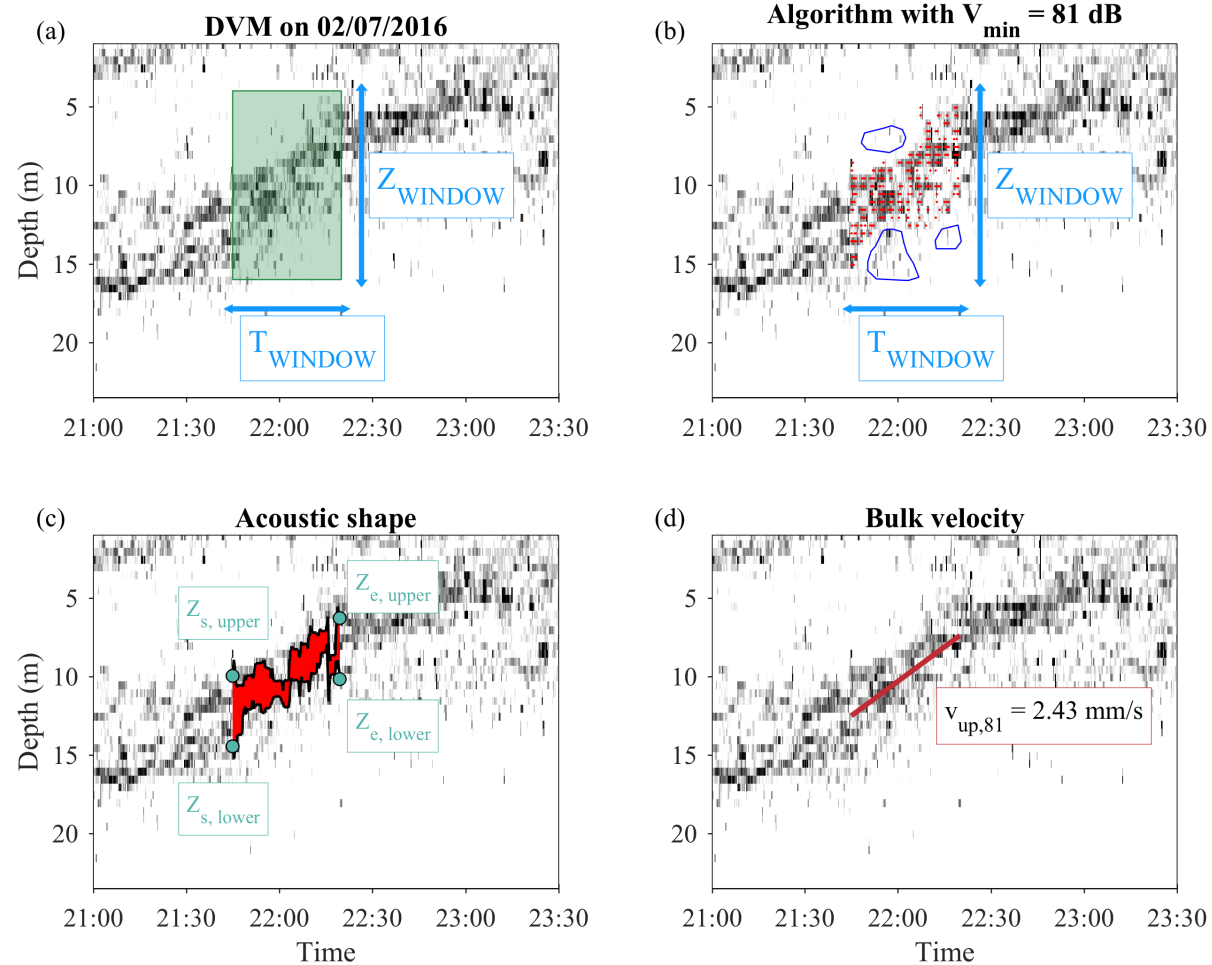


Figure 4.2: Schematic of how the algorithm computes the bulk velocity. The four panels show the DVM captured by the ADCP on 02/07/16. The grey-scale shading is the VBS and shows the position of the zooplankton in the water column as a function of the time. Panel a shows the green box delimited by  $Z_{\text{WINDOW}}$  and  $T_{\text{WINDOW}}$  and used by the model to detect the migrating layer. Red dots in panel b show the zooplankton layer where  $81 \text{ dB} \leq VBS \leq 85 \text{ dB}$ . Blue shapes delimit isolated zooplankton patches removed from the algorithm. The red patch in panel c highlights the layer identified by the algorithm.  $Z_{s, \text{lower}}$ ,  $Z_{s, \text{upper}}$ ,  $Z_{e, \text{lower}}$  and  $Z_{e, \text{upper}}$  provide the upper and lower position of the layer when the DVM begins and ends. Panel d shows the resulting slope of the layer and the bulk velocity  $v_{\text{up},81}$  for  $V_{\min} = 81$  dB.

To objectively and automatically estimate  $v_{up}$  from the VBS data, an image-detection algorithm was developed to detect the acoustic shape of the zooplankton layer and to estimate its slope. Two input parameters need to be provided by the user: (1) the box (target area) containing the layer and delimited by  $Z_{WINDOW}$  and  $T_{WINDOW}$  limits (see Fig. 4.2a); when the DVM begins and ends and its limits can be immediately identified from the acoustic image; (2) the VBS range  $V_{range} = [V_{min}, V_{max}]$  of the zooplankton in the migrating layer. This range is characteristic of the zooplankton for that day and is affected by the organism abundance and size. Because the VBS always reaches the maximum in the migrating layer, the algorithm can be controlled just by adjusting the lower limit  $V_{min}$  and setting  $V_{max}$  to the observed maximum of 85 dB.

Once these two groups of parameters are set, to detect the layer, the algorithm picks the points in the target area where  $V_{min} \leq VBS \leq 85$  dB (see red dots in Fig. 4.2b). The acoustic shape then can be identified by selecting the outer points of the layer (Fig. 4.2c). A line can be finally fitted to the red points to estimate  $v_{up}$ . Fig. 4.2d shows  $v_{up,81} = 2.43$  mm/s for  $V_{min} = 81$  dB.

Some of the VBS data, representing isolated patches of zooplankton or environmental noise within the target area, had to be manually removed. An example is provided in Fig. 4.2b, where the three blue patches show dense aggregations of zooplankton with high VBS not belonging to the migrating layer. These points would be selected by the algorithm and affect the velocity computation in the layer.



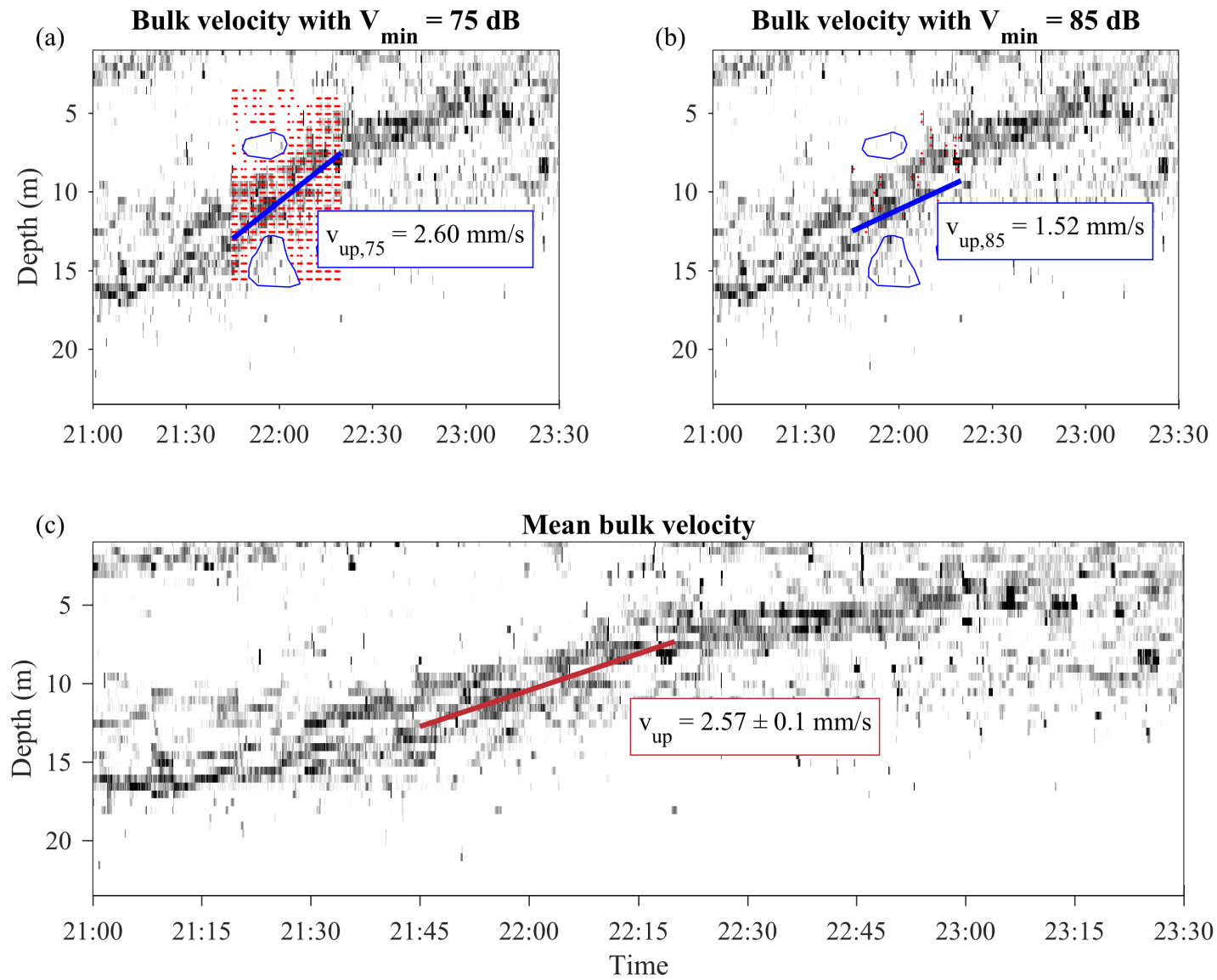


Figure 4.3: Algorithm results with two other values of  $V_{\min}$ . Panel a shows the case with a low value, where almost all the points in the target area are selected. When  $V_{\min}$  is too high as in panel b, the resulting slope is off. In both cases the slope is marked as invalid. Panel c depicts the final result of  $v_{\text{up}}$  via bootstrapping.

Because the choice of  $V_{min}$  can be arbitrary, the algorithm was run by changing  $V_{min}$  from 75 dB, which was the lowest observed value, to  $V_{min} = V_{max} = 85$  dB, generating 11 different layer detection and fitting results. Two examples are shown in Fig. 4.3 for  $V_{min} = 75$  dB and  $V_{min} = 85$  dB. Each image can be then inspected manually to remove spurious results and bad fits, when at least one of the following conditions are met: (1) the algorithm selects points within the target area but outside the layer; this occurs when  $V_{min}$  is too low, such as the case in Fig. 4.3a; (2) the fitted line cuts across the migrating layer rather than follows its centroid; this condition is met when  $V_{min}$  is too low or high. When  $V_{min} = 85$  dB (Fig. 4.3b), too few points, which lack alignment with the centre of the target layer, were picked to correctly estimate the slope.

After excluding the fits that meet the rejection criteria previously defined, the velocity of the accepted fits can be bootstrapped to estimate the mean bulk velocity  $v_{up}$  and its 95% confidence interval. For example, by choosing  $V_{min}$  from 78 to 83 dB for the 2 July migration,  $v_{up} = 2.57 \pm 0.1$  mm/s (Fig. 4.3c). This procedure was applied for both 2015 and 2016, producing a time-series of sunset migration velocities  $v_{up}$ .

#### 4.2.4 Temperature measurements

The vertical temperature stratification was assessed with a thermistor chain deployed in location "T" (Fig. 4.1). The chain consisted of 10 RBR thermistors (Solo T, RBR Ltd.) with a temperature accuracy of  $\pm 0.002$  °C and 5 Hobo loggers (TidbiT v2, Onset Computer) with an accuracy of  $\pm 0.2$  °C. Data were sampled every 5 minutes. Data were available from June to October 2015 and from May until mid-August 2016.

### 4.2.5 Turbulence estimation

To assess the effect of turbulence on zooplankton swimming velocity, profiles of temperature fluctuations were acquired at location "S" (Fig. 4.1) with a Self-Contained Autonomous MicroProfiler (SCAMP), a temperature microstructure profiler. After splitting each profile into 256-point (25 cm) segments, turbulence was assessed in terms of turbulent kinetic energy (TKE) dissipation rates  $\varepsilon$ . Dissipation rates were estimated for each segment using the theoretical spectrum proposed by Batchelor (1959):

$$S_B(k) = \sqrt{\frac{q}{2}} \frac{\chi_T}{k_B D_T} \alpha \left( e^{-\alpha^2/2} / 2 - \alpha \int_{\alpha}^{-\infty} e^{-x^2/2} dx \right) \quad (4.2)$$

where  $q=3.4$  is an universal constant (Ruddick et al., 2000),  $k_B = (\varepsilon/\nu D_T^2)^{1/4}$  the Batchelor wavenumber,  $k$  the wavenumber and  $\alpha = k k_B^{-1} \sqrt{2q}$ . By fitting the observed spectrum  $S_{obs}$  to  $S_B(k)$ , it was possible to estimate  $k_B$  and then  $\varepsilon$ . Bad fits, that provided invalid  $\varepsilon$ , were rejected and removed using the statistical criteria proposed by Ruddick et al. (2000).

On each date, an average of six turbulence profiles were acquired to ensure a statistically-reliable estimation of  $\varepsilon$ . Profiles were then time-averaged to obtain one profile per sampling date. Profiles from 17 September 2015 and 9 June 2016 were not processed because the SCAMP thermistors provided unreliable data.

### 4.2.6 Chlorophyll-*a* concentration

Chlorophyll-*a* concentration profiles were acquired at the sampling station "S" (Fig. 4.1). Data were collected from approximately 0.5 m from the lake surface with a depth resolution of 2 mm between 5 hours and 5 minutes before dusk. Chlorophyll-*a* was sampled five times in July-August 2015 and ten times between

May and August 2016 (see black triangles in Fig. 4.9). At least five profiles were sampled on each date.

Profiles were acquired using a fluorometer mounted on the SCAMP. The sensor excites the water with a blue L.E.D. emitter at 455 nm in a glass tube to avoid interference with ambient lighting. It then measures the voltage from the light emitted from the chlorophyll with a photo-diode. On each date, voltage profiles were binned every 30 cm and time-averaged to obtain one profile. Voltage data were finally converted to chlorophyll-*a* concentration using a linear calibration curve provided in Appendix 4.7.1.

### 4.2.7 Underwater light conditions

To characterise the underwater light conditions, surface solar radiation  $I_0$  was measured with a frequency of 5 minutes by a meteorological station located in Kilmersdon (Radstock, UK), 2 km from the site. Data were available for the studied period with the exception of 4 July 2016. Photosynthetically active radiation (PAR) profiles  $I_{PAR}$  were also collected at the same time as chlorophyll-*a* concentration profiles. The PAR was measured with a Li-Cor LT-192SA underwater radiation sensor mounted facing upwards on the SCAMP. On each sampling date,  $I_{PAR}$  profiles were filtered with a moving average filter to remove noise and then binned and time-averaged to obtain a mean PAR profile  $\overline{I_{PAR}}$ . Profiles collected on 16 July 2016 were discarded because no valid data were recorded. A 20-cm Secchi disk was employed to measure the Secchi depth  $z_{SD}$  in June-July 2015 and April-August 2016.

## 4.2.8 Zooplankton concentration

Zooplankton samples were also collected to characterise the zooplankton population density and their vertical distribution. A conical net (Hydro-Bios) mounted on a stainless-steel hoop with a cowl cone (mesh=100  $\mu\text{m}$ , diameter  $d=100$  mm, length approximately 50 cm) was used for this purpose. The water column was sampled at location "S" (Fig. 4.1) before the DVM, by towing the net through consecutive layers of thickness  $h=3$  m. Three samples ( $n = 3$ ) were collected and pooled for each stratum. Samples were then stored in a 70% ethanol solution to fix and preserve the organisms and prevent decomposition (Black and Dodson, 2003). Four tows were acquired in June-July 2015 and 10 tows from May to August 2016.

Zooplankton were enumerated by counting the organisms under a dissecting microscope in three replicate sub-samples of each sample. Four zooplankton groups were distinguished: *Daphnia* spp., adult and copepodite-stage copepods, small Cladocera and copepods nauplii. The concentration of each group was then estimated by dividing the abundance by the filtered water volume  $V = \pi/4 \cdot d^2 \cdot h/n$ .

## 4.3 Results

### 4.3.1 Bulk velocity

Fig. 4.4 shows the time series of bulk velocity  $v_{up}$  (grey dots) at sunset for both years using the developed image-detection algorithm. Each point in the figure also includes error bars (the 95% confidence interval from the bootstrap analysis of the valid fittings of  $v_{up}$ ). Some error bars are not visible because the interval is too small.

Bulk velocity at sunset in 2015 ranged from a minimum of  $2.23 \text{ mm s}^{-1}$  on 12 July to a maximum of  $3.55 \text{ mm s}^{-1}$  on 22 July. The time series of  $v_{up}$  in 2016 showed similar values with a lowest of  $2 \text{ mm s}^{-1}$  at the beginning of June and a maximum of  $4.5 \text{ mm s}^{-1}$  in mid-August. Both time series showed a positive increasing trend over time, as suggested by the dashed lines fitted to the data. The bulk velocity at sunrise showed instead a weak trend over time with a mean of  $1.78 \pm 0.08 \text{ mm s}^{-1}$  in 2015 and  $1.71 \pm 0.1 \text{ mm s}^{-1}$  in the following year.

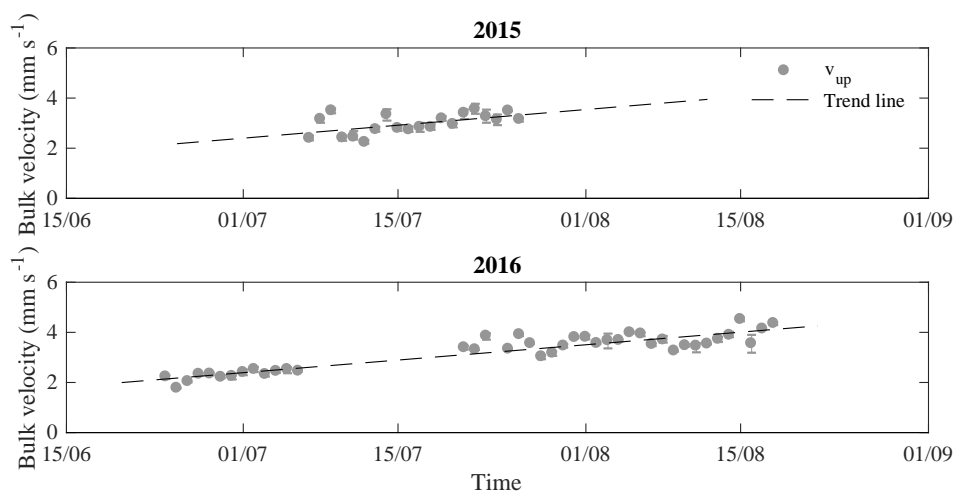


Figure 4.4: Time series of bulk velocity  $v_{up}$  at sunset in 2015 and 2016. Error bars show the 95% confidence interval from the bootstrap method. The black dashed lines show the trend lines fitted to the points.

### 4.3.2 Temperature measurements

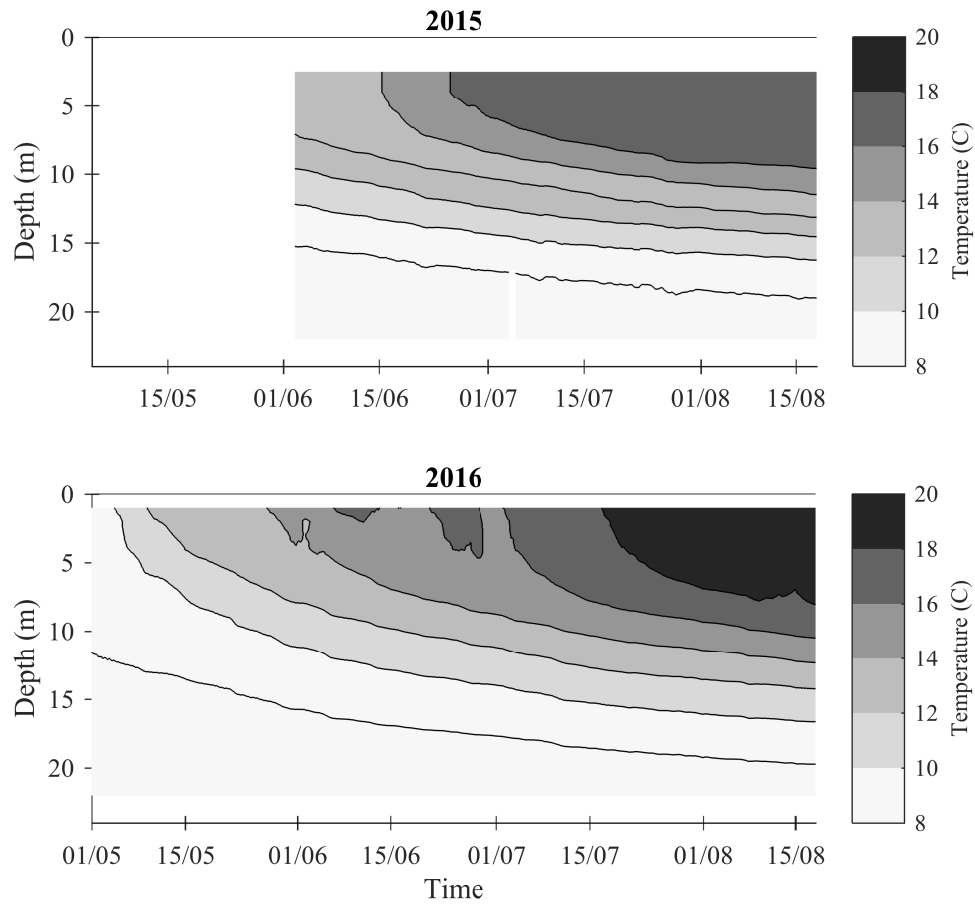


Figure 4.5: Contour plot of temperature in 2015 (panel above) and 2016 (panel below) from the thermistor chain.

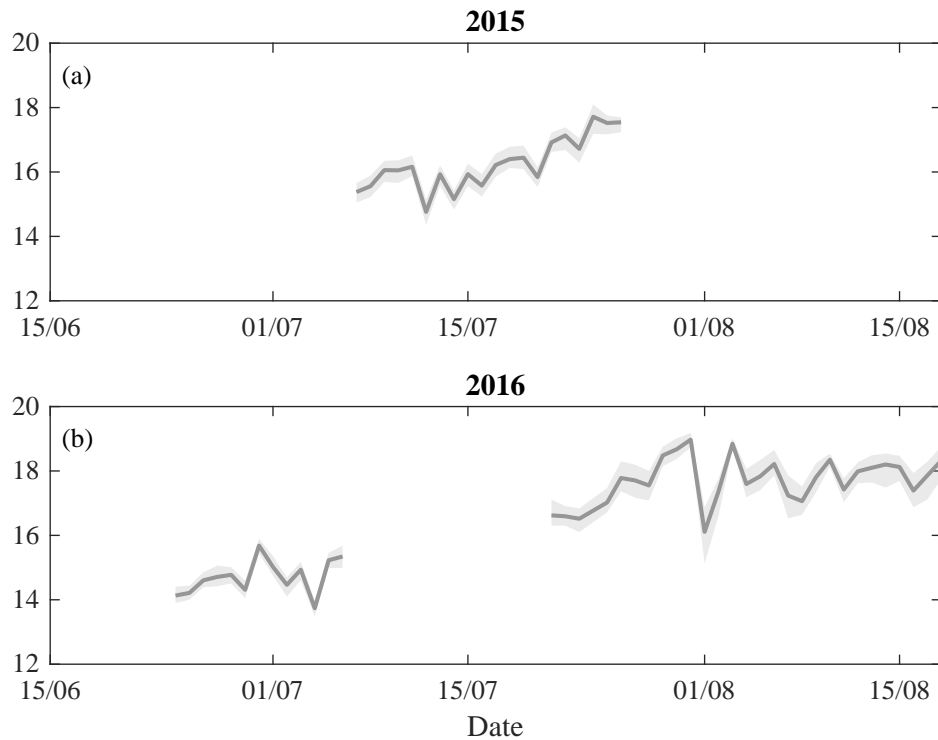


Figure 4.6: Mean temperature in the migrating layer (thick line) and its 95% confidence interval (shaded area).

The daily average temperature in Fig. 4.5 showed that the lake was already stratified in June 2015 and the epilimnion started to deepen at the end of the same month. In 2016 the water temperature varied little with depth in early May and stratification began to form in mid-May. During the summer months, the water temperature reached 20°C. The mean temperature that the zooplankton experienced during the ascent phase of the DVM can be obtained by overlapping the thermistor chain data with the position and timing of the zooplankton acoustic layer for each migration date. The mean temperature is reported in Fig. 4.6 (thick line) with the 95% confidence interval (shaded area).



### 4.3.3 Dissipation rates of TKE

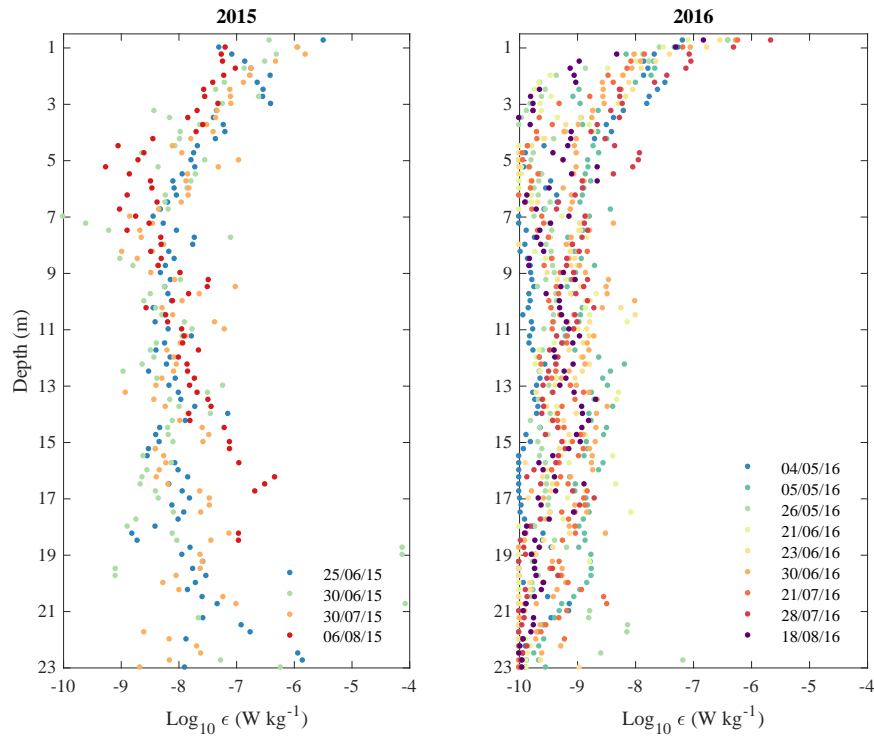


Figure 4.7: Mean profiles of TKE dissipation rates  $\varepsilon$  (dots) on a logarithmic scale.

Averaged profiles of  $\varepsilon$  are reported in Fig. 4.7 and showed that the TKE dissipation rates were highest in the surface layer, with  $\varepsilon$  approaching  $10^{-6} \text{ W kg}^{-1}$  in both years. Turbulence decreased moving away from the surface with  $\varepsilon < 10^{-8} \text{ W kg}^{-1}$ . Fig. 4.8 reports instead the time series of  $\varepsilon$  after depth-averaging the profiles. The mean dissipation level in the water column showed little evidence of a systematic trend over time in both years with  $\varepsilon \sim 10^{-8} \text{ W kg}^{-1}$  in 2015 and with calmer conditions in 2016 ( $\varepsilon \sim 10^{-9.3} \text{ W kg}^{-1}$ ).

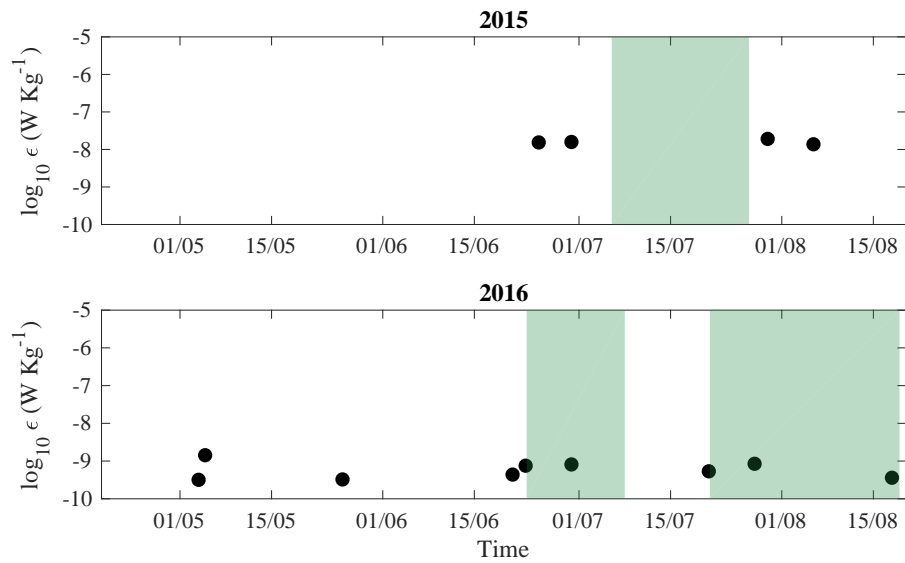


Figure 4.8: Time series of time and depth-average TKE dissipation rates  $\epsilon$  (dots) on a logarithmic scale. The green areas show the time period when the acoustic measurements are available.

#### 4.3.4 Chlorophyll-*a* concentration

The concentration of chlorophyll-*a* was very low for both years (Fig. 4.9). In 2015 the concentration in the water column peaked at  $2.5 \mu\text{g L}^{-1}$  near the lake bottom at the end of June. In 2016 the concentration showed a maximum at the beginning of the time series (early May) and it reached a deep maximum of  $5 \mu\text{g L}^{-1}$  in July below 10 m. For most of the stratification period, the vertical distribution was nearly homogenous with very little variations.

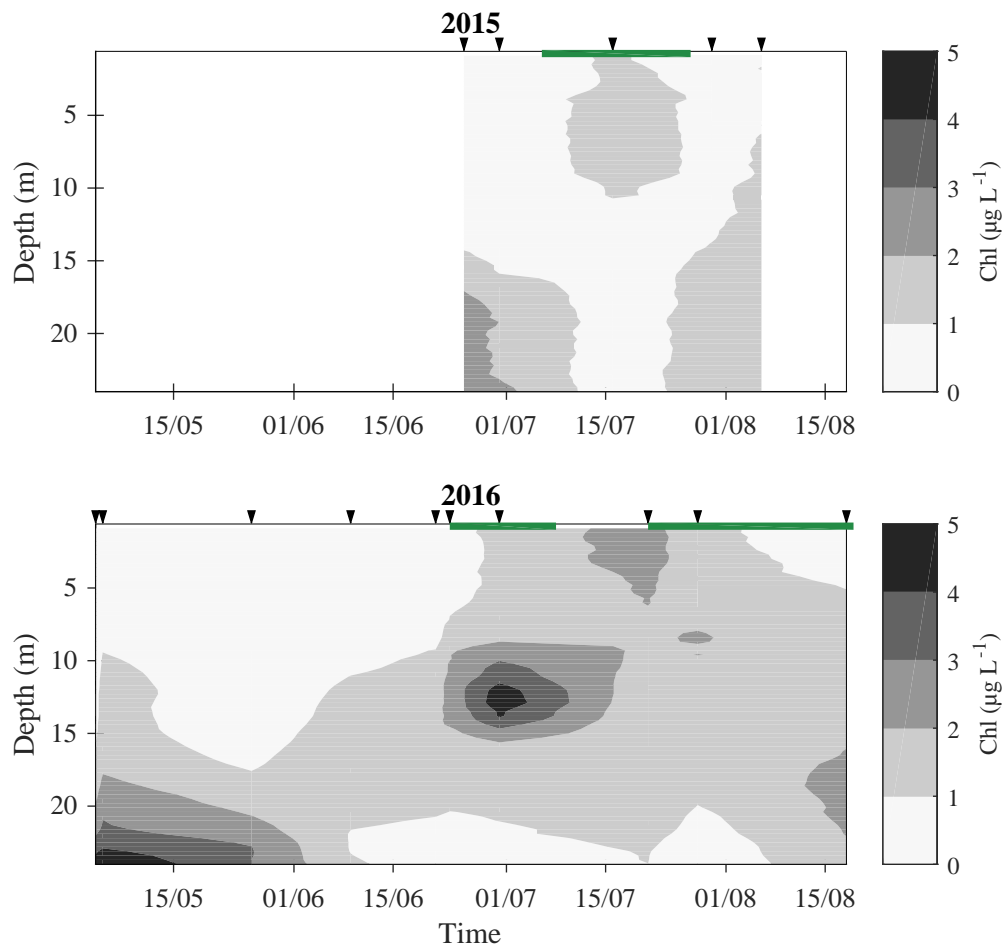


Figure 4.9: Contour plot of chlorophyll-a concentration profiles collected in the lake in 2015 and 2016. The colour-bar on the right shows the measured concentration while the black triangles indicate the time when vertical profiles were collected with the SCAMP fluorometer. The green lines show the periods when the acoustic measurements were taken.

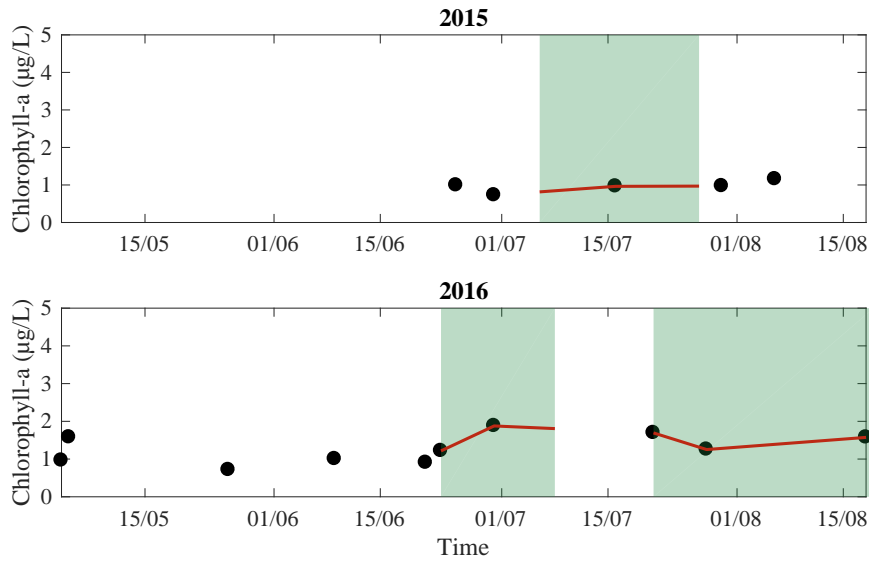


Figure 4.10: Time series of water-column-averaged concentration of chlorophyll-*a* in 2015 and 2016. Black dots indicate the day when the chlorophyll-*a* profiles were averaged. The red line represents the time series employed in the correlation. The green areas show the time period when the acoustic measurements are available.

Potential food availability during the DVM was estimated by vertically-averaging the chlorophyll-*a* concentration from the available chlorophyll-*a* profiles. The dots in Fig. 4.10 depicts the resulting time series. Since chlorophyll concentration was not available for all the dates with the acoustic measurements (green areas), a linear interpolation was used to estimate missing chlorophyll concentration data between the available observations. The red line is the final time series used in subsequent correlations.

### 4.3.5 Underwater light conditions

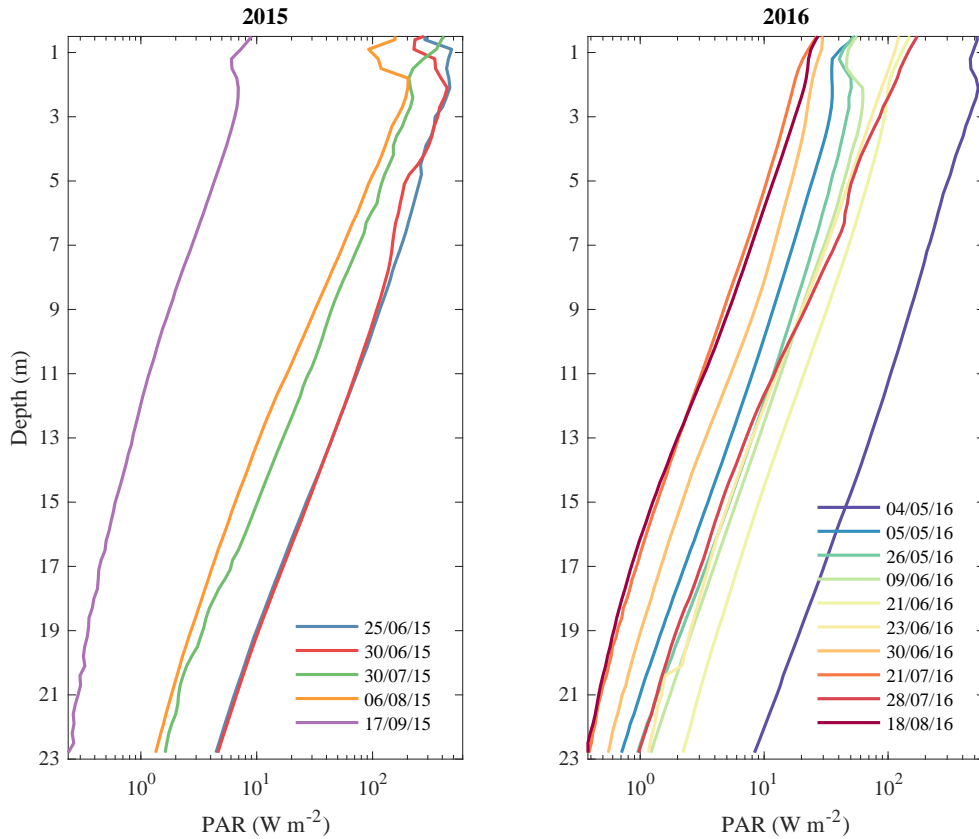


Figure 4.11: *Photosynthetically active radiation (PAR) profiles in 2015 and 2016 on a logarithmic scale.*

PAR profiles are reported in Fig. 4.11 on a semi-logarithmic scale. All profiles showed a linear trend, with the exception of the data above 1 m, indicating an exponential decay with depth of the ambient light in the water column. Some profiles provided  $\overline{I_{PAR}} < 50 \text{ W m}^{-2}$  because they were collected near dusk. The Secchi disk depths in Fig. 4.12 showed a mean depth of  $10.4 \pm 2 \text{ m}$  in 2015 with a decreasing trend after the beginning of July despite a constant and low

chlorophyll concentration in the water column (see Fig. 4.9). In 2016  $z_{SD}$  was on average  $10.1 \pm 1$  m and never fell below 8 m.

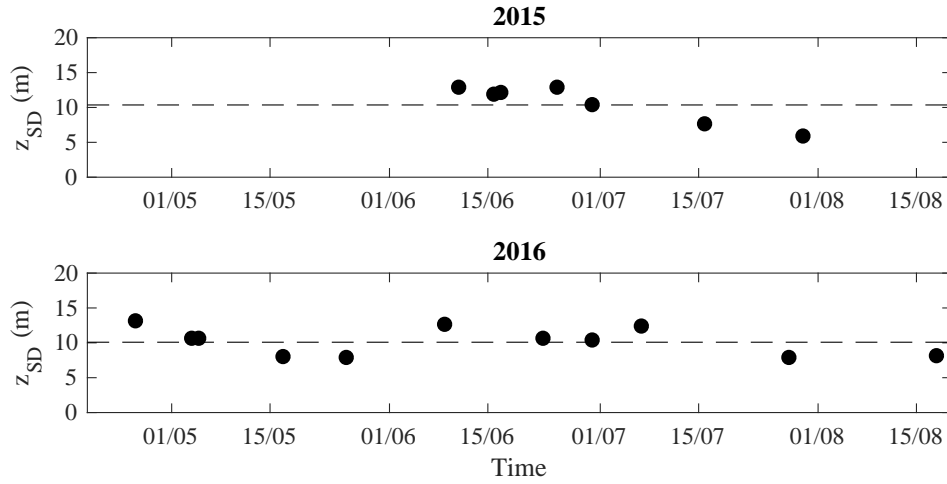


Figure 4.12: Time series of Secchi disk depth  $z_{SD}$  in 2015 and 2016. The dashed horizontal line represents the mean depth from the data.

The light extinction coefficient  $K_{PAR}$  was then estimated by fitting the Lambert-Beer equation to each  $\overline{I_{PAR}}$  profile (Armengol et al., 2003):

$$\overline{I_{PAR}} = \overline{I_{PAR,0}} \cdot e^{-K_{PAR} \cdot z} \quad (4.3)$$

where  $\overline{I_{PAR,0}}$  is the surface PAR. The ambient attenuation coefficients were also determined from the Secchi disk depth  $z_{SD}$  using the following empirical relationship (Armengol et al., 2003):

$$K_{SD} = 1.7/z_{SD} \quad (4.4)$$

The time series of  $K_{PAR}$  and  $K_{SD}$  in Fig. 4.13 showed a good agreement between the two methods. The coefficient  $K$  showed a negative trend in 2015, with a mean value of  $0.19 \pm 0.03 \text{ m}^{-1}$ , and stationary conditions in 2016 with a mean of  $0.18 \pm 0.01 \text{ m}^{-1}$ . It never exceeded  $0.22 \text{ m}^{-1}$ , with the exception of  $K_{SD}$  at the end of July.

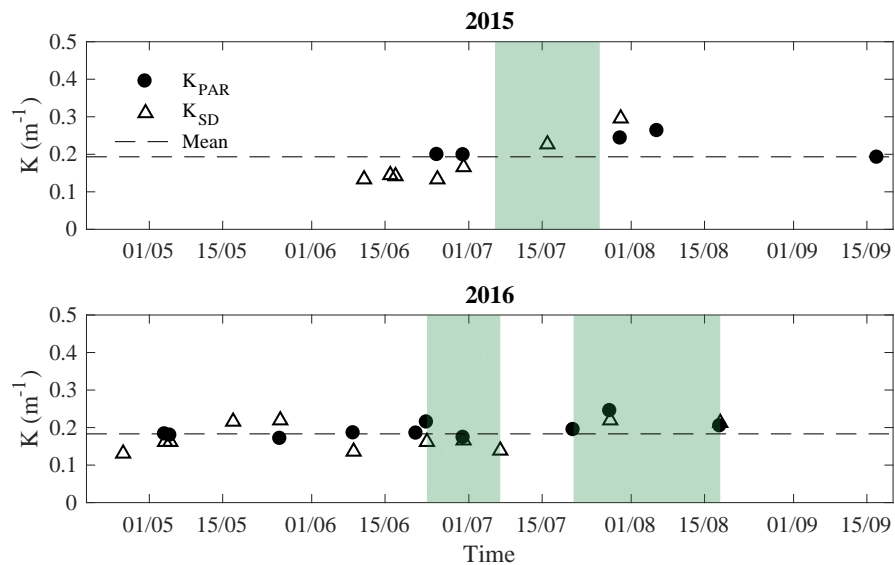


Figure 4.13: Time series of light extinction coefficients from PAR profiles (black circles) and Secchi depths (empty triangles). The green areas show the time period when the acoustic measurements are available.

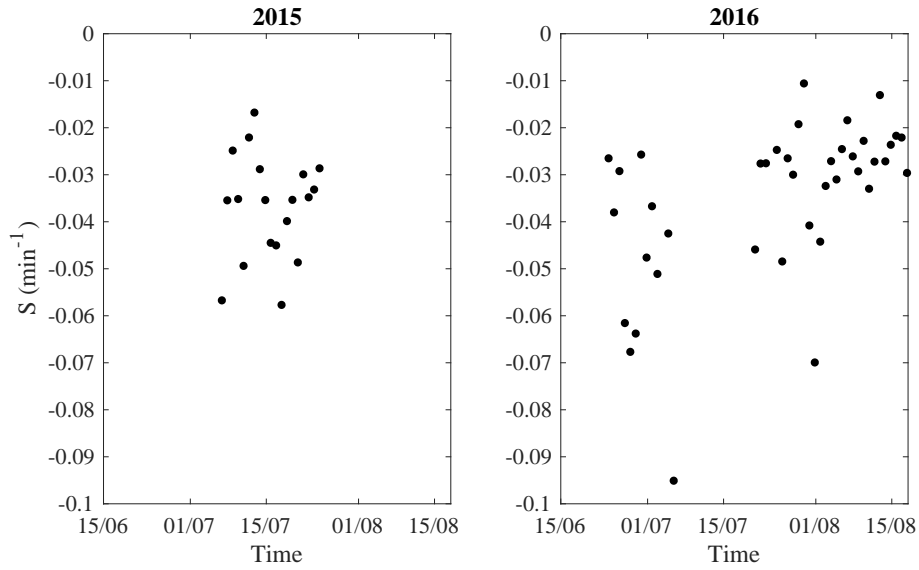


Figure 4.14: Time series of mean relative change in light intensity  $S$  during the migration.

The underwater light conditions, at the depth where the zooplankton started the DVM, can be described in terms of relative change in light intensity  $S$  (Ringelberg and Flik, 1994). This quantity can be estimated by using the definition provided by Ringelberg (1999) and assuming that the light intensity  $I$  in the water column decayed exponentially with the depth  $z$ :

$$S = \frac{d \ln I(t)}{dt} = \frac{d \ln I_0(t)}{dt} - \frac{dK(t)}{dt} \cdot z \quad (4.5)$$

where  $t$  is the time,  $I_0$  the surface solar radiation and  $K$  the light extinction coefficient. Because  $K$  could be assumed to be time-independent (Fig. 4.13),  $S$  was depth-independent and reduced to:

$$S = \frac{d \ln I_0(t)}{dt} \quad (4.6)$$



By employing a linear correlation to the time series of the natural log of the solar radiation ( $\ln I_0(t)$ ) during the DVM, a slope can be estimated that provided the mean value of  $S$  (Fig. 4.14).  $S$  was always negative and in most of the cases was within the range  $S = -[0.04, 0.1] \text{ min}^{-1}$  suggested for inducing phototactic behaviour in *Daphnia* (Ringelberg, 2010).

### 4.3.6 Zooplankton concentration

The time series of the average and maximum vertical concentration in the water column for the four zooplankton groups are reported in Fig. 4.15.

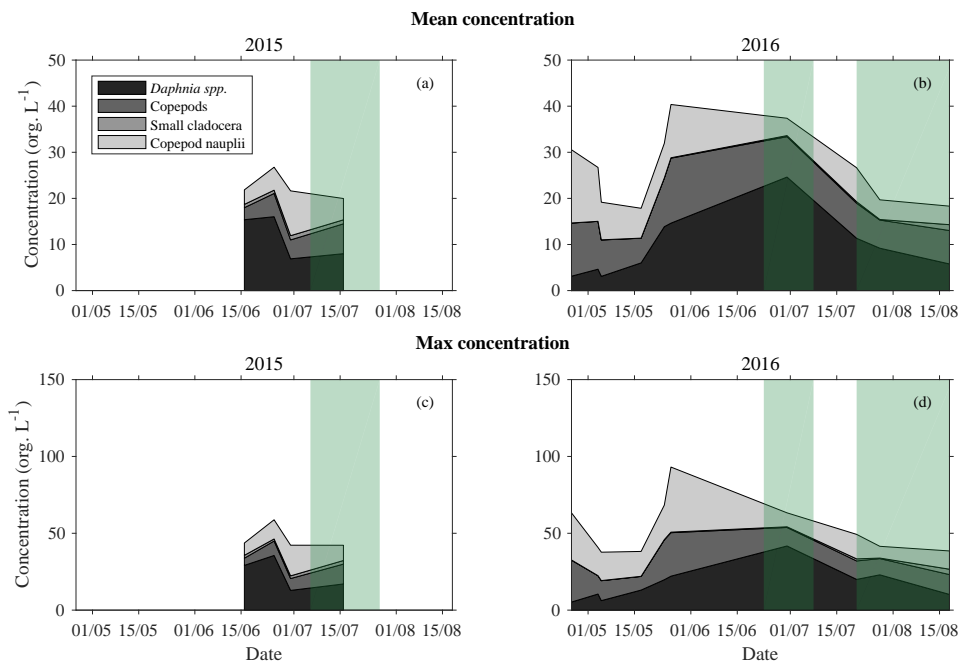


Figure 4.15: Stacked plots of mean concentration in the water column (panel a and b) and maximum concentration (panel c and d) of *Daphnia spp.*, adult and copepodite-stage copepods, small Cladocera and copepod nauplii. The green areas show the time period when the acoustic measurements are available.

The time series in 2015 (panel a) showed that *Daphnia* was dominant, accounting for up the 80% of the mean concentration in the water column in June. The concentration remained almost constant until the end of the same month and then it started decreasing reaching a minimum of 7 org. L<sup>-1</sup> in July. The concentration of adult, copepodite and naupliar stages of copepods was very small in June (~ 5 org. L<sup>-1</sup>) but in mid-July they became as abundant as *Daphnia* with an average density of up 10 org L<sup>-1</sup>. The maximum concentration of zooplankton (panel c) followed the same trend with a peak of 35 org. L<sup>-1</sup> of *Daphnia* at the end of June and a maximum of 20 org. L<sup>-1</sup> of copepods (including nauplii).

Data in 2016 displayed a more complete picture of the zooplankton density dynamics. From late April until June, copepods dominated with an average concentration of 27 org. L<sup>-1</sup> (panel b). The *Daphnia* population increased throughout May peaking at 25 org. L<sup>-1</sup> in July. The density of small cladocera remained very low and negligible with respect to the other species. For the remainder of the summer the total zooplankton abundance decreased, until the end of August where a maximum of 5 org. L<sup>-1</sup> of *Daphnia* and 11 org. L<sup>-1</sup> of copepods were observed. The maximum abundance in 2016 (panel d) was very similar in magnitude to that observed in 2015 with the exception of copepod nauplii whose abundance reached 42 org. L<sup>-1</sup> in late May. The concentration declined quickly with a minimum of 12 org. L<sup>-1</sup> at the end of the time series.

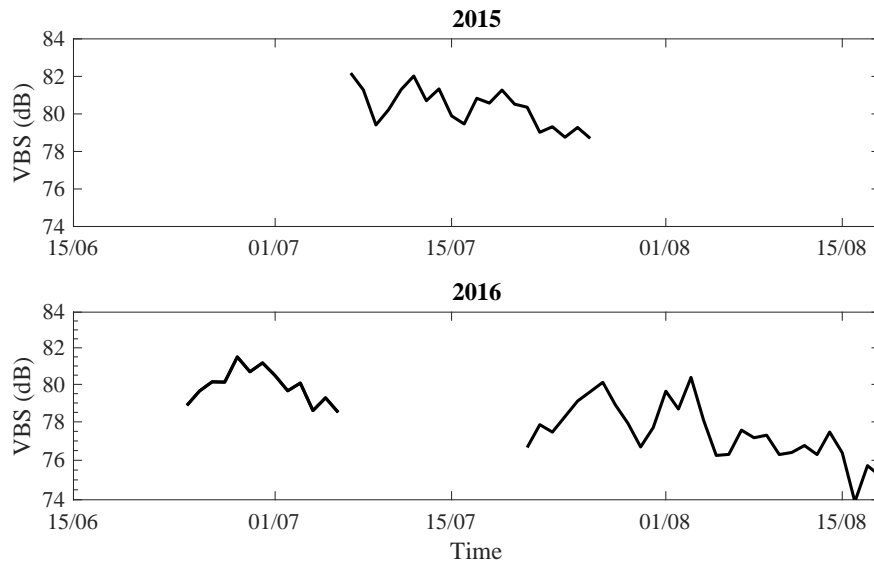


Figure 4.16: Mean volume backscatter strength of the migrating layer during the DVM in 2015 and 2016.

Net tows do not however quantify zooplankton concentration within the migrating layer and during the DVM with adequate time and vertical resolution. However, the VBS can be used to provide suitably-resolved data on zooplankton concentration and size (Barth et al., 2014; Hembre and Megard, 2003; Huber et al., 2011; Inoue et al., 2016; Record and de Young, 2006; Sutor et al., 2005) and was available during the DVM. Fig. 4.16 reports the mean value of VBS within the layer on each migration date. The 95% confidence interval was not reported because was too small.

### 4.3.7 Zooplankton position

The VBS data can be further used to extract more information about the zooplankton behaviour in relation to the DVM. The acoustic shape (Fig. 4.2c) from

the image-processing algorithm also provides the zooplankton position in the water column prior the DVM and when the migration ends. By taking the average of the upper and lower limits of the shape when the DVM begins ( $Z_{s, \text{lower}}$  and  $Z_{s, \text{upper}}$ ), it is possible to infer the average depth range within which the organisms were found before moving. The result is reported in Fig. 4.17 for both years (black dots). By repeating the same operation when the DVM stops, the two depths  $Z_{e, \text{lower}}$  and  $Z_{e, \text{upper}}$  once averaged, provide the mean location where the organisms completed the migration and started spreading out near the surface. This is shown by the empty dots. Prior to migration, zooplankton were found at an average depth of 12.2 m in both years with a 95% confidence interval  $CI_{95}=[11.8, 12.6]$  m in 2015 and  $CI_{95}=[11.9, 12.4]$  m in 2016. The depth where they stopped migrating was 5 m with  $CI_{95}=[4.7, 5.5]$  m in 2015 and  $CI_{95}=[4.5, 5.3]$  m in 2016.

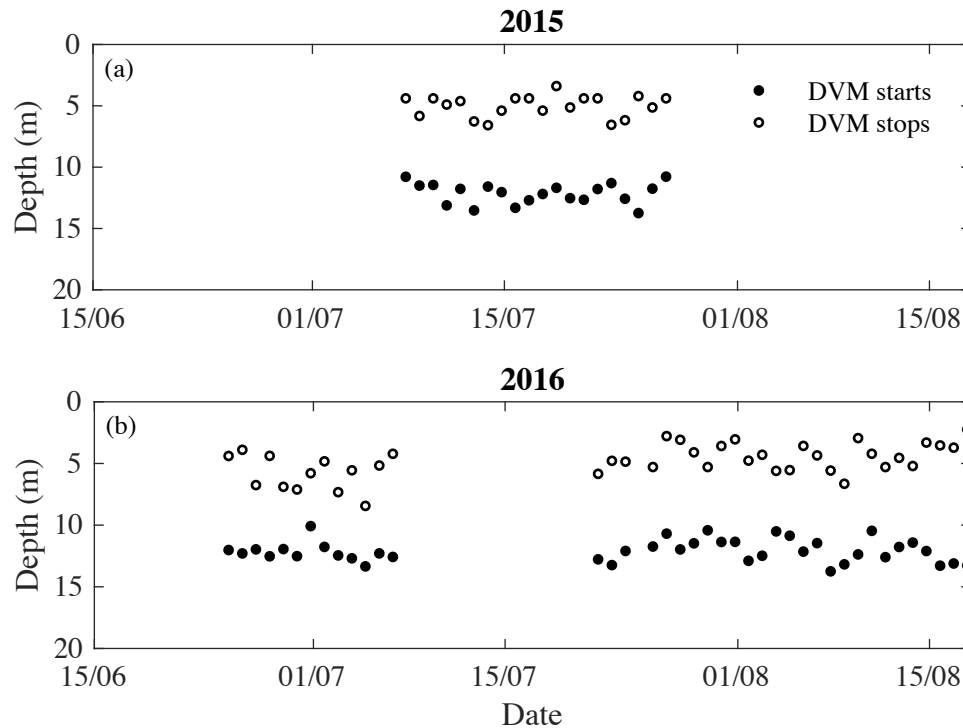


Figure 4.17: Mean zooplankton position before the DVM (full dots) and after DVM (empty dots) when they reach the surface in 2015 (panel a) and 2016 (panel b).

## Correlation

To investigate potential drivers of the observed variability in  $v_{up}$ , the upwards bulk velocity was linearly correlated with the temperature (Fig. 4.6), chlorophyll-*a* concentration (Fig. 4.10), the light conditions during the DVM (Fig. 4.14) and the VBS as a proxy for the *in situ* concentration and size (Fig. 4.16). The dissipation rates  $\varepsilon$  (Fig. 4.8) were not used in the correlation. Turbulence values could not be interpolated because of their patchy and unsteady nature. Prior to further analysis, we removed one sampling date due to the absence of data on  $S$  in 2016.

The predictors to be included in the multiple linear regression model were

Table 4.1: *Correlation matrix of the regression coefficient for the volume backscatter strength (VBS), temperature (T), chlorophyll concentration (Chl) and relative change in light intensity (S)*

	VBS	T	Chl	S
VBS	1			
T	-0.645	1		
Chl	-0.376	-0.076	1	
S	-0.088	-0.364	0.649	1

Table 4.2: *Variance inflation factor (VIF) for the predictors*

$VIF_{VBS}$	$VIF_T$	$VIF_{Chl}$	$VIF_S$
2.532	2.513	2.135	2.123

tested to assess any possible multicollinearity. The correlation matrix of the variables (Table 4.1) shows that the *VBS* was negatively correlated with the temperature *T* ( $R_{VBS,T} = -0.645$ ) and weakly related to the chlorophyll-*a* concentration ( $R_{VBS,Chl} = -0.375$ ). Chlorophyll concentration was also correlated with the light availability with  $R_{S,Chl} = 0.649$ . However, the variance inflation factor (VIF) index for each of the predictors in Table 4.2 shows that the collinearity among the three variables was weak and unimportant ( $VIF_{VBS} = 2.532$ ,  $VBS_{Chl} = 2.123$  and  $VIF_S = 2.123 < 5$ ). Variations in the chlorophyll-*a* concentration were in reality very small and any small interdependence was a numeric artefact.

A model fitting dataset was created from the data by extracting 46 random observations (about 80% of the original sample). The remaining 12 observations constituted the validation dataset that was later used to validate the prediction of the fitted model. A multiple linear regression was applied to the 46 observations with a significance level  $\alpha = 0.01$ . The model results indicated that there was no significant statistical correlation between  $v_{up}$  and the relative change in light intensity *S* ( $F$  statistic =  $-0.927$ ,  $p$  value =  $0.358$ ), the food (chlorophyll) concentration ( $F = -0.2420$ ,  $p = 0.810$ ) and *VBS* ( $F = -2.0328$ ,  $p = 0.0482$ ).

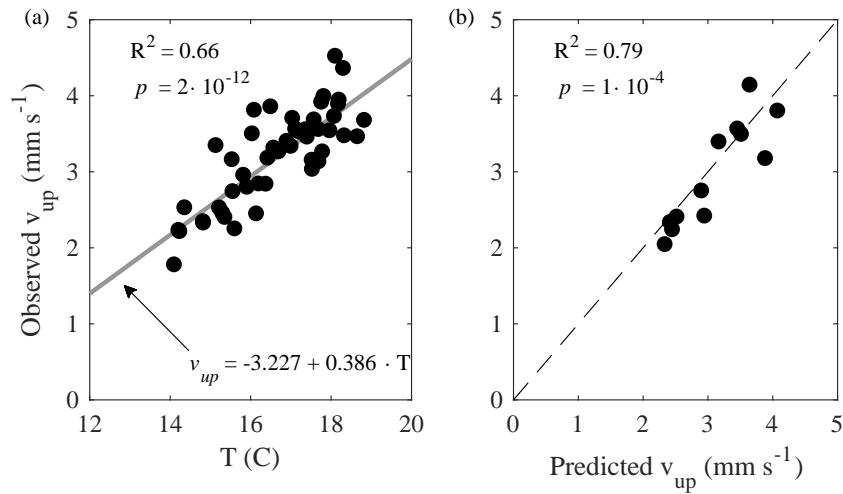


Figure 4.18: Panel a shows the correlation between  $T$  and the observed upwards velocity. The grey line represents the fitted model to the regression dataset whose equation is reported in the bottom right corner. The upper left corner displays the coefficient of determination  $R^2$  and the  $p$  value of the regression. Panel b shows the relation between the observed  $v_{up}$  from the validation dataset and the prediction from the regression model (dots). The dashed line is the 1:1 relationship.

The upwards velocity was, instead, significantly correlated with changes in temperature  $T$  ( $F = 4.933$  and  $p = 1.26 \cdot 10^{-5}$ ). The linear regression model was further simplified by excluding the other predictors and the result is reported in Fig. 4.18a with  $p = 2 \cdot 10^{-12}$  and a coefficient of determination  $R^2 = 0.66$ . The final regression model also predicted reasonably well the observations from the validation dataset (Fig. 4.18b) with  $p = 1 \cdot 10^{-4}$  and  $R^2 = 0.79$ .

## 4.4 Discussion

We used for the first time acoustic measurements to quantify the time series of zooplankton displacement velocity during the DVM in an oligotrophic lake.

Based upon environmental measurements we aimed to infer the environmental drivers that might influence the rate of zooplankton migration in the field.

#### 4.4.1 Upwards bulk velocity

In our correlation model, we hypothesised that  $v_{up}$  may depend on temperature, zooplankton density, food availability, and light intensity. Because of lack of sufficient data, fish abundance and turbulence were not included in the correlation. The effect of temperature on zooplankton swimming velocity has been demonstrated by laboratory studies of single swimming organisms (Ringelberg, 2010). When temperature increases, zooplankton metabolic activity rates change (Beveridge et al., 2010; Gorski and Dodson, 1996; Heinle, 1969), and they can also swim faster because of the reduced drag exerted on their swimming appendages (Larsen and Riisgård, 2009). Temperature can also enhance *Daphnia* phototactic response (Van Gool and Ringelberg, 2003) and indirectly affect their displacement velocity during migration. The strong correlation between  $v_{up}$  and temperature is a likely signal of this effect in the field.

In principle, if zooplankton are present at very high population densities while migrating, organisms would have to reduce the velocity they can swim at to avoid encounter with other animals (i.e. the surrounding space for moving would be limited). The instantaneous speed and the resulting bulk velocity would be smaller. In the opposite scenario, with a low abundance within the migrating layer, organisms would be free to swim unobstructed, reaching the maximum thrust they can propel at, resulting in a higher bulk velocity. Our dataset showed however that the  $VBS$  was weakly correlated with  $v_{up}$  probably because the zooplankton concentration was not high enough to yield such collective swimming behaviour.

Food availability can both positively and negatively affect *Daphnia* migration velocity depending on environmental conditions and genetic differences



(Dodson et al., 1997a). Our analysis, however, did not provide evidence of this effect because of the stationary chlorophyll-*a* concentration during the period over which the migration velocities changed. Surprisingly the bulk velocity was not affected by the average change in light intensity. Light changes can influence zooplankton displacement velocity during the DVM (Ringelberg and Flik, 1994; Ringelberg et al., 1991) but this reaction likely disappears when the displacement velocity is averaged over the whole migration duration. Moreover our analysis focused on changes in migration velocity at a seasonal scale rather than the response from a single DVM.

The lack of data on fish abundance and kairomone concentrations did not allow direct inclusion of predation pressure in our analyses. However, some speculations can be made about its possible effect. While we observed an increasing near-linear temporal trend in  $v_{up}$ , predation often has a seasonal peak coinciding with the time at which larval fish hatch and begin actively feeding upon zooplankton; this leads to a stronger zooplankton responsiveness to light limited to that specific period (Van Gool and Ringelberg, 2003). The zooplankton layer depth prior the DVM (black dots in Fig. 4.17) suggests that the organisms did not change their vertical position during the observation period and they resided on average at the same depth in both years. If a strong pressure had appeared at some point, a repositioning of the population towards deeper layers would have been expected (Dodson, 1990; Leach et al., 2014). However, the near-constant migration amplitude suggests that visual predation pressure was present and consistent throughout the whole study period, and thus a sudden increase in that pressure appears unlikely.

Turbulence was not included in our model either. Available measurements could not be interpolated to fill the gaps of missing observations. However, Fig. 4.8 shows that  $\varepsilon$  was constant and very low, approaching the background dissipation level. The lack of a clear temporal trend in turbulence, suggest that this could not be an important driver of the observed trend in zooplankton migration velocity.

The correlation model showed that temperature was a primary factor in controlling migration speed in the field. Because zooplankton swim in a low-Reynolds-number environment, temperature dependent viscosity is a crucial mediator of their motility. Assuming that the viscosity mainly controls the organism swimming response (Larsen and Riisgård, 2009), our dataset showed that a viscosity variation of 13% led to an increase in velocity of about 61%, from  $\nu = 1.1 \cdot 10^{-6} \text{ m}^2 \text{ s}^{-1}$  at the start of the dataset to  $\nu = 1.8 \cdot 10^{-6} \text{ m}^2 \text{ s}^{-1}$  in August. The same variation was observed by Larsen et al. (2008) in the lab, but over a wider viscosity range (about 36%) for the instantaneous velocity of the copepod *Acartia tonsa*. Moison et al. (2012) found instead an increase of 29% in the speed of *Temora longicornis* for a viscosity variation of 15%. Because we were dealing with a mean velocity during the migration and no further studies were available, it was not possible to make any direct comparisons with other experiments.

#### 4.4.2 Ecological implications

Understanding the behaviour and responses of diel migrators to environmental conditions is essential to knowledge of ecosystem functioning. Zooplankton experience varying temperatures in lakes due to short-term meteorological forcing and seasonality or as a function of the water depth, when organisms swim vertically. According to our analyses, changes in water temperature and viscosity can affect migration velocity, and by extension, escape reactions from predators. Since zooplankton are a food resource for planktivorous fish, temperature changes may indirectly alter patterns of predation, and thus trophic interactions and energy flows in lake food webs via this mechanism. Finally, temperature also affects zooplankton metabolism potentially impacting patterns in excretion and faecal pellet production throughout the water column and altering biogeochemical fluxes of nutrients and carbon.

## 4.5 Conclusions

In this study we assessed the mean displacement velocity of zooplankton from the slope of the zooplankton layer during the DVM at sunset and sunrise. The upwards bulk velocity  $v_{up}$  exhibited an increasing pattern over time which was strongly correlated with the temperature in the layer during the migration. Based upon our analysis, chlorophyll concentration, relative change of light intensity, and zooplankton concentration and size during the DVM did not seem to play an important role in affecting  $v_{up}$ . This suggests that temperature may be a key mechanical factor controlling swimming activity. Temperature can increase metabolic rates and zooplankton require less effort to propel themselves in a less viscous fluid. The relationship between temperature and velocity has, so far, only been demonstrated under greatly-simplified conditions in lab experiments (Larsen and Riisgård, 2009). We demonstrate, for the first time, the potential for the same effect to be significant in the field. In the field it is not however possible to separate the direct effect of the temperature (physiological effect) and the indirect impact of viscosity (mechanical effect). Our correlation did not account for any effect due to predation pressure. However, because we did not observe changes in the zooplankton daytime-depth or migration amplitude during the two years, we hypothesise that the intensity of visual predation was consistent throughout our study period, and could not explain the changes in migration velocity that occurred. Although predation pressure may be important in determining whether migration happens at all, temperature may be more important in governing migration velocity, when this behaviour does occur.

Since temperature is a key component controlling zooplankton hydrodynamics, changes in zooplankton swimming velocity may have implications in relation to nutrient and carbon transport, trophic interactions and web food structure. Therefore, understanding zooplankton behaviour and responses to exogenous factors during the upwards DVM is ecologically important.

## 4.6 Acknowledgements

Funding for this work was provided by a UK Royal Society Research Grant (Y0106-WAIN) and an EU Marie Curie Career Integration Grant (PCIG14-GA-2013-630917) awarded to D. J. Wain. We would also like to thanks Tim Clements for allowing us access to Vobster Quay.

## 4.7 Appendix

### 4.7.1 SCAMP fluorometer calibration curve

Voltage data from the SCAMP fluorometer can be linearly related to chlorophyll-*a* concentration, once the SCAMP calibration curve is known. This relationship has been produced by comparing voltage and chlorophyll-*a* profiles collected in 2016 from Blagdon Lake, an eutrophic lake located in Blagdon (England) and Llandegfedd Reservoir, an oligotrophic basin in Pontypool (Wales).

Chlorophyll-*a* was measured using a calibrated fluorometer from an EXO3 multi-parameter sonde manufactured by YSI with a vertical resolution of 30 cm. Four profiles in four different locations were available from Blagdon lake and one profile from Llandegfedd Reservoir.

Five SCAMP voltage profiles were acquired at the same time in each location with a depth increment of 2 mm. In each site, the five SCAMP profiles have been binned every 30 cm and time-averaged to obtain one profile.

From each bin of the voltage and chlorophyll-*a* profiles, the corresponding sampled points have been extracted (stars and circles in Fig. 4.19). A line was finally fitted to the points to obtain the calibration equation reported in the figure. The coefficient of determination  $R^2 = 0.93$  suggests that the correlation was strong.

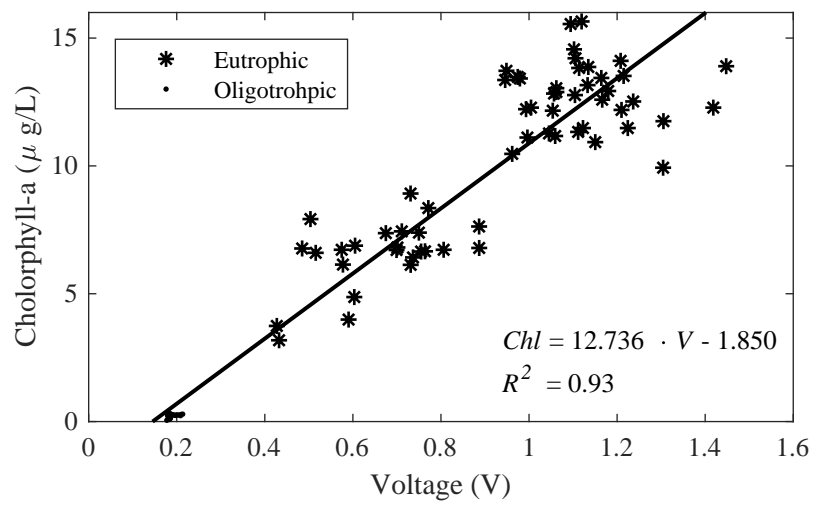


Figure 4.19: *In situ* calibration curve used to convert the SCAMP voltage profiles to chlorophyll-a concentration. Stars indicate data from the Blagdon lake, while the circles refer to Llandegfedd Reservoir. The conversion equation is reported in the right-bottom corner of the figure along with the coefficient of determination  $R^2$ .

Chapter **5**

# Modelling sinking rate of *Daphnia* during the downward vertical migration

S. Simoncelli<sup>1</sup>, S. J. Thackeray<sup>2</sup> and D. J. Wain<sup>1</sup>

<sup>1</sup> Department of Architecture and Civil Engineering, University of Bath


<sup>2</sup> Centre for Ecology & Hydrology, Lancaster Environment Centre

## Abstract

**M** EASURING and modelling zooplankton sinking velocity in the field can help us to understand how zooplankton respond to EXogenous ecological factors during the downward phase of DVM and how residence times of carcasses can affect aquatic carbon and nutrient cycling in lakes. Existing parameterisations of sinking rates of live zooplankton rely only on laboratory experiments yielding highly variable results even when performed under the same environmental conditions. These experiments do not provide realistic sinking velocities of organisms in the field. In the field, measurements of sinking rates are very limited and little is known about which parameters really drive this velocity and how it changes during the stratified period. In this study, we measured the velocity of the migrating layer at sunrise (bulk velocity) when zooplankton usually sink. The velocity was estimated from the backscatter strength (VBS) from an acoustic Doppler current profiler in summer 2015 and 2016. We also measured in the laboratory *Daphnia* mean density and body sizes from specimens collected in the field. Our data show that bulk velocity was constant for both years and zooplankton likely sank during the reverse DVM. We modelled the *Daphnia* body as a sinking ellipse and its antennae as cylindrical needles accounting for water temperature, and zooplankton shape, size and density. The good agreement of the sinking model with the field data indicates that buoyancy and gravity are the governing parameters of the reverse migration. The model also shows that  $v_{down}$  changes very little with the water temperature. In our study system, zooplankton appear to sink passively, rather than swim actively, during the downward phase of DVM to preserve energy and avoid hydrodynamic disturbances that allow them to be detected by predators.



## Statement of Authorship

<b>This declaration concerns the article entitled</b>				
Modelling sinking rate of <i>Daphnia</i> during the downward vertical migration				
<b>Authors</b>				
Simoncelli, S. (SS), Thackeray, S. J. (SJT) and Wain, D. J. (DJW)				
<b>Publication status (tick one)</b>				
Draft manuscript	Submitted	✓ <u>In review</u>	Accepted	Published
<b>Publication details (reference)</b>				
Hydrobiologia (Chapter 4 and 5 have been submitted as one paper)				
<b>Candidate's contribution to the paper (detailed, and also given as a percentage)</b>				
Designed the experiments: DJW, SJT, SS (90%).				
Performed the experiments: DJW, SS (90%).				
Analysed the data: SS (100%).				
Wrote the paper: SS.				
Editorial support in writing the manuscript: DJW, SJT				
Interpretation of the results: DJW, SJT, SS (90%).				
<b>Statement from Candidate</b>				
This paper reports on original research I conducted during the period of my Higher Degree by Research candidature.				
<b>Signed</b>			<b>Date</b>	13/02/2018

## 5.1 Introduction

*Daphnia* is the most common taxa of crustacean zooplankton in freshwater bodies (Benzie, 2005). Its swimming behaviours have been widely studied in laboratory experiments via analysis of video recordings (Beveridge et al., 2010; Dodson et al., 1997b; Gorski and Dodson, 1996; Gries et al., 1999; Van Gool and Ringelberg, 1998b) and more recently with PIV techniques (Wickramarathna et al., 2014) and laser-induced fluorescence methods (Noss and Lorke, 2014). Field studies about *Daphnia* are limited and restricted to the evaluation of displacement velocity during the DVM (Huber et al., 2011; Ringelberg and Flik, 1994) and to calibration of acoustic devices to continuously estimate the organisms concentration without relying on net collection (Huber et al., 2011; Lorke et al., 2004).

*Daphnia* normally swim by hopping and sinking: they push water downwards by beating the second set of antennae during the power stroke phase, performing a quick forward jump; they then pause and sink during the recovery stage for a few milliseconds. Organisms create a vortex ring in their wake whose size is dictated by the animal's size and water density (Gries et al., 1999). Other swimming patterns have been observed such as cruising, looping (Wickramarathna et al., 2014) and sinking (Noss and Lorke, 2014).

Sinking behaviour has been analysed either during the descent phase of the hop-and-sink pattern (Dodson et al., 1997a; Dodson et al., 1997b; Gorski and Dodson, 1996; Ringelberg, 2010) or when *Daphnia* passively and purely sink (Eyden, 1923; Hutchinson, 1967; Noss and Lorke, 2014). The sinking phase in the first scenario differs from that assessed in the latter: animals after hopping may still have a residual momentum and their downwards velocity may still be affected by the thrust during the hop phase. For passive sinking, an additional distinction should be made when the sinking rate is assessed with a live (Hutchinson, 1967; Noss and Lorke, 2014) or narcotised (Eyden, 1923; Gorski

and Dodson, 1996) specimen. For example, Gorski and Dodson (1996) hypothesised that *Daphnia* in the field may sink slower; when the water temperature  $T$  increases *Daphnia* metabolism is enhanced and the organism may generate a stronger downwards feeding current, that slows it down with respect to a narcotised specimen. Live organisms can also alter their drag by changing the carapace gape, the angle of the second set of antennas, when outstretched or folded (Eyden, 1923) and they can also change the setae gaps, creating a sieve-like or paddle-like effect (Gorski and Dodson, 1996). Finally, sinking rates can be lake-dependant based on the residing species of *Daphnia* (Dodson et al., 1997a) and their density (i.e. eggs in brood chamber) (Eyden, 1923).

An exhaustive summary of sinking rates derived from laboratory studies is reported in Table 5.2. Sinking rates of anaesthetised *Daphnia* range between 2.27 and 5 mm s<sup>-1</sup>. Experiments on live specimens report instead values between 2.78 and 3.5 mm s<sup>-1</sup> from the hop-and-sink behaviour, while live samples from 0.6 to 5 mm s<sup>-1</sup> when purely sinking. All the reported velocities are very variable and cannot be directly compared because they strongly depend on the *Daphnia* species and length, and the water temperature. However, sometimes results are contradictory. For example Eyden (1923) reports an average speed of 6 mm s<sup>-1</sup> at 18 °C, while Gorski and Dodson (1996) measured a maximum speed of 3.85 mm s<sup>-1</sup> for a narcotised specimen with same length. Finally Noss and Lorke (2014) provide 1 mm s<sup>-1</sup>, but within a water column stratified by salinity.

Measuring and modelling zooplankton sinking velocity in the field can help understanding of how zooplankton respond to ecological factors during the reverse DVM and how residence time of carcasses can affect aquatic carbon and nutrient cycling in lakes. Existing parameterisations of sinking rates of live zooplankton rely only on laboratory experiments (Eyden, 1923; Gorski and Dodson, 1996), whose results are highly dissimilar from each another (see Table 5.2), even when performed under the same environmental conditions. These experiments do not therefore provide realistic or consistent sinking velocities of organisms in the field. In the field, only the studies by Lorke et al. (2004) and Huber et al.

(2011) assessed the sinking rate of zooplankton under real environmental conditions. Nevertheless, little is known about how *Daphnia* sinking rates change in lakes during the stratified period and which parameters really drive this velocity. In this study we measured the sinking rates of zooplankton ( $v_{down}$ ) in the field using the backscatter strength of an Acoustic Current Doppler Profiler (ADCP) in two different years. We then formulated a physical-based model that describes  $v_{down}$  as a function of environmental parameters, such as the water temperature, and zooplankton shape, size and density.

Study	Sinking rate (mm s <sup>-1</sup> )	T (°C)	Length (mm)	Notes
Eyden (1923)	6 (mean)	18	1.6	Anaesthetised
	6 (mean)		1.8-2	Anaesthetised
Hutchinson (1967)	1-3 ( <i>D.galeata mendotae</i> )	-	1-2	Alive in testing tube
	0.6-4.5 ( <i>D. schloederi</i> )	-	1-2	
	4.5-5 ( <i>D. hyalina</i> )	-	-	
Ringelberg and Flik (1994)	5	-	2.5	Narcotised
Gorski and Dodson (1996)	2.78, 3.44	5, 25	1.5	Alive during hop-and-sink
	2.27, 3.85			Anaesthetised
Dodson et al. (1997a)	3.44 ( <i>D. Magna</i> )	20.5	-	Mean velocity during hop-and-sink
	3.5 ( <i>D. Pulicaria</i> )		-	
	3 ( <i>D. Pulex</i> )		-	
	2.4 ( <i>D. Hyalina</i> )		-	
Ringelberg (2010)	0.8-2.7	-	-	Alive during hop-and-sink
Kirillin et al. (2012)	0.9-1.9	21	-	Carcass in the lab
Noss and Lorke (2014)	1	18	1	With salt stratification
Dodson et al. (1997b)	3-4	-	-	-

Table 5.2: *Sinking rates of Daphnia from the literature*

## 5.2 Materials and Methods

### 5.2.1 Velocity measurements

Zooplankton velocity  $v_{down}$  was measured in Vobster Quay (see Section 4.2.1) during the reverse phase of the zooplankton DVM. The volume backscatter strength (VBS) data from the ADCP were processed using the image-detection algorithm described in Chapter 4. This allowed estimation of the zooplankton sinking rate or mean displacement velocity (DV) from the slope of the migrating layer.

### 5.2.2 Laboratory experiments

Laboratory experiments were performed to independently quantify zooplankton sinking velocities during the descending phase of the DVM. Results from these analyses were used to calibrate a physical-based model of the sinking rates to compare them with  $v_{down}$  quantified from the study site. Since results of sinking rates from the field are highly limited, our estimations of the sinking velocities from the model can be compared only with data derived from other laboratory experiments. We limited our attention to *Daphnia* because its hydrodynamics can be easily described by mathematical models with respect to other migrating genera and exhaustive studies were available in the literature about their sinking behaviour.

#### Daphnia density

The density of *Daphnia* carcasses was assessed using the density gradient method proposed in Kirillin et al. (2012). Nine different fluid densities were created in different cylinders by mixing freshwater with different volumes of sodium chlo-

ride solute ( $1 \text{ g mL}^{-1}$ ). The cylinder densities were verified with a portable densimeter (DMA 35 by Anton Paar) after the water reached the equilibrium with room temperature.

Twenty specimens were then individually tested. Each organism was gently injected and moved from the cylinder with the lowest density ( $\rho_w = 1000 \text{ kg m}^{-3}$ ) to the one with the highest density ( $\rho_w = 1050 \text{ kg m}^{-3}$ ) until the cylinder where the animal reached the neutral buoyancy was found. When the organism stops sinking, it can be assumed that the carcass has a density between the fluid density of the cylinder where it floats and the previous cylinder where it sank.

### Daphnia size

Morphometric data for each specimen were also measured under a Leica M205C dissecting microscope. The measured lengths are indicated in Fig. 5.1:  $b_e$  is half the body length  $l$  and  $a_e$  half the body width. The arm length is  $b_c$  and its width  $a_c$ .

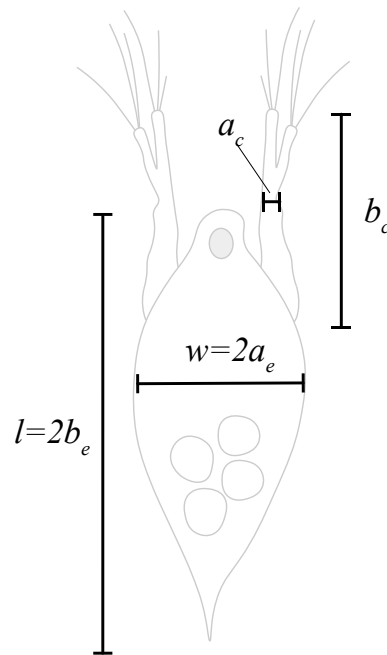


Figure 5.1: Measured lengths of *Daphnia*.  $l$  is the body length,  $w$  its width. The second antennae length is  $b_c$  while its width  $a_c$ .

## 5.3 Results

### 5.3.1 Bulk velocity

Fig. 5.2 shows the time series of bulk velocity  $v_{down}$  (grey triangles) at sunrise for both years using the developed image-detection algorithm described in Chapter 4. Each point in the figure also includes error bars (the 95% confidence inter-



val from the bootstrap analysis of the valid fittings of  $v_{down}$ ). The bulk velocity showed a weak trend over time with a mean of  $1.78 \pm 0.08 \text{ mm s}^{-1}$  in 2015 and  $1.71 \pm 0.1 \text{ mm s}^{-1}$  in the following year.

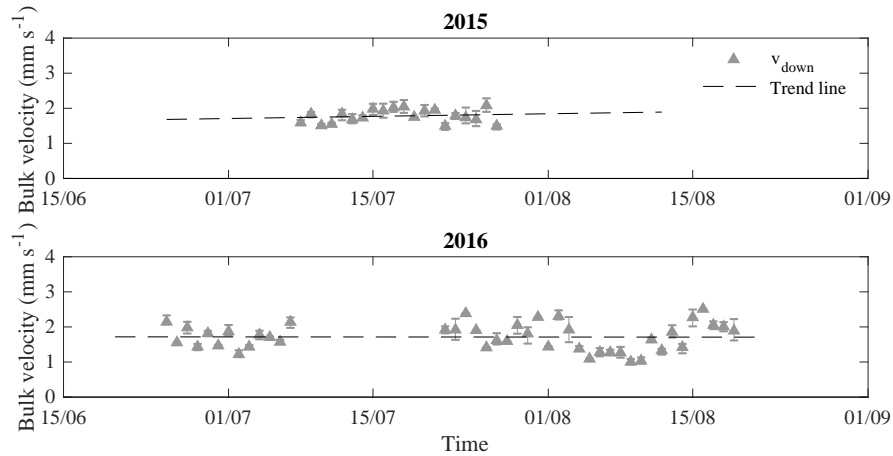


Figure 5.2: Time series of bulk velocity  $v_{down}$  at sunrise (grey triangles) in 2015 and 2016. Error bars show the 95% confidence interval from the bootstrap method. The black dashed lines show the trend lines fitted to the points.

### 5.3.2 Laboratory experiments

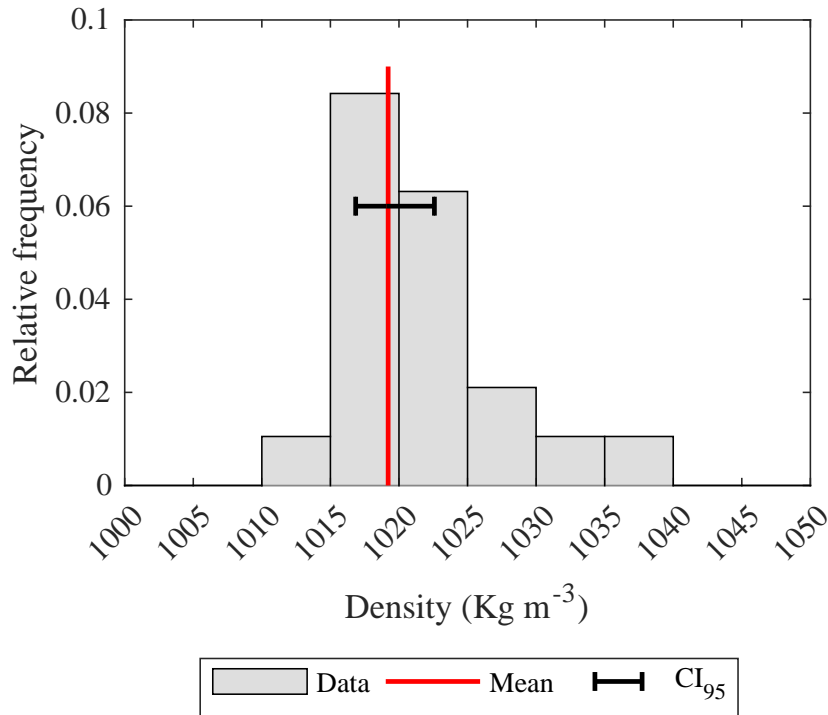


Figure 5.3: Frequency distribution of the density of individual *Daphnia* specimens ( $n=20$ ). The red line is the sample mean and the horizontal error bar its 95% confidence interval.

Fig. 5.3 shows the discrete distribution of the density of individual *Daphnia*. The mean density of a single *Daphnia* was  $1019.2 \text{ kg m}^{-3}$  (red line) with  $CI_{95}=[1016.8, 1022.5] \text{ kg m}^{-3}$  (black error bar). The lengths of each specimen are reported in Table 5.3. For each size, the mean and the 95% confidence interval  $CI_{95}$  was computed via bootstrapping.

Specimen #	$b_e$ (mm)	$a_e$ (mm)	$b_c$ (mm)	$a_c$ (mm)
1	0.406	0.217	0.624	0.029
2	0.421	0.218	0.492	0.050
3	0.415	0.221	0.404	0.044
4	0.326	0.129	0.226	0.028
5	0.479	0.153	0.422	0.038
6	0.448	0.230	0.439	0.028
7	0.477	0.203	0.473	0.051
8	0.518	0.170	0.342	0.044
9	0.490	0.151	0.381	0.034
10	0.422	0.234	0.360	0.052
11	0.342	0.116	0.425	0.033
12	0.499	0.207	0.421	0.034
13	0.518	0.170	0.342	0.044
14	0.490	0.151	0.381	0.034
15	0.422	0.234	0.360	0.052
16	0.342	0.116	0.425	0.033
17	0.499	0.207	0.421	0.034
18	0.491	0.172	0.573	0.046
19	0.462	0.202	0.606	0.045
20	0.384	0.265	0.384	0.027
<i>Mean</i>	0.443	0.189	0.425	0.039
$CI_{95}$	0.419, 0.476	0.164, 0.201	0.390, 0.466	0.035, 0.043

Table 5.3: *Body sizes (see Fig. 5.1) measured for Daphnia. The last two rows report the mean and the 95% confidence interval  $CI_{95}$  via bootstrapping.*

### 5.3.3 Modelling of $v_{down}$

If zooplankton passively descended during the DVM,  $v_{down}$  would depend only on the gravity, fluid characteristics and individual size and shape (Kirillin et al., 2012; Ringelberg and Flik, 1994). Assuming that zooplankton did not interfere with each other while sinking,  $v_{down}$  can be approximated by using the average sinking rate of a single organism. In the following, only the sinking rate of *Daphnia* was modelled. No data exist on the rate of sinking of live copepods. Moreover, they sink frequently with the body orientated in a horizontal or oblique position (Paffenhöfer and Mazzocchi, 2002) and that angle is not known. *Daphnia* sink instead mostly vertically (Dodson et al., 1995).

The sinking rate  $U_s$  of a spherical *Daphnia*, as a function of the water temperature  $T$ , can be found by balancing the Stokes drag force exerted by the fluid ( $F = 6\pi\mu R U_s$ ) with the body buoyancy ( $B = Vg(\rho_d - \rho_w)/\rho_w$ ):

$$U_s(T) = \frac{2}{9} R^2 g \frac{\rho_d - \rho_w(T)}{\mu(T)} \quad (5.1)$$

where  $V$  is the animal volume,  $R$  the body radius,  $g$  the gravitational acceleration,  $\rho_d$  the *Daphnia* density, and  $\rho_w(T)$  and  $\mu(T)$  the water density and dynamic viscosity respectively. By using  $R = b_E = 0.433$  mm (Table 5.3) and  $\rho_d = 1019.2$  kg m<sup>-3</sup> (Fig. 5.3), the average sinking rate is shown in Fig. 5.5 (orange curve). The shaded area in the figure shows the 95% confidence interval of  $U_s$ , calculated using the interval limits  $CI_{95} = [0.419, 0.476]$  mm for  $b_E$  and  $CI_{95} = [1016.8, 1022.4]$  kg m<sup>-3</sup> for  $\rho_d$ . The model provided velocities consistently above the falling rates reported in the literature for narcotised animals (Dore et al., 2009; Gorski and Dodson, 1996; Hutchinson, 1967; Ringelberg and Flik, 1994), because *Daphnia* is not sphere-shaped.

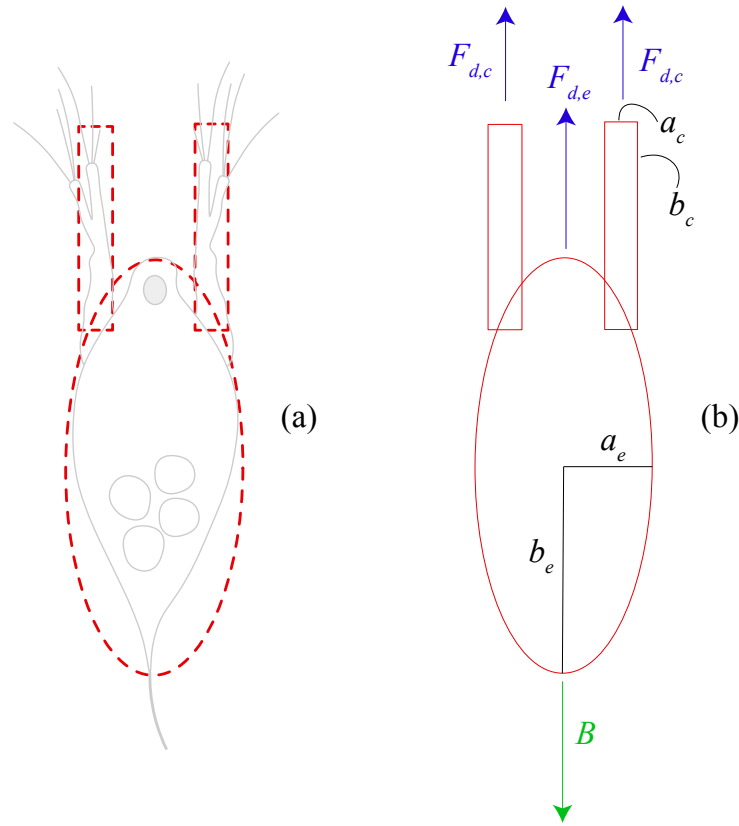


Figure 5.4: *Daphnia* is modelled using an ellipsoid for the body and two cylinders for the antennae (panel a). The new model (panel b) balances the buoyancy  $B$  with the additional drag ( $F_{d,c}$  and  $F_{d,e}$ ) accounting for the body lengths  $a_e$ ,  $b_e$ ,  $a_c$  and  $b_c$ .

The model was thus improved by assuming that *Daphnia* body is an ellipsoid (Fig. 5.4b) with width  $w = 2a_e$  and length  $l = 2b_e$  (Fig. 5.4c). The new body drag is:

$$F_{d,c} = F \cdot K_e \quad \text{with} \quad K_e = \frac{4}{3} \cdot \frac{\beta_e^2 - 1}{\frac{2 \cdot \beta_e^2 - 1}{\sqrt{\beta_e^2 - 1}} \cdot \ln(\beta_e + \sqrt{\beta_e^2 - 1}) - \beta_e} \quad (5.2)$$

where  $\beta_e = b_e/a_e$ . The new mean velocity (green line in Fig. 5.5) with  $a_e = 0.189$  mm and  $b_e = 0.443$  (Table 5.3)

$$U_e(T) = \frac{U_s(T)}{\beta_e \cdot K_e} \quad (5.3)$$

still overestimated the observed velocity (black dots and grey box). Because the second set of antennae affects the organism sinking rate (Dore et al., 2009; Gorski and Dodson, 1996), the additional drag  $F_{d,e}$  from the antennae was accounted by modelling the two appendages as two cylindrical needles with dimensions  $a_c$  and  $b_c$  (Fig. 5.4b). The resulting velocity was:

$$U(T) = \frac{2}{3} \cdot g \cdot \frac{\rho_d - \rho_w(T)}{\mu(T)} \cdot \frac{2 \cdot a_c^2 \cdot b_c + a_e^2 \cdot b_e}{\frac{4 \cdot b_c}{\ln(2 \cdot \beta_c)} + 3 \cdot a_e \cdot K_e} \quad (5.4)$$

where and  $\beta_c = b_c/a_c$ . By employing the mean values of  $a_c = 0.425$  mm and  $b_c = 0.039$  mm (Table 5.3), the modelled velocity (blue line in Fig. 5.5) matched the observed range of  $v_{down}$  in the field (black dots and grey box) within the 95% confidence interval (blue shaded area).

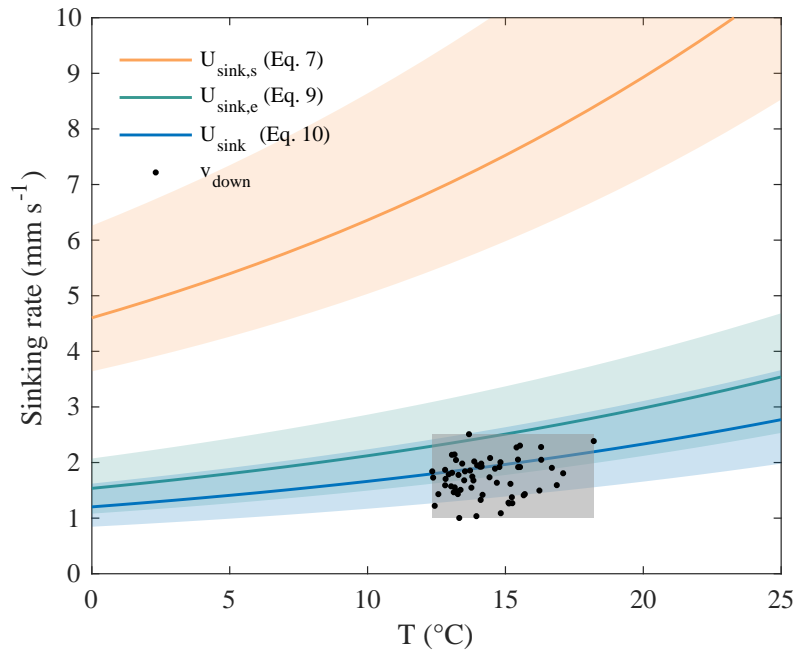


Figure 5.5: Average sinking rates of *Daphnia* as a function of the temperature  $T$ . Orange line shows the organism modelled as a spherical body (with  $R = b_E = 0.433$  mm), the green line as an ellipses (with  $a_e = 0.189$  mm and  $b_e = 0.443$ ) and the blue line with the new model (with  $a_c = 0.425$  mm and  $b_c = 0.039$  mm). Each thick line shows the mean velocity and the shaded areas the 95% confidence intervals. Dots report the measured values of  $v_{\text{down}}$  with the corresponding temperature  $T$  observed in the migrating layer. Grey box shows instead the observed range of  $v_{\text{down}}$  and  $T$ .

## 5.4 Discussion

Zooplankton descent can occur by active swimming, when organisms orient downwards, or by passive sinking (Dodson et al., 1997b; Ringelberg, 2010). Ringelberg and Flik (1994) reported that *Daphnia* swim downwards only when the light stimulus  $S$  is high and above an unknown threshold. However, several reasons suggests that zooplankton sank passively during the DVM observed here. First, according to the meteorological station measurements, zooplankton started migrating several minutes before sunrise when the solar radiation was still zero or undetectable by the solar sensor. This may be an indication that the organisms passively sank and  $S$  was not a causal factor for active downwards DVM (Ringelberg and Flik, 1994). Second,  $v_{down}$  (Fig. 5.2) did not exhibit any seasonal trend and therefore correlation with any predictors. Active swimming can be energetically costly for zooplankton (Power, 1989) and generate hydrodynamic disturbances detectable by predators. Lastly, the good agreement of the sinking model (Fig. 5.5, blue line) with the field data (Fig. 5.2, negative values) indicates that organisms sank during the DVM because the velocity depends on the Stokes's law (Ringelberg and Flik, 1994). The model shows that the velocity changed very little with the temperature, as seen in Kirillin et al. (2012). This explains why  $v_{down}$  was constant during the observations and did not correlate with  $T$ . The model also suggests that accounting for additional drag is important when modelling *Daphnia* sinking rate. Results from the literature cannot be directly compared with our model and observations because organisms have different lengths or density (i.e. eggs in brood chamber) and experiments were performed under different conditions of  $T$ .

Although the goal was to model the sinking rates of live *Daphnia* during the DVM, our model can be applied and extended to assess the sinking velocity of zooplankton carcasses in the water column. Dead organisms constitute an important energy source for microbial activity (Bickel and Tang, 2010; Kirillin et al., 2012; Reinfelder et al., 1993) and assessing their residence time can help to



provide insights into aquatic carbon and nutrient cycling in lakes. Thanks to the model linearity and flexibility, different carcass shapes can be accommodated in our equations to account for significant changes in organism's body dimensions and hydrodynamics due to microbial decomposition and lake stratification. Existing sinking rates of carcasses do not account for changes in organism's shape and sizes as they are degraded by bacteria, because they are based on the sinking velocity of spheric bodies (Kirillin et al., 2012).

Our measurements of *Daphnia* sinking rates ( $v_{down}$ ) are lake-specific. Different environmental parameters can significantly impact their sinking behaviour, in particular in the lake epilimnion. Convective cells from nocturnal penetrative convection or energetic turbulent eddies may drift organisms downwards more rapidly. When the density stratification becomes very strong, the thermocline may act as a physical barrier preventing them from sinking. In this scenario zooplankton may change their swimming behaviour to active downwards swimming in order to overcome the density gradient. Results from our study site suggest that the lake was weakly stratified (see Fig. 4.5) and that turbulence was on average very low in the water column (see Fig. 4.7). These two factors may have played an important role in determining the *Daphnia* sinking behaviour and velocities observed in this study. Finally, underwater light conditions at sunrise is another crucial parameter in determining the swimming behaviour. Diverse light conditions in other basins may trigger a different swimming response and the thresholds in the light stimulus  $S$  may be different depending on the residing zooplankton species.

## 5.5 Conclusions

In this study we assessed the mean displacement velocity of zooplankton from the slope of the zooplankton layer during the DVM at sunrise. The velocity at sunrise  $v_{down}$  was constant. The lack of variation in  $v_{down}$  is likely because *Daph-*

*nia* passively sink instead of swimming during the reverse migration. Modelling the *Daphnia* body as sinking ellipses and its second antennas as cylindrical needles confirmed that buoyancy and gravity are the governing parameters of the reverse migration. The developed model suggests that accounting for additional drag is important when modelling *Daphnia* sinking rate. We also suggests that zooplankton may favour passive sinking than active swimming during the reverse DVM to preserve energy and generate hydrodynamic disturbances not detectable by predators. Finally, we suggest that the proposed model can be employed in modelling sinking rate of carcasses and evaluate the potential of dead zooplankton in affecting aquatic carbon and nutrient cycling in lakes. Since sinking rates are mainly controlled by zooplankton size and density, this may alter zooplankton residence time in the water column and the carbon availability to bacteria.

# Conclusions

## 6.1 Introduction

Zooplankton play an important role in governing ecologically-important processes, trophic interactions and budgets of salt, heat and dissolved substances in ocean and lakes (Castellani and Edwards, 2017; Hays, 2003). This thesis investigated the interactions between zooplankton hydrodynamics and their environment during the diel vertical migration (DVM) in lakes (see Fig. 6.1). The aims of this work were to (1) explore the potential for swimming zooplankton to generate turbulent and mixing in a lake environment (blue block “a” in Fig. 6.1); and (2) understand how changes in the ecosystem conditions affect zooplankton hydrodynamics and their swimming behaviour (green block “b” in Fig. 6.1). In the following, the first research topic and its conclusions are discussed in Section 6.2, while the second research topic is addressed in Section 6.3.

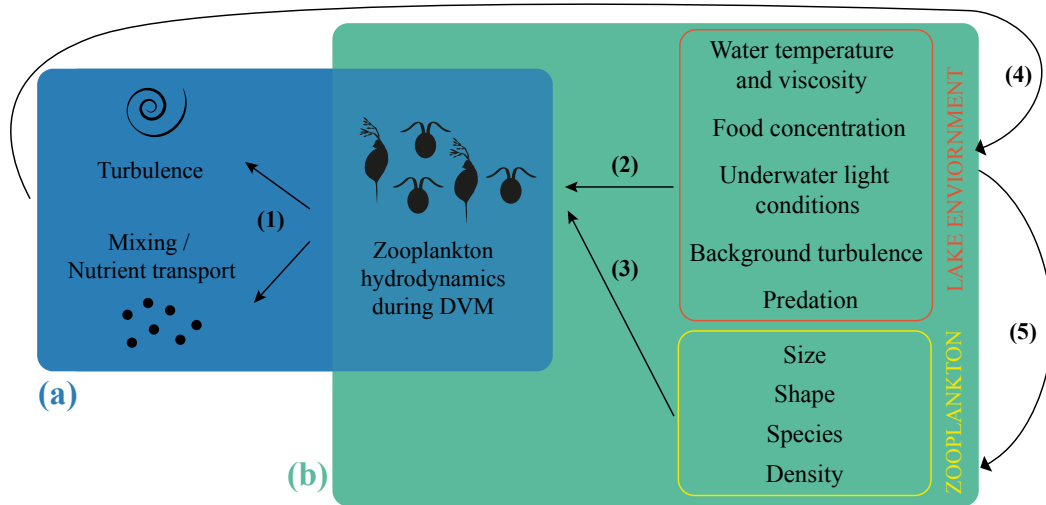


Figure 6.1: Conceptual diagram showing interactions between zooplankton hydrodynamics and their environment during the DVM. Block (a) and (b) show the two explored research topics, while numbers 1 to 5 indicate the connections between different elements.

## 6.2 Effect of swimming zooplankton on the environment

As many studies have shown, swimming organisms may be able to produce turbulent kinetic energy (TKE) in lakes and oceans and enhance vertical mixing with a direct impact on transport of important chemical compounds (Huntley and Zhou, 2004; Katija, 2012; Wang and Ardekani, 2015; Wilhelmus and Dabiri, 2014). Past research about biomixing has been conducted in the ocean (Katija, 2012; Kunze et al., 2006; Rousseau et al., 2010) and laboratory only (Noss and Lorke, 2012; 2014; Wilhelmus and Dabiri, 2014). However, for freshwater zooplankton, no *in situ* studies exist that assess the real role of biomixing. This precluded definitive conclusions regarding the potential importance of biomixing from zooplankton because the problem needs to be explored in the field,

to overcome limitations arising from experiments and without altering the behaviour of the animals under study. This thesis focused on small zooplankton in freshwater bodies where organisms may create hydrodynamic instabilities with their swimming appendages and inject TKE during the DVM at dusk (block (a) in Fig. 6.1).

In order to build upon, and advance, knowledge of zooplankton biomixing in freshwaters, the following objectives have been tackled:

1. Measure the turbulence generated by zooplankton during the diel vertical migration in a lake environment by using a microstructure profiler.
2. Estimate the mixing and Thorpe overturning scales due to zooplankton migration.
3. Compare the results and the importance of this mechanism with other investigations regarding small zooplankton.

To address objective 1, turbulence data were collected on three different migration dates with a microstructure profiler in Vobster Quay, a small made-man lake in Radstock (UK), with an active population of *Daphnia*. Microstructure data were used to estimate dissipation rates of thermal variance  $\chi_T$  and TKE  $\varepsilon$ , possibly arising from swimming zooplankton. Measurements were also combined with acoustic measurements to continuously estimate *Daphnia* concentration during the vertical ascent and estimate their concentration within the migrating layer. Results of  $\chi_T$  and  $\varepsilon$  show that the highest heat and energy production was in the unstratified surface layer. Below the thermocline and within the migrating layer, no important and persistent turbulent enhancements of  $\chi_T$  and  $\varepsilon$  were observed with respect to the background levels, even when *Daphnia* concentrations peaked at 40 org. L<sup>-1</sup>. Moreover, no correlations between *Daphnia* concentration and dissipation rates were measured for all the three datasets.

This suggests that migrating *Daphnia* do not affect mixing in lakes at the observed concentrations (pathways 1 and 4 in Fig. 6.1). However, this does not rule out the possibility that collective action and synchronised movements of larger zooplankton and/or higher abundances may produce significant instabilities in other lakes.

To address objective 2, mixing was estimated from microstructure profiles data using the Osborn and Cox model. Results showed that, below the epilimnion, mixing did not increase and consistently approached the molecular heat diffusivity. Limited patches with higher mixing up to  $K_T = 10^{-6} \text{ m}^2 \text{ s}^{-1}$  were detected but they were short-lived. This is an indication that mixing was not intensified during the DVM. Overturning length scales were also computed from profiles of temperature fluctuations to verify the presence of small fluctuations produced by swimming zooplankton. For this purpose, Thorpe scales  $L_T$  and  $L_{OZ}$  were compared inside and outside the migrating layer during the DVM. This was essential to determine if any differences in overturning were present between the undisturbed water column and that part affected by the zooplankton migration. The observed fluctuations of  $L_T$  were always above the size of a single *Daphnia*, however, no significant and persistent differences in the displacements were generally observed between the situation outside and inside the migrating layer. This further suggests the hypothesis that no important fluctuations were generated by the migrating *Daphnia* and that no potential energy was created.

To address objective 3, dissipation rates of TKE and mixing were compared with existing studies about zooplankton-generated mixing. In this study, TKE dissipation rates  $\varepsilon$  always approached values as low as  $10^{-9} \text{ W kg}^{-1}$ . Noss and Lorke (2012) measured instead  $\varepsilon \sim 10^{-6} \text{ W kg}^{-1}$  near the body of a single swimming *Daphnia*, but this was not observed in this study in the vicinity of multiple swimming organisms. Dissipation rates of TKE were also below the prediction of Huntley and Zhou (2004)'s model with  $\varepsilon \sim 10^{-5} \text{ W kg}^{-1}$ . Mixing results indicate that in this study no mixing was generated, because  $K_T = K_V \sim 10^{-7}$

$\text{m}^2 \text{s}^{-1}$ , even with *Daphnia* concentrations as high as  $40 \text{ org. L}^{-1}$ . The result is in accordance with the laboratory experiment by Noss and Lorke (2014) where just  $4 \text{ org. L}^{-1}$  were used. Numerical simulations by Wang and Ardekani (2015) suggest instead that biomixing by zooplankton is a likely mechanism and that  $K_V$  can be enhanced up to  $10^{-5} \text{ m}^2 \text{ s}^{-1}$ , but only using unrealistic concentrations of *Daphnia* of  $10,000 \text{ org. L}^{-1}$ . The observed mean concentration within the turbulent patches in this study varied instead between 4 and  $60 \text{ org. L}^{-1}$ . These values were above the concentration employed by Noss and Lorke (2014) and three order magnitudes smaller than those used in Wang and Ardekani (2015)'s simulations. This study clearly demonstrates that, with the organisms concentrations normally found in lakes, small and vertically-swimming zooplankton cannot affect the vertical thermal stratification in freshwater bodies (pathway 4 in Fig. 6.1).

### 6.3 Effect of the environment on zooplankton

The focus of this second study was to assess the effect of the environment on the zooplankton displacement velocity (DV) during the DVM. Currently, it is not known which factors are key in driving this velocity because available measurements of DV during the DVM in the field are rare. The aim of this research was therefore to explore and explain the seasonal variability of DV as a function of different environmental drivers (block (b) in Fig. 6.1). The objectives of this work were to:

1. Measure the zooplankton displacement velocity during the DVM at sunset and sunrise with a new technique based upon acoustic measurements.
2. Correlate the time series of the measured velocity at sunset with time series of possible DVM drivers in the field, such as food concentration, underwater light conditions, water temperature.

### 3. Explain and model the zooplankton sinking velocity at sunrise.

To address objective 1, acoustic measurements were employed to track the zooplankton position during the DVM in two different years. From these data, it was possible to measure the slope of the zooplankton layer during the DVM, which provides the mean DV of zooplankton in the field. To objectively and automatically compute DV, an image-detection algorithm was developed to process and detect the acoustic shape of the zooplankton migrating layer and to estimate its slope throughout the stratified period. The new technique allows reliable estimation of a time series of DV in lakes in which zooplankton migration takes place. From the acoustic data collected in Vobster Quay (UK), the DV was estimated in summer 2015 and 2016. Data showed that the upwards bulk velocity ( $v_{up}$ ) had a positive increasing trend over time, while the downward bulk velocity ( $v_{down}$ ) was constant.

To address objective 2, the upwards bulk velocity of zooplankton ( $v_{up}$ ) was correlated with measured DVM drivers in the field: chlorophyll-a concentration, underwater light conditions, water temperature, background turbulence, and zooplankton concentration and size. Results show that  $v_{up}$  was strongly correlated with the water temperature in the layer during the migration. Chlorophyll concentration, relative change of light intensity, and zooplankton concentration and size during the DVM did not seem to play an important role in affecting the velocity. Temperature may be a key mechanical factor controlling swimming activity (pathway 2 in Fig. 6.1). Temperature can increase metabolic rates and zooplankton require less effort to propel themselves in a less viscous fluid. The relationship between temperature and velocity has, so far, only been demonstrated under greatly-simplified conditions in lab experiments. This study shows, for the first time, the potential for the same effect to be significant in the field. Finally, the temperature can also influence, by extension, escape reactions from predators, patterns of predation, and thus trophic interactions, energy flows in lake food webs and biogeochemical fluxes of nutrients and carbon.



To address objective 3, it was first argued that the downwards bulk velocity ( $v_{down}$ ) represents the *Daphnia* sinking rate: the measured velocity did not exhibit any seasonal trend and correlation with any environmental parameters; moreover, the reverse DVM was not light-driven because organisms started migrating when the light stimulus, measured by the meteorological station, was still zero.  $v_{down}$  was therefore modelled by assuming that *Daphnia* body behaves as a sinking ellipse and its second set of antennas as cylindrical needles. The new proposed physical-based model also accounts for changes in water temperature, and zooplankton shape, size and density (pathways 2 and 3 in Fig. 6.1). The good agreement of the sinking model with the field data is a strong indication that organisms sank during the reverse DVM. The model also indicates that accounting for the additional drag from the organism's antennae is important when modelling *Daphnia* sinking rate and that existing parameterisations based only on the Stokes' law are inaccurate. Models in the literature show conflicting conclusions because the sinking rate is not correctly modelled. The main ecological implications is that *Daphnia* may favour passive sinking than active swimming during the reverse DVM. This is fundamental to preserve energy and generate hydrodynamic disturbances not detectable by predators (i.e. reduce predation risk).

## 6.4 Links between zooplankton hydrodynamics and environment

Fig. 6.1 depicts an overview of the two main research topics covered in this thesis. Block (a) shows the influence of the hydrodynamics of swimming zooplankton on the environment, while block (b) deals with the potential effect of the environment on the zooplankton swimming behaviour. The figure also depicts the complex relations (pathways 1 to 5) between the explored issues.

Turbulence and mixing, generated from hydrodynamic instabilities during the zooplankton vertical ascent (pathway 1), can indirectly modify the lake environment (pathway 4 to red box). Mixing can partially destroy the stable vertical stratification and affect temperature and viscosity of water in which organisms swim. Dissolved substances such as food concentration, kairomone levels and other nutrients can further be redistributed in the water column, influencing predation pressure on zooplankton and stimulating primary production. Underwater light condition can also be altered when suspended material, contributing to turbidity, is dispersed in the lake. According to the conclusions drawn in Section 6.2, this feedback did not occur in the study site because turbulence and mixing were not intensified. Nonetheless, larger zooplankton or different species (yellow box), with different swimming velocities (pathway 3), may be favoured under other environmental conditions (pathway 5) and may still create stronger water instabilities during the DVM and enhance turbulence and water transport (pathway 1) in the same lake.

The green block (b) in Fig. 6.1 shows the direct (red box and pathway 2) and indirect (yellow box and pathway 3) feedback of the environment on the zooplankton hydrodynamics. The results contained in this work have shown that the water temperature mostly affected the zooplankton swimming velocity during the upwards phase of the DVM. Other parameters such as food level, underwater light intensity, and zooplankton concentration and size did not seem to play an important role in affecting the organisms velocity and their hydrodynamics. The employed model did not however account for any direct effect of predation pressure. Higher kairomone levels can lead to faster swimming reactions (Dodson et al., 1997a; Loose and Dawidowicz, 1994; Ringelberg, 1999; 2010) and further enhance turbulence and mixing production (pathway 2 to 1). During the reverse phase of the DVM, the results from the study site indicate instead that zooplankton size, shape, species and density (pathway 5) contributed the most to determining the downwards velocity. The direct impact of the environment (pathway 2) did not play an important role, even though this may

depend on the lake environment under investigation.

## Prospects for future work

### 7.1 Further development of this thesis

Future research can be divided into two categories related to the two analysed research topics. In this study, measurements of zooplankton-generated turbulence were accomplished in a small lake with a *Daphnia* concentration up to 60 org. L<sup>-1</sup> in late summer. In order to understand if the findings in this work are lake-specific, turbulence and mixing measurements should be collected with the same methodology proposed in Section 3.2 in other lakes. Collection should be carried out at different times of year, in particular in early summer when it is more likely that peaks in zooplankton concentration will occur. This would allow us to understand if a higher zooplankton concentration may still generate turbulence and trigger vertical mixing. Measurements should also be collected in a range of basins, with different stratification and zooplankton species and abundances. In this study, zooplankton-generated mixing has been investigated using temperature microstructure measurements which are based on the principle that probe thermistors cannot measure diffusivities  $K_V$  below the molecular heat diffusivity  $D_T = 10^{-7} \text{ m}^2 \text{ s}^{-1}$ . The measured eddy diffusivity in the study site always approached  $D_T$  and results showed that migrating zooplankton could not affect the vertical thermal stratification in lakes. However, this

does not rule out the possibility that swimming organisms can still enhance the vertical diffusivity above  $D_G = 10^{-9} \text{ m}^2 \text{ s}^{-1}$  and therefore affect transport of gases or dissolved substance whose molecular diffusion is above  $D_G$ . In the field, tracer studies can be employed to estimate  $K_V$  before and during the DVM. Dye studies allow (1) direct assessment of  $K_V$ , without relying to models, such as that used in this study, (2) direct assessment of diffusivities smaller than those estimated from microstructure profilers and (3) understanding of whether the stratification can restore the initial water column density structure affected by the zooplankton migration.

For the second research topic, the correlation between the displacement velocity (DV) and the DVM drivers can be further strengthened by collecting additional data from more years and study sites. Information about predation should also be collected and included in empirical models to investigate whether predation pressure may explain part of the observed DV. These measurements may rely on fish net sampling, hydro-acoustics, or water analysis of kairomone levels. Finally, in this study the chlorophyll-a concentration and water transparency were nearly constant during the observational period. Acoustic measurements, the proposed image-detection algorithm and correlative approach can be applied to other lakes where stronger variations in the aforementioned DVM drivers take place. This allows accounting for other possible effects on the zooplankton DV.

In relation to zooplankton sinking rates, future work can further explore how zooplankton swimming behaviour is affected in the field during the reverse DVM. In this study it was proposed that *Daphnia* sank at sunrise. However, when *Daphnia* actively swim downwards instead of sinking, it is not known which parameters really govern their swimming velocity. Finally, the formulated sinking rate model can be used in studying the sinking of carcasses in relation to aquatic carbon and nutrient cycling in lakes. More complex parameterisations can be developed to account for changes in zooplankton density, shape and size and better model nutrients fluxes.

## 7.2 Future Directions in Zooplankton Hydrodynamics

In addition to future work related to the questions in this thesis, there are other important questions in zooplankton hydrodynamics to be explored. Theoretical and empirical studies in the literature suggest that zooplankton behaviour is strongly altered when organisms are exposed to different levels of turbulence intensity in lake water column (Visser and Stips, 2002). For example, grazing zooplankton feed more efficiently in moderate turbulence because small-scale fluctuations increases encounter rate with their prey (Alcaraz et al., 1994). At the same time, fast-moving instabilities can significantly decrease interaction time with their food (Ross et al., 2007), preventing organisms from feeding effectively with respect to a turbulence-free environment. When turbulence dissipations become too intense, most organisms generally respond by escaping toward calmer waters (Dower et al., 1998; Prairie et al., 2012; Seuront et al., 2004; Visser and Stips, 2002; Wickramarathna, 2016). However, when velocities are too strong, organisms are passively advected with the flow by surface or internal waves and other wind-driven mechanisms (Huber et al., 2011; Rinke et al., 2007; 2009).

Interactions between turbulence and zooplankton motility have been experimentally investigated under controlled laboratory conditions, but only for some species of marine copepods and under mechanically-generated turbulence (Michalec et al., 2015; Saiz and Alcaraz, 1992; Saiz et al., 2013; Seuront et al., 2004; Webster et al., 2015). These experiments present however varying outcomes depending on the species under observation, how turbulence is generated and the parameters used to assess changes in zooplankton behaviours. Only a field study by Huber et al. (2011) documented vertical and horizontal passive migrations of *Daphnia* due to the internal wave field. However, to date, no other field study exists to understand how behaviour of small zooplankton is affected by small-scale motions in lakes.

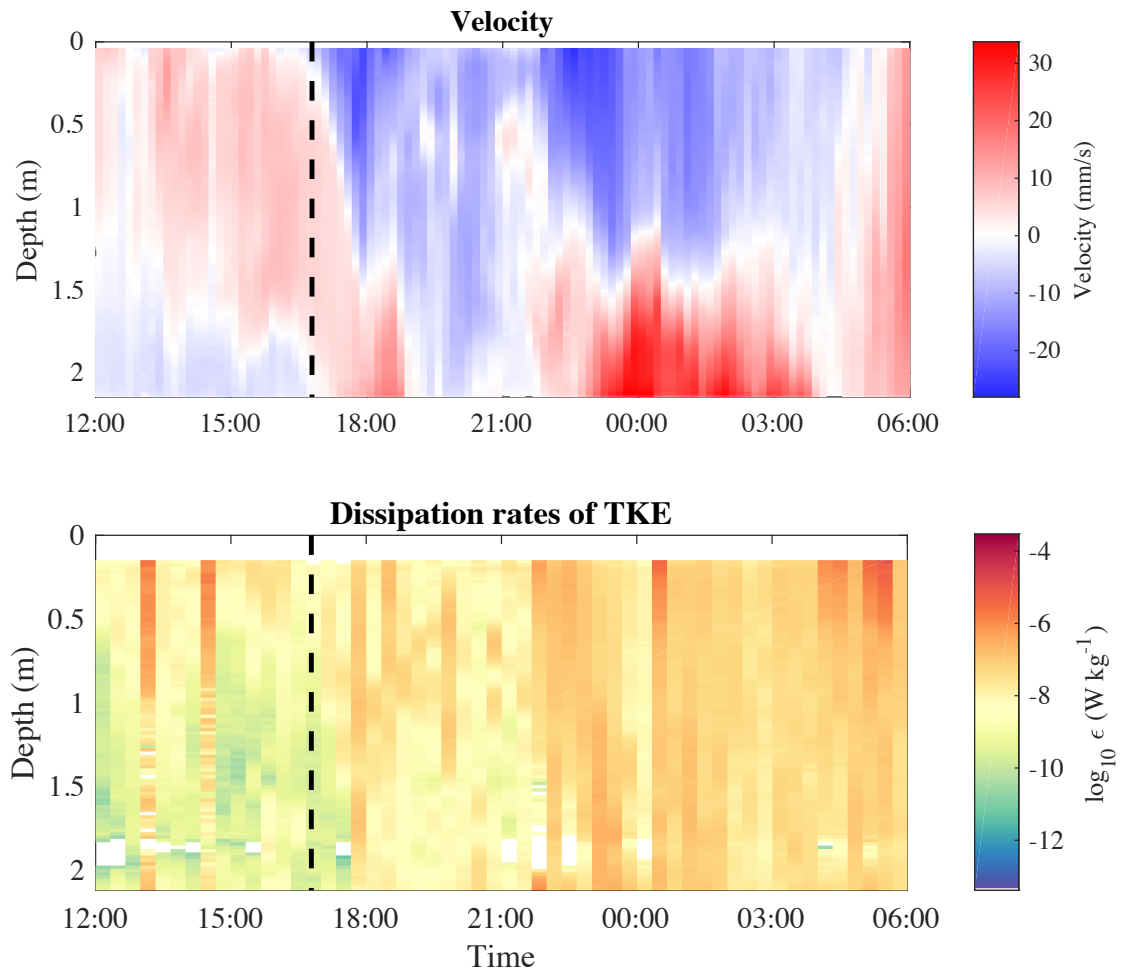


Figure 7.1: *Vertical velocities (upper panel) and turbulence dissipation rates (lower panel) measured from an Aquadopp and 1000-kHz ADCP in Lake Stechlin, Germany. Black lines highlight the time when night convection approximately begins.*

When zooplankton migrate towards the surface food-rich water at sunset to graze on phytoplankton, the key mechanisms driving turbulence and mixing at nighttime is thermal convection as a result of surface cooling (Jonas et al., 2003; Wüest and Lorke, 2003). Fig. 7.1 (upper panel) shows an example of the typical vertical velocities in Lake Stechlin (by G. Kirillin, unpublished) when night convection begins (black line). Similar vertical velocities have been observed

in other lakes (Wüest and Lorke, 2003). In this dataset, the vertical velocity increases and becomes negative, indicating downwards motions, and the turbulence dissipation rates of TKE (lower panel) increase from  $10^{-10} \text{ W kg}^{-1}$  up to  $10^{-6} \text{ W kg}^{-1}$  in the first few metres of the water column. Convective cells also deepen the mixed lake layer as shown by the turbulence enhancement below 0.5m after the black line.

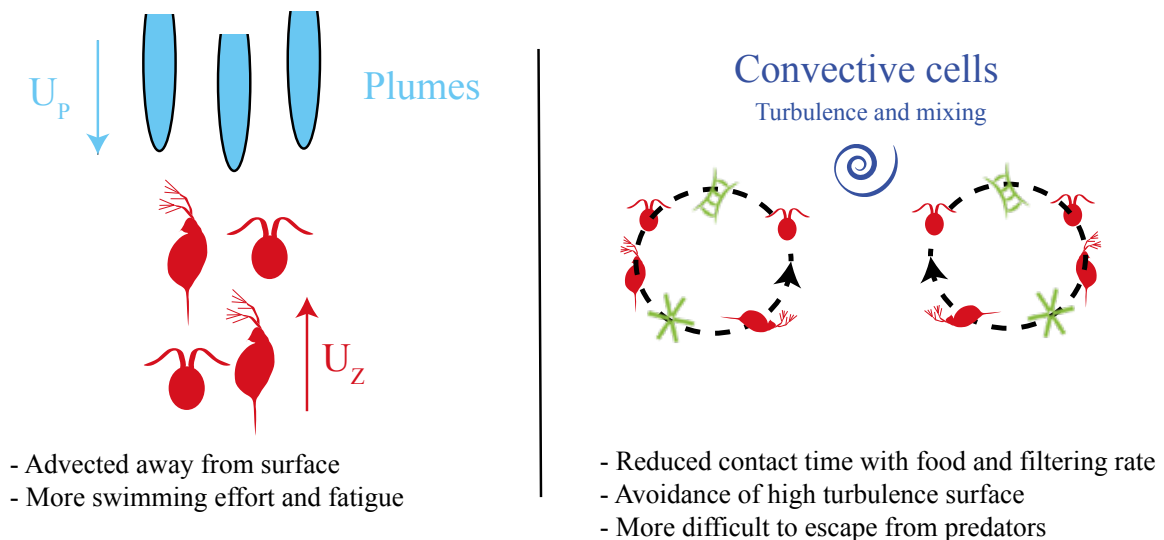


Figure 7.2: Sketch of interaction between convective cells and plumes during penetrative convection at nighttime.

As a result of this mechanism, zooplankton motility and food availability may be affected. Since zooplankton swimming speed  $U_Z \sim 10^{-3} \text{ m s}^{-1}$  is notably smaller than the plume's downwelling velocities  $U_P \sim 10^{-2} \text{ m s}^{-1}$ , zooplankton organisms are dragged away from the surface (Fig. 7.2, left panel). If convection is strong enough to affect the thermocline position, organisms can be further dragged downwards, partially jeopardising their swimming effort. Moreover, when convective cells form, organisms can be moved upwards and downwards in the water column, preventing them from efficiently feeding because contact



time and filtering rates are reduced (Fig. 7.2, right panel). *Daphnia* may also avoid the surface due to high turbulence (Wickramarathna, 2016) or find it more difficult to escape from predators because of their reduced motility.

If zooplankton matched the upwelling/downwelling velocity to maintain their depth, they would be able to do that only for a limited amount of time. This interaction between convection and zooplankton suggests a potential trade-off between feeding, but at the expense of their energy reserve, and preserving energy but being advected and risking starvation or being preyed upon.

Thus there are several unanswered questions regarding the interaction between zooplankton and convective mixing, such as: What is the zooplankton abundance and velocities during grazing and how does that relate to the mixed layer properties? Can zooplankton swim against upwelling and downwelling currents to maintain their depth? If they can, can they maintain the velocity for long periods of time? How is the zooplankton feeding efficiency affected by convection?

To achieve the proposed objective, field experiments can be conducted in lakes where penetrative convection processes are important and with an active population of zooplankton feeding at nighttime. Experiments may be performed in a mesocosm facility to easily control predation, zooplankton population and food concentration.



# Bibliography

- Alcaraz, M., Saiz, E., and Calbet, A., 1994. Small-scale turbulence and zooplankton metabolism: Effects of turbulence on heartbeat rates of planktonic crustaceans. *Limnol. Oceanogr.* 39(6), pp.1465–1470.
- Andersen Borg, C.M., Bruno, E., and Kiørboe, T., 2012. The kinematics of swimming and relocation jumps in copepod nauplii. *PLoS One*, 7(10), pp.33–35.
- Armengol, J., Caputo, L., Comerma, M., Feijoo, C., Garcia, J.C., Marce, R., Navarro, E., and Ordonez, J., 2003. Sau reservoir's light climate: Relationships between Secchi depth and light extinction coefficient. *Limnetica*, 22(1-2), pp.195–210.
- Barth, L.E., Sprules, W.G., Wells, M., Coman, M., and Prairie, Y., 2014. Seasonal changes in the diel vertical migration of *Chaoborus punctipennis* larval instars. *Can. J. Fish. Aquat. Sci.* 71(5), pp.665–674.
- Batchelor, G.K., 1959. Small-scale variations of convected quantities like temperature in turbulent fluid. part I: General discussion and the case of small conductivity. *J. Fluid Mech.* 5(1), pp.113–133.
- Beck, J.L. and Turingan, R.G., 2007. The effects of zooplankton swimming behavior on prey-capture kinematics of red drum larvae, *Sciaenops ocellatus*. *Mar. Biol.* 151(4), pp.1463–1470.

- Beklioglu, M., Gozen, A.G., Yildirim, F., Zorlu, P., and Onde, S., 2008. Impact of food concentration on diel vertical migration behaviour of *Daphnia pulex* under fish predation risk. *Hydrobiologia*, 614(1), pp.321–327.
- Benoit-Bird, K.J., Moline, M.A., Schofield, O.M., Robbins, I.C., and Waluk, C.M., 2010. Zooplankton avoidance of a profiled open-path fluorometer. *J. Plankton Res.* 32(10), pp.1413–1419.
- Benzie, J.A.H., 2005. *The Genus Daphnia (including Daphniopsis)*. Vol. 21. Kenobi Productions.
- Beutel, M., Hannoun, I., Pasek, J., and Kavanagh, K.B., 2007. Evaluation of Hypolimnetic Oxygen Demand in a Large Eutrophic Raw Water Reservoir, San Vicente Reservoir, Calif. *J. Environ. Eng.* 133(2), pp.130–138.
- Beveridge, O.S., Petchey, O.L., and Humphries, S., 2010. Mechanisms of temperature-dependent swimming: the importance of physics, physiology and body size in determining protist swimming speed. *J. Exp. Biol.* 213(24), pp.4223–4231.
- Bickel, S.L. and Tang, K.W., 2010. Microbial decomposition of proteins and lipids in copepod versus rotifer carcasses. *Mar. Biol.* 157(7), pp.1613–1624.
- Black, A.R. and Dodson, S.I., 2003. Ethanol: a better preservation technique for *Daphnia*. *Limnol. Oceanogr. Methods*, 1, pp.45–50.
- Blake, J.R., 1971. A spherical envelope approach to ciliary propulsion. *J. Fluid Mech.* 46(01), p.199.
- Blukacz, E.A., Shuter, B.J., and Sprules, W.G., 2009. Towards understanding the relationship between wind conditions and plankton patchiness. *Limnol. Oceanogr.* 54(5), pp.1530–1540.
- Boehrer, B. and Schultze, M., 2008. Stratification of lakes. *Rev. Geophys.* 46(RG2005), pp.1–27.

- Boeing, W.J., Leech, D.M., and Williamson, C.E., 2003. Opposing predation pressures and induced vertical migration responses in *Daphnia*. *Limnol. Oceanogr.* 48(4), pp.1306–1311.
- Bouffard, D. and Boegman, L., 2012. Basin-Scale Internal Waves. *Encycl. lakes reserv.* Dordrecht: Springer Netherlands, pp.102–107.
- Bouffard, D. and Boegman, L., 2013. A diapycnal diffusivity model for stratified environmental flows. *Dyn. Atmos. Ocean.* 61-62, pp.14–34.
- Brinton, E., 1967. Vertical migration and avoidance capability of euphausiids in the California Current. *Limnol. Oceanogr.* 12, pp.451–483.
- Buchanan, C., Goldberg, B., and McCartney, R., 1982. A laboratory method for studying zooplankton swimming behaviors. *Hydrobiologia*, 94(1), pp.77–89.
- Castellani, C. and Edwards, M., 2017. *Marine Plankton: A Practical Guide to Ecology, Methodology, and Taxonomy*, p.704.
- Chen, H.-L., Hondzo, M., and Rao, A.R., 2002. Segmentation of temperature microstructure. *J. Geophys. Res.* 107(C12, 3211), pp.4–13.
- Cohen, J.H. and Forward, R.B., 2009. Zooplankton diel vertical migration - A review of proximate control. *Oceanogr. Mar. Biol.* 47, pp.77–110.
- De Robertis, A., 2002. Size-dependent visual predation risk and the timing of vertical migration: An optimization model. *Limnol. Oceanogr.* 47(4), pp.925–933.
- Dean, C., Soloviev, A., Hirons, A., Frank, T., and Wood, J., 2016. Biomixing due to diel vertical migrations of zooplankton: Comparison of computational fluid dynamics model with observations. *Ocean Model.* 98, pp.51–64.
- Deines, K., 1999. Backscatter estimation using Broadband acoustic Doppler current profilers. *Proc. IEEE Sixth Work. Conf. Curr. Meas. (Cat. No.99CH36331)*.

- Dewar, W.K., Bingham, R.J., Iverson, R.L., Nowacek, D.P., St. Laurent, L.C., and Wiebe, P.H., 2006. Does the marine biosphere mix the ocean? *J. Mar. Res.* 64(4), pp.541–561.
- Dodson, S.I, Ryan, S., Tollrian, R., and Lampert, W., 1997a. Individual swimming behavior of *Daphnia*: effects of food, light and container size in four clones. *J. Plankton Res.* 19(10), pp.1537–1552.
- Dodson, S., 1988. The ecological role of chemical stimuli for the zooplankton: predator-avoidance behavior in *Daphnia*. *Limnology*, 33(6), pp.1431–1439.
- Dodson, S., 1990. Predicting diel vertical migration of zooplankton. *Limnol. Oceanogr.* 35(5), pp.1195–1200.
- Dodson, S.I., Hanazato, T., and Gorski, P.R., 1995. Behavioral responses of *Daphnia pulex* exposed to carbaryl and *Chaoborus* kairomone. *Environ. Toxicol. Chem.* 14(1), pp.43–50.
- Dodson, S.I., Tollrian, R., and Lampert, W., 1997b. *Daphnia* swimming behavior during vertical migration. *J. Plankton Res.* 19(8), pp.969–978.
- Dore, V., Moroni, M., Menach, M.L., and Cenedese, A., 2009. Investigation of penetrative convection in stratified fluids through 3D-PTV. *Exp Fluids*, 47, pp.811–825.
- Dower, J.F., Pepin, P., and Leggett, W.C., 1998. Enhanced gut fullness and an apparent shift in size selectivity by radiated shanny (*Ulvaria subbifurcata*) larvae in response to increased turbulence. *Can. J. Fish. Aquat. Sci.* 55(1), pp.128–142.
- Eyden, B.Y.D., 1923. Specific gravity as a factor in the vertical distribution of plankton. *Biol. Rev. Camb. Philos. Soc.* 1(1), pp.49–55.
- Fielding, S., Griffiths, G., and Roe, H.S.J., 2004. The biological validation of ADCP acoustic backscatter through direct comparison with net samples and model predictions based on acoustic-scattering models. *ICES J. Mar. Sci.* 61(2), pp.184–200.

- Fischer, H.B., List, E.J., Koh, R.C.Y., Imberger, J., and Brooks, N.H., 1979. *Mixing in Inland and Coastal Waters*. Vol. 114. Academic San Diego Calif, p.315.
- Francois, R.E., 1982. Sound absorption based on ocean measurements: Part I: Pure water and magnesium sulfate contributions. *J. Acoust. Soc. Am.* 72(3), pp.896–907.
- George, D.G. and Hewitt, D.P., 1999. The influence of year-to-year variations in winter weather on the dynamics of *Daphnia* and *Eudiaptomus* in Esthwaite Water, Cumbria. *Funct. Ecol.* 13, pp.45–54.
- Gool, E.V. and Ringelberg, J., 1995. Swimming of *Daphnia galeata x hyalina* in response to changing light intensities: influence of food availability and predator kairomone. *Mar. Freshw. Behav. Physiol.* 26(2-4), pp.259–265.
- Gorski, P.R. and Dodson, S.I., 1996. Free-swimming *Daphnia pulex* can avoid following Stokes law. *Limnol. Oceanogr.* 41(8), pp.1815–1821.
- Goudsmit, G, Peeters, F, Gloor, M, and Wüest, A, 1997. Boundary versus internal diapycnal mixing in stratified natural waters. *J. Geophys. Res.* 12(1997), pp.27,903–27,914.
- Gregg, M.C. and Horne, J.K., 2009. Turbulence, acoustic backscatter, and pelagic nekton in Monterey Bay. *J. Phys. Oceanogr.* 39(5), pp.1097–1114.
- Gries, T., Jöhnk, K., Fields, D., and Strickler, J.R., 1999. Size and structure of 'footprints' produced by *Daphnia*: Impact of animal size and density gradients. *J. Plankton Res.* 21(3), pp.509–523.
- Harris, R., Wiebe, P., Lenz, J., Skjoldal, H.R., and Huntley, M., 2000. *Zooplankton Methodology Manual*.
- Haupt, F., Stockenreiter, M., Reichwaldt, E.S., Baumgartner, M., Lampert, W., Boersma, M., and Stibor, H., 2010. Upward phosphorus transport by *Daphnia* diel vertical migration. *Limnol. Oceanogr.* 55(2), pp.529–534.

- Hays, G.C., 2003. A review of the adaptive significance and ecosystem consequences of zooplankton diel vertical migrations. *Hydrobiologia*, 503, pp.163–170.
- Heinle, D.R., 1969. Temperature and zooplankton. *Chesap. Sci.* 10(3), pp.186–209.
- Hembre, L.K. and Megard, R.O., 2003. Seasonal and diel patchiness of a *Daphnia* population: An acoustic analysis. *Limnol. Oceanogr.* 48(6), pp.2221–2233.
- Hessen, D.O. and Kaartvedt, S., 2014. Top-down cascades in lakes and oceans: Different perspectives but same story? *J. Plankton Res.* 36(4), pp.914–924.
- Huber, A.M.R., Peeters, F., and Lorke, A., 2011. Active and passive vertical motion of zooplankton in a lake. *Limnol. Oceanogr.* 56(2), pp.695–706.
- Humphries, S., 2013. A physical explanation of the temperature dependence of physiological processes mediated by cilia and flagella. *Proc. Natl. Acad. Sci. U. S. A.* 110(36), 14693–14698.
- Huntley, M.E. and Zhou, M., 2004. Influence of animals on turbulence in the sea. *Mar. Ecol. Prog. Ser.* 273, pp.65–79.
- Hutchinson, G.E., 1967. *A treatise on limnology*. Wiley.
- Ianson, D., Jackson, G.A., Angel, M.V., Lampitt, R.S., and Burd, A.B., 2004. Effect of net avoidance on estimates of diel vertical migration. *Limnol. Oceanogr.* 49(6), pp.2297–2303.
- Imboden, D.M. and Wuest, A., 1995. *Mixing Mechanisms in Lakes*. Springer-Verlag, p.334.
- Inoue, R., Kitamura, M., and Fujiki, T., 2016. Diel vertical migration of zooplankton at the S1 biogeochemical mooring revealed from acoustic backscattering strength. *J. Geophys. Res. Ocean.* 121, 1031–1050.



- Ivey, G.N. and Imberger, J., 1991. On the Nature of Turbulence in a Stratified Fluid. Part I: The Energetics of Mixing. *EN. J. Phys. Oceanogr.* 21(5), pp.650–658.
- Ivey, G.N., Winters, K.B., and Koseff, J.R., 2008. Density Stratification, Turbulence, but How Much Mixing? *Annu. Rev. Fluid Mech.* 40(1), pp.169–184.
- Iwasa, Y., 1982. Vertical migration of zooplankton: A game between predator and prey. *Am. Nat.* 120(2), pp.171–180.
- Jiang, H. and Kjørboe, T., 2011. The fluid dynamics of swimming by jumping in copepods. *J. R. Soc. Interface*, 8(61), pp.1090–1103.
- Jonas, T., Stips, A., Eugster, W., and Wuest, A., 2003. Observations of a quasi shear-free lacustrine convective boundary layer: Stratification and its implications on turbulence. *J. Geophys. Res.* 108(C10, 3328), pp.1–15.
- Jung, I., Powers, T.R., and Valles, J.M., 2014. Evidence for two extremes of ciliary motor response in a single swimming microorganism. *Biophys. J.* 106(1), pp.106–113.
- Katija, K., 2012. Biogenic inputs to ocean mixing. *J. Exp. Biol.* 215(Pt 6), pp.1040–1049.
- Kils, U., 1993. Formation of micropatches by zooplankton-driven microturbulences. *Bull. Mar. Sci.* 53(1), pp.160–169.
- Kjørboe, T., Jiang, H., Goncalves, R.J., Nielsen, L.T., and Wadhwa, N., 2014. Flow disturbances generated by feeding and swimming zooplankton. *Proc. Natl. Acad. Sci.* 111(32), pp.11738–11743.
- Kirillin, G., Grossart, H.-P., and Tang, K.W., 2012. Modeling sinking rate of zooplankton carcasses: Effects of stratification and mixing. *Limnol. Oceanogr.* 57(3), pp.881–894.

- Kunze, E., 2011. Fluid mixing by swimming organisms in the low-Reynolds-number limit. *J. Mar. Res.* 69(4-6), pp.591–601.
- Kunze, E., Dower, J.F., Beveridge, I., Dewey, R., and Bartlett, K.P., 2006. Observations of biologically generated turbulence in a coastal inlet. *Science (80- )*. 313(5794), pp.1768–1770.
- Larsen, P.S. and Riisgård, H.U., 2009. Viscosity and not biological mechanisms often controls the effects of temperature on ciliary activity and swimming velocity of small aquatic organisms. *J. Exp. Mar. Bio. Ecol.* 381(2), pp.67–73.
- Larsen, P.S., Madsen, C.V., and Riisgard, H.U., 2008. Effect of temperature and viscosity on swimming velocity of the copepod *Acartia tonsa*, brine shrimp *Artemia salina* and rotifer *Brachionus plicatilis*. *Aquat. Biol.* 4(1), pp.47–54.
- Lass, S. and Spaak, P., 2003. Chemically induced anti-predator defences in plankton: A review. *Hydrobiologia*. Vol. 491, pp.221–239.
- Leach, T.H., Williamson, C.E., Theodore, N., Fischer, J.M., and Olson, M.H., 2014. The role of ultraviolet radiation in the diel vertical migration of zooplankton: An experimental test of the transparency-regulator hypothesis. *J. Plankton Res.* 37(5), pp.886–896.
- Leshansky, A.M. and Pismen, L.M., 2010. Do small swimmers mix the ocean? *Phys. Rev. E*, 82(2), p.025301.
- Lighthill, M.J., 1952. On the Squirming Motion of Nearly Spherical Defomable Bodies through Liquids at Very Small Reynolds Numbers. *Commun. Pure Appl. Math.* 5(2), pp.109–118.
- Loose, C.J. and Dawidowicz, P., 1994. Trade-offs in diel vertical migration by zooplankton: The costs of predator avoidance. *Ecology*, 75(8), pp.2255–2263.
- Lorke, A. and Probst, W.N., 2010. In situ measurements of turbulence in fish shoals. *Limnol. Oceanogr.* 55(1), pp.354–364.

- Lorke, A., McGinnis, D.F., Spaak, P., and Wüest, A., 2004. Acoustic observations of zooplankton in lakes using a Doppler current profiler. *Freshw. Biol.* 49, pp.1280–1292.
- Machemer, H., 1972. Ciliary activity and the origin of metachrony in *Paramecium*: Effects of increased viscosity. *J. Exp. Biol.* 57(1), pp.239–259.
- MacIntyre, S., Flynn, K.M., Jellison, R., and Romero, J.R., 1999. Boundary mixing and nutrient fluxes in Mono Lake, California. *Limnol. Oceanogr.* 3, pp.512–529.
- Masson, S., Angeli, N., Guillard, J., and Pinel-Alloul, B., 2001. Diel vertical and horizontal distribution of crustacean zooplankton and young of the year fish in a sub-alpine lake: an approach based on high frequency sampling. *J. Plankton Res.* 23, pp.1041–1060.
- Michalec, F.-G., Souissi, S., and Holzner, M., 2015. Turbulence triggers vigorous swimming but hinders motion strategy in planktonic copepods. *J. R. Soc. Interface*, 12(106), pp.20150158–20150158.
- Moison, M., Schmitt, F.G., and Souissi, S., 2012. Effect of temperature on *Temora longicornis* swimming behaviour: Illustration of seasonal effects in a temperate ecosystem. *Aquat. Biol.* 16(2), pp.149–161.
- Neill, W.E., 1990. Induced vertical migration in copepods as a defence against invertebrate predation. *Nature*, 345(6275), pp.524–526.
- Noss, C. and Lorke, A., 2012. Zooplankton induced currents and fluxes in stratified waters. *Water Qual. Res. J. Canada*, 47(3-4), pp.276–286.
- Noss, C. and Lorke, A., 2014. Direct observation of biomixing by vertically migrating zooplankton. *Limnol. Oceanogr.* 59(3), pp.724–732.
- Osborn, T.R., 1980. Estimates of the local rate of vertical diffusion from dissipation measurements. *J. Phys. Oceanogr.* 10(1), pp.83–89.

- Osborn, T.R. and Cox, C.S., 1972. Oceanic fine structure. *Geophys. Fluid Dyn.* 3(1), pp.321–345.
- Paffenhöfer, G.A. and Mazzocchi, M.G., 2002. On some aspects of the behaviour of *Oithona plumifera* (Copepoda: Cyclopoida). *J. Plankton Res.* 24(2), pp.129–135.
- Piera, J., Roget, E., and Catalan, J., 2002. Turbulent patch identification in microstructure profiles: A method based on wavelet denoising and thorpe displacement analysis. *EN. J. Atmos. Ocean. Technol.* 19(9), pp.1390–1402.
- Power, J.H., 1989. Sink or Swim : Growth Dynamics and Zooplankton Hydromechanics. *Am. Nat.* 133(5), pp.706–721.
- Prairie, J.C., Sutherland, K.R., Nickols, K.J., and Kaltenberg, A.M., 2012. Biophysical interactions in the plankton: A cross-scale review. *Limnol. Oceanogr. Fluids Environ.* 2(1), pp.121–145.
- Pujiana, K., Moum, J.N., Smyth, W.D., and Warner, S.J., 2015. Distinguishing ichthyogenic turbulence from geophysical turbulence. *J. Geophys. Res. Ocean.* 120(5), pp.3792–3804.
- Rahkola-Sorsa, M., Voutilainen, A., and Viljanen, M., 2014. Intercalibration of an acoustic technique, two optical ones, and a simple seston dry mass method for freshwater zooplankton sampling. *Limnol. Oceanogr. Methods*, 12, pp.102–113.
- Rao, Y.R., Hawley, N., Charlton, M.N., and Schertzer, W.M., 2008. Physical processes and hypoxia in the central basin of Lake Erie. *Limnol. Oceanogr.* 53(5), pp.2007–2020.
- Record, N.R. and de Young, B., 2006. Patterns of diel vertical migration of zooplankton in acoustic Doppler velocity and backscatter data on the Newfoundland Shelf. *Can. J. Fish. Aquat. Sci.* 63(12), pp.2708–2721.

- Reinfelder, J.R., Fisher, N.S., and Fowler, S.W., 1993. Release rates of trace elements and protein from decomposing planktonic debris . 2 . Copepod carcasses and sediment trap particulate matter. *J. Mar. Res.* 51, pp.423–442.
- Ringelberg, J and Flik, B.J.G., 1994. Increased phototaxis in the field leads to enhanced diel vertical migration. *Limnol. Ocean.* 39(8), pp.1855–1864.
- Ringelberg, J., Flik, B.J.G., Lindenaar, D., and Royackers, K., 1991. Diel vertical migration of *Daphnia hyalina* (*sensu latiori*) in Lake Maarsseveen: Part 1. Aspects of seasonal and daily timing. *Arch. Hydrobiol.* 121, pp.129–145.
- Ringelberg, J., 1999. The photobehaviour of *Daphnia* spp. as a model to explain diel vertical migration in zooplankton. *Biol. Rev. Camb. Philos. Soc.* 74(04), pp.397–423.
- Ringelberg, J., 2010. *Diel vertical migration of Zooplankton in Lakes and Oceans*. Springer. Springer Netherlands.
- Rinke, K. and Petzoldt, T., 2008. Individual-based simulation of diel vertical migration of *Daphnia*: A synthesis of proximate and ultimate factors. *Limnologia*, 38(3-4), pp.269–285.
- Rinke, K., Hübner, I., Petzoldt, T., Rolinski, S., König-Rinke, M., Post, J., Lorke, A., and Benndorf, J., 2007. How internal waves influence the vertical distribution of zooplankton. *Freshw. Biol.* 52(1), pp.137–144.
- Rinke, K., Huber, A.M., Kempke, S., Eder, M., Wolf, T., Probst, W.N., and Rothhaupt, K.O., 2009. Lake-wide distributions of temperature, phytoplankton, zooplankton, and fish in the pelagic zone of a large lake. *Limnol. Oceanogr.* 54(4), pp.1306–1322.
- Rippeth, T., Gascoigne, J.C., Green, J.A.M., Inall, M.E., Palmer, M.R., Simpson, J.H., and Wiles, P.J., 2007. Turbulent Dissipation of Coastal Seas, a response to "Observations of Biologically Generated Turbulence in a Coastal Inlet".

*Science Electronic Letters*. Available from: <https://www.sciencemag.org/content/313/5794/1768> [Accessed 30 March 2016].

Ross, T., 2014. A video-plankton and microstructure profiler for the exploration of in situ connections between zooplankton and turbulence. *Deep. Res. Part I*, 89, pp.1–10.

Ross, T., Gaboury, I., and Lueck, R., 2007. Simultaneous acoustic observations of turbulence and zooplankton in the ocean. *Deep. Res. Part I Oceanogr. Res. Pap.* 54(1), pp.143–153.

Rousseau, S., Kunze, E., Dewey, R., Bartlett, K., and Dower, J., 2010. On Turbulence Production by Swimming Marine Organisms in the Open Ocean and Coastal Waters. *J. Phys. Oceanogr.* 40(1966), pp.2107–2121.

Ruddick, B., Anis, A., and Thompson, K., 2000. Maximum Likelihood Spectral Fitting: The Batchelor Spectrum. *J. Atmos. Ocean. Technol.* 17(11), pp.1541–1555.

Saiz, E. and Alcaraz, M., 1992. Enhanced excretion rates induced by small-scale turbulence in *Acartia* (Copepoda: Calanoida). *J. Plankton Res.* 14(5), pp.681–689.

Saiz, E., Calbet, A., and Broglio, E., 2013. Effects of small-scale turbulence on copepods: The case of *Oithona davisae*. *Limnol. Ocean.* 48(3), pp.1304–1311.

Seuront, L., Yamazaki, H., and Souissi, S., 2004. Hydrodynamic disturbance and zooplankton swimming behavior. *Zool. Stud.* 43(2), pp.376–387.

Simoncelli, S., Thackeray, S.J., and Wain, D.J., 2017. Can small zooplankton mix lakes? *Limnol. Oceanogr. Lett.* 2(5), pp.167–176.

Sommer, T., Danza, F., Berg, J., Sengupta, A., Constantinescu, G., Tokyay, T., Bürgmann, H., Dressler, Y., Sepúlveda Steiner, O.R., Schubert, C.J., Tonolla, M., and Wüest, A., 2017. Bacteria-induced mixing in natural waters. *Geophys. Res. Lett.* 44(18), pp.9424–9432.

- Stoecker, D.K. and Capuzzo, J.M., 1990. Predation on Protozoa: its importance to zooplankton. *J. Plankton Res.* 12(5), pp.891–908.
- Straile, D. and Adrian, R., 2000. The North Atlantic Oscillation and plankton dynamics in two European lakes - two variations on a general theme. *Glob. Chang. Biol.* 6(6), pp.663–670.
- Subramanian, G., 2010. Viscosity-enhanced bio-mixing of the oceans. *Curr. Sci.* 98(8), pp.1103–1108.
- Sutor, M., Cowles, T.J., Peterson, W.T., and Lamb, J., 2005. Comparison of acoustic and net sampling systems to determine patterns in zooplankton distribution. *J. Geophys. Res. C Ocean.* 110(10), pp.1–11.
- Talling, J.F., 2003. Phytoplankton-zooplankton seasonal timing and the 'clear-water phase' in some English lakes. *Freshw. Biol.* 48(1), pp.39–52.
- Tanaka, M., Nagai, T., Okada, T., and Yamazaki, H., 2017. Measurement of sardine-generated turbulence in a large tank. *Mar Ecol Prog Ser*, 571, pp.207–220.
- Thackeray, S.J., George, D.G., Jones, R.I., and Winfield, I.J., 2004. Quantitative analysis of the importance of wind-induced circulation for the spatial structuring of planktonic populations. *Freshw. Biol.* 49(9), pp.1091–1102.
- Thiffeault, J.-L. and Childress, S., 2010. Stirring by swimming bodies. *Phys. Lett. A*, 374(34), pp.3487–3490.
- Thorpe, S.A., 2005. *The Turbulent Ocean*. Cambridge University Press, p.485.
- Thorpe, S., 2007. *An Introduction to Ocean Turbulence*. Cambridge University Press, p.264.
- Tiberti, R. and Iacobuzio, R., 2013. Does the fish presence influence the diurnal vertical distribution of zooplankton in high transparency lakes? *Hydrobiologia*, 709(1), pp.27–39.

- Unesco, 1968. *Zooplankton Sampling*. Unesco, p.174.
- Van Gool, E., 1997. Light-induced swimming of *Daphnia*: can laboratory experiments predict diel vertical migration? *Hydrobiologia*, 360, pp.161–167.
- Van Gool, E. and Ringelberg, J., 1998a. Light-induced migration behaviour of *Daphnia* modified by food and predator kairomones. *Anim. Behav.* 56(3), pp.741–747.
- Van Gool, E. and Ringelberg, J., 1998b. Quantitative effects of fish kairomones and successive light stimuli on downward swimming responses of *Daphnia*. *Aquat. Ecol.* 32(4), pp.291–296.
- Van Gool, E. and Ringelberg, J., 2003. What goes down must come up: Symmetry in light-induced migration behaviour of *Daphnia*. *Hydrobiologia*, 491, pp.301–307.
- Visser, A.W., 2007a. Visser's response to Kunze (2006). *Science* (80-. ). 318, pp.1239–1239.
- Visser, A.W., 2007b. Biomixing of the Oceans? *Science*, 316(5826), pp.838–839.
- Visser, A.W. and Stips, A., 2002. Turbulence and zooplankton production: Insights from PROVESS. *J. Sea Res.* 47(3-4), pp.317–329.
- Wagner, G.L., Young, W.R., and Lauga, E., 2014. Mixing by microorganisms in stratified fluids. *J. Mar. Res.* 72(2), pp.47–72.
- Wain, D, Kohn, M., Scanlon, J., and Rehmann, C., 2013. Internal wave driven transport of fluid away from the boundary of a lake. *Limnol. Oceanogr.* 58(2), pp.429–442.
- Wain, D.J. and Rehmann, C.R., 2010. Transport by an intrusion generated by boundary mixing in a lake. *Water Resour. Res.* 46(W08517), pp.1–11.
- Wang, S. and Ardekani, A.M., 2015. Biogenic mixing induced by intermediate Reynolds number swimming in stratified fluids. *Sci. Rep.* 5, pp.1–12.



- Wayu, R., 2004. Diel vertical migration of zooplankton in the Tanzanian waters of lake Victoria. *Tanzania Journal Sci.* 30(1), pp.123–124.
- Weber, A. and Van Noordwijk, A., 2002. Swimming behaviour of *Daphnia* clones: Differentiation through predator infochemicals. *J. Plankton Res.* 24(12), pp.1335–1348.
- Webster, D.R., Young, D.L., and Yen, J., 2015. Copepods' Response to Burgers' vortex: Deconstructing interactions of copepods with turbulence. *Integr. Comp. Biol.* 55(4), pp.706–718.
- Wickramarathna, L.N., 2016. *Kinematics and Energetics of Swimming Zooplankton*. PhD thesis. Universität Koblenz-Landau.
- Wickramarathna, L.N., Noss, C., and Lorke, A., 2014. Hydrodynamic trails produced by *Daphnia*: size and energetics. *PLoS One*, 9(3), pp.1–10.
- Wilhelmus, M.M. and Dabiri, J.O., 2014. Observations of large-scale fluid transport by laser-guided plankton aggregations. *Phys. Fluids*, 26(10), p.101302.
- Williamson, C.E., Fischer, J.M., Bollens, S.M., Overholt, E.P., and Breckenridge, J.K., 2011. Towards a more comprehensive theory of zooplankton diel vertical migration: Integrating ultraviolet radiation and water transparency into the biotic paradigm. *Limnol. Oceanogr.* 56(5), pp.1603–1623.
- Work, K.A. and Havens, K.E., 2003. Zooplankton grazing on bacteria and cyanobacteria in a eutrophic lake. *J. Plankton Res.* 25(10), pp.1301–1306.
- Wu, R.S., Zhou, B.S., Randall, D.J., Woo, N.Y., and Lam, P.K., 2003. Aquatic hypoxia is an endocrine disruptor and impairs fish reproduction. *Environ. Sci. Technol.* 37(6), pp.1137–1141.
- Wüest, A, Senden, D.C. van, Imberger, J, Piepke, G, Gloor, M, Wijest, A, Piepke, G, and Gloor, M, 1996. Comparison of diapycnal diffusivity measured by tracer and microstructure techniques. *Dyn. Atmos. Ocean.* 24(1–4), pp.27–39.

Wüest, A. and Lorke, A., 2003. Small Scale Hydrodynamics in Lakes. *Annu. Rev. Fluid Mech.* 35(1), pp.373–412.